THESIS FOR THE DEGREE OF DOCTOR OF PHILOSOPHY

A Chemical Perspective on the Tellurium Source Term in the Context of Severe Nuclear Power Plant Accidents

Fredrik J. C. Espegren

Department of Chemistry and Chemical Engineering

CHALMERS UNIVERSITY OF TECHNOLOGY

Gothenburg, Sweden 2020

A Chemical Perspective on the Tellurium Source Term in the Context of Severe Nuclear Power Plant Accidents
Fredrik J. C. Espegren
ISBN 978-91-7905-352-9

Doktorsavhandlingar vid Chalmers tekniska högskola
Ny serie nr 4819
ISSN 0346-718X

Nuclear Chemistry
Department of Chemistry and Chemical Engineering
Chalmers University of Technology
SE-412 96 Gothenburg
Sweden
Telephone + 46 (0)31-772 1000

Cover:
Samples of tellurium and sodium chloride heated to increasingly higher temperature.

Chalmers Reproservice
Gothenburg, Sweden 2020

A Chemical Perspective on the Tellurium Source Term in the Context of Severe Nuclear Power Plant Accidents

Fredrik J.C. Espegren

Department of Chemistry and Chemical Engineering
Nuclear Chemistry and Industrial Materials Recycling
Chalmers University of Technology

Abstract

In the event of a severe nuclear accident, one of the biggest concerns is the release of radioactive nuclides. Typically, the most volatile is likely to be released. One that is considered among the most volatile is tellurium. Additionally, health implications towards the public by tellurium can be by itself or the decay product iodine.

Several aspects concerning the volatility under mainly oxidizing (e.g., air ingress) and inert (injection of inert gas preventing hydrogen explosion) conditions of the tellurium source term from a chemical perspective have been explored. These aspects are the consequence of seawater as an emergency cooling medium, the effect of cesium iodide on the transport on and interaction in the reactor coolant system (RCS), and the effect of surfaces located inside a boiling water reactor (BWR). Finally, the effectiveness of the containment spray system (CSS) using different solutions was investigated.

Under oxidizing conditions, tellurium was noticeably affected by all aspects. The seawater experiments showed that tellurium was enhanced by sodium chloride. From the RCS experiments, the addition of cesium iodide decreased the transported amount of tellurium and a new tellurium species was observed, but uncertain if it was correlated to cesium. Regarding the BWR surfaces, only zinc was removed from the surface by the tellurium when humidity was high. However, neither if this enhanced the volatility or if a new compound formed were clear. Finally, high removal efficiency was observed of the spray system under all conditions.

The investigation of tellurium under inert conditions had less of the investigated aspect affecting the volatility. The seawater experiment showed no change to the volatilization of tellurium. However, in the RCS the addition of cesium iodide resulted in both an increase in transported tellurium and new tellurium species, potentially correlated to cesium. None of the BWR surfaces had any effect on tellurium. Finally, the effectiveness of the CSS was lower than under oxidizing conditions but still above 50%. However, the addition of cesium iodide considerably enhanced the removal. Therefore, indicating a change of the tellurium speciation.

From this work, it is clear that the chemistry concerning the volatility of tellurium still needs further attention. Under an air ingress scenario, using seawater would enhance the release of tellurium. Opposed to the cesium iodide, that would reduce it. In the containment, tellurium would interact with surfaces made out of zinc. For a scenario when inert gas has been injected, the use of seawater would have less impact if any and the presence of cesium iodide would enhance the transport of tellurium. No surface in the BWR containment would interfere. However, under both scenarios, an intact containment and a functional CSS would effectively trap the tellurium in the sump.

Keywords: Tellurium, Cesium Telluride, Nuclear Accident, Fission Products, Seawater Cooling, Reactor Coolant System, Containment, Containment Spray System

List of Publications

The thesis is based on the work found in the publications stated below and the contribution by the author of this thesis is included:

I. Espegren, F., Glänneskog, H., Foreman, M.R.S., Ekberg, C. "*Chemical interaction between sea-salt and tellurium, between 300 and 1180 K*". In: "*Journal of Radioanalytical and Nuclear Chemistry*" 317 (2018), pp. 535–543 DOI: 10.1007/s10967-018-5922-1

   Contribution: *Main author, all experimental work, all data acquisition and interpretation.*

II. Espegren, F. and Ekberg, C. "*Potential tellurium deposits in the BWR containment during a severe nuclear accident*". In: "*Annals of Nuclear Energy*" 146 (2020), pp. 107629, ISSN: 0306-4549, DOI: 10.1016/j.anucene.2020.107629

   Contribution: *Main author, all experimental work, all data acquisition and interpretation.*

III. Espegren, F., Kärkelä, Pasi, A.E., Tapper, U., Kučera, J., Lerum, V.L., Omtvedt, J.P., Ekberg, C. "*Tellurium Transport in the RCS under conditions relevant for severe nuclear accidents*". Submitted to: "*Progress in Nuclear Energy*"

   Contribution: *Main author, collaborated on all experimental work, part of data acquisition and interpretation.*

IV. Kärkelä, Pasi, A.E., Espegren, F., Sevon, T., Tapper, U., Ekberg, C. "*Tellurium Retention by Containment Spray System*". Manuscript to be submitted in September. Input from other authors still missing. Journal aim: "Nuclear Engineering and Technology", "Progress in Nuclear Energy", "Annals of Nuclear Energy", or "Nuclear Technology".

   Contribution: *Editing of article, participation in most of the experimental work, part of data acquisition and interpretation.*

V. Kučera, J., Pasi, A.E., Espergen, F., Kärkelä, T., Lerum, H.V., Omtvedt, J.P., Ekberg, C. "*Tellurium determination by three modes of instrumental neutron activation analysis in aerosol filters and trap solutions for the simulation of a severe nuclear accident*". In: "*Microchemical Journal*" 58 (2020), pp. 105139, ISSN: 0026-265X, DOI: 10.1016/j.microc.2020.105139

   Contribution: *Editing of article concerning the TETRA part, participated in the analysis.*

Contents

1 Introduction

Starting from 2007 and continuing through to 2017, the global primary energy consumption was increased by an average of 1.5% per year. The following year of 2018, the global energy consumption exceeded this by doubling the average of prior years to 2.9%. To meet such an increase in demand for energy, several sources were expanded over the 10-year period as well as during the year 2018 [1]. Among these sources were fossil, hydro, renewables, and nuclear. The corresponding individual annual increase for these sources can be found in Table 1.

Table 1. The global energy production increase of some of the primary energy sources. Values given are for 2007-2017 average annual increase and the 2018-year increase. Renewable includes solar and wind production [1].

Energy source	Coal	Oil	Natural gas	Nuclear	Hydro	Renewable
2007-2017	0.7%	1.0%	2.2%	-0.4%	2.8%	16.4%
2018	1.4%	1.2%	5.3%	2.4%	3.1%	14.5%

A major concern associated with energy production today is the CO_2-emission [2]. According to the Intergovernmental Panel on climate change [3] and the European Union [4], one energy source that can deliver low emission of CO_2 energy is nuclear power and as shown in Table 1, was expanded during 2018. Using nuclear power comes with some drawbacks and these are operational safety, waste management, and fissile material proliferation. Therefore, if nuclear power is to be part of the future energy mix of any country, these aforementioned drawbacks need to be mitigated and research.

During a nuclear accidents, one of the biggest issues is the release of radionuclides. On this topic a considerable effort has already been made. Still, if the safe use of nuclear power is to be continued, more is needed. Historically, such research has been carried out in large fission product release research programs such as e.g., VERCORS [5, 6, 7], VERDON [8, 9, 10], PHÉBUS [11, 12, 13, 14, 15]. In such programs, a large number of radionuclides, phenomena, and parameters have been investigated simultaneously and as such closer mimics an actual nuclear power plant accident scenario. However, to better understand specific phenomena observed during these programs, they need to be supplemented by bench-scale work [16, 17, 18, 19, 20, 21, 22]. Such work usually focuses on one or a few radionuclides (e.g., cesium, iodine, ruthenium) and relevant phenomena (e.g., core melt, corium concrete interaction, air ingress). When observing these works, and many others, a lack of tellurium research is noticeable concerning both the reactor coolant system (RCS) and the containment. Thus, the focus of this work is to better understand the chemical behavior of tellurium in these locations as well as other relevant phenomena.

One important contributing factor to the tellurium release is its volatility during and possibly after a nuclear accident under different conditions. Based on already occurred nuclear accidents and identified shortcomings in literature areas/topics have been found needing further attention. Of those, the following has been deemed relevant for the volatility of the tellurium source term: the effect caused of using seawater as an emergency cooling, the effect by cesium iodide under different conditions inside the RCS, and the interaction with surfaces found throughout a boiling water reactor containment. Finally, the efficiency of the containment spray system in preventing the release of tellurium has also been investigated.

2 Background

The consequences of a nuclear power plant accident will depend on the type, the severity, and the circumstances as it occurs. One of the main concerns and possible contributors to the health consequences of a nuclear power plant accident is the release of radionuclides. Minor accidents/incidents may only release small amounts of radionuclides, which may be contained within the reactor vessel or the containment. Still, even an accident characterized as less problematic may have releases to the surrounding areas (e.g., the Three Mile Island accident [23]). However, in the event of a severe nuclear power plant accident, the consequences may be considerably more extensive, to the point that the releases of the radionuclides are not limited to the nuclear power plant site or the vicinity of it, and instead reach beyond it (e.g., the Fukushima Daiichi nuclear accident [24]).

To the general public, the two most infamous severe nuclear power plant accidents to have occurred were the *Chernobyl accident* (1986) [25] and the *Fukushima Daiichi nuclear accident* (2011) [26]. Other less known, but still problematic were e.g., the Windscale fire (1957) [27], the Three Mile Island accident (1979) [23], and the Forsmark incident (2006) [28]. In terms of severity, the Chernobyl and the Fukushima Daiichi accidents are classified as the most severe based on the impact towards the environment and people. Considering the reactor designs used at the different sites, an important difference exists. In the case of Chernobyl, a critical safety feature used almost exclusively at all nuclear power plants today was lacking; the concrete containment enclosure [29]. However, at Fukushima Daiichi nuclear power plant the containment existed and is from a strict safety research perspective more relevant for the majority of the world's nuclear power plants.

To mitigate and prevent an accident at a nuclear power plant, the concept of defense-in-depth strategy is commonly utilized [30]. It consists of several aspects relating to safety, one being physical barriers. Of which several exist and three important ones that are all capable of preventing the release of radionuclides are the cladding, the reactor vessel, and the containment [31]. The cladding encloses the fuel and the cladding can be fabricated [32] from a range of materials (e.g., austenitic stainless steel, magnesium alloys, and zirconium alloys). Next is the reactor pressure vessel [33], which contains the reactor core. The third barrier is the aforementioned concrete containment [34] and it houses the reactor pressure vessel as well as other safety features. In addition, other features exist to prevent or mitigate incidents and accidents at nuclear power plants. These vary from e.g., nuclear fail-safe redundancy [35], early fault detection system [36], emergency shutdown (e.g., Scram or reactor trip) [37], emergency core cooling system (ECCS) [38], filtered containment venting system (FCVS) [39], and containment spray system (CSS) [40].

The release of radionuclides can be a complex topic, with several aspects and phenomena to consider. This depending on the radionuclide investigated, prevailing atmosphere conditions, as well as the location (e.g., vicinity of the core, RCS, or containment). Thus, a need exists for a term that includes a broader perspective of each radionuclide. This has been achieved with the terminology "*Source Term*", for which one definition is: "the quantity, time, history, chemical and physical form of radionuclides released to the environment, or present in the containment atmosphere, during the course of a severe accident" [41].

2.1 Accident - General

A more general description of a severe nuclear accident, where the result is a core meltdown and the failure of all physical safety barrier with the consequences that radionuclides are released to the environment, can be divided into different phases that occur concurrently and/or sequentially; starting from the ”coolant activity phase”, followed by the ”gap activity phase” and then the two main release phases. The latter two phases revolve around whether the release is occurring, inside the vessel or outside. These are referred to as the ”in-vessel phase” and ”ex-vessel phase” respectively. However, it is also possible that a containment by-pass may occur during these phases, resulting in a direct release to the environment of radionuclides. An overview of these phases can be seen in Table 2.

Table 2. Overview of the different phases and corresponding duration for a BWR and PWR [42].

Sequence	Phase	Duration, BWR	Duration, PWR
1	Coolant activity	10-30 s	30 s
2	Gap activity phase	30 min	30 min
3	Early in-vessel phase	1.3 h	1.5 h
4	Ex-vessel phase	2 h	3 h
	Late in-vessel phase	10 h	10 h

BWR: Boiling water reactor; PWR: Pressure water reactor

The first phase of an accident is the **coolant activity**, which can start with a postulated pipe rupture and ends when the failure of the first fuel rod is estimated to occur. During this phase, the amount of radionuclides released will be very small and dissolve in the coolant. The time range for this phase (for a large loss of cooling accident) ranges from 10 to 30 seconds, depending on the reactor type [41, 42].

As the cladding encapsulating the fuel starts to fail[1] the next phase begins, i.e., the **gap activity phase**. Consequently, the accumulated radionuclides in the gap (between the fuel and cladding) would then be released. These released radionuclides are the most volatile e.g., xenon, krypton, iodine, and cesium. The release fractions of these are typically very small compared to what remains in the fuel. This phase is estimated to last around 30 minutes. The definite end of this phase occurs when the temperature has reached a level where considerable releases of the radionuclides from the core take place [41, 42].

Once the accident has progressed to the point that the core no longer maintains its full structural integrity, but still with an intact reactor vessel, the next phase begins and is referred to as the **early in-vessel phase**. This phase is characterized by considerable releases of the volatile radionuclides and the start of the releases of the lesser volatile radionuclides. The released radionuclides will at this stage of the accident, enter the RCS. In which, they will be exposed to the conditions found therein, other released species, and the surfaces found in the RCS [43]. This phase lasts until the core melts and falls to the bottom of the reactor vessel. The duration of this phase is estimated to be around 10 minutes up to 1.5 h, which will depend on e.g., reactor type and accident scenario. Once the corium (molten core debris) finally breach the reactor vessel, the two next phases begin [41, 42].

[1]This may occur during normal operation as well, without severe consequences.

At the moment, which the reactor vessel fails and the corium drops to the concrete floor, a new pathway opens up for the radionuclide release. That is, that the radionuclides can directly enter the containment, without passing through the RCS. This is generally referred to as the **ex-vessel phase**. During this phase, the releases of radionuclides will be affected by several phenomena e.g., the boiling of the sump water, concrete-corium interaction, and re-suspension of deposited material on the containment wall [43]. The ex-vessel phase ends when the temperature of the corium has dropped sufficiently, which is expected to take a few hours. Concurrently with the ex-vessel phase, it is still possible that radionuclides can enter the RCS and that the radionuclides already present within it will become re-suspended. This location and stage are referred to as the **late in-vessel phase**. The expected duration of this phases is around ten hours [41, 42].

Inside the reactor containment enclosure, several features exists to reduce the transport, and consequently mitigate the release of the radionuclides beyond the containment and site. Some of these that directly or indirectly prevent releases are: the CSS (reducing airborne particles, decrease of the containment pressure in the long run, hydrogen-burning) [40], the FCVS (vented gas is filtered through a scrubber, containment pressure reduction and removal of decay heat) [39], the catalytic hydrogen recombiners and the ignitors (preventing strong deflagrations or detonations) [44], and the core melt stabilization concepts (CMSC, mitigating basemat penetration, overpressure, damage to internal structure) [45].

For the radionuclides to reach the environment, the containment enclosure needs to fail. This may occur by e.g., hydrogen combustion [46], direct containment heating [47], diffuse leakage (e.g., through valves, gaskets) [48], or steam explosion [49]. Alternatively, the radionuclides can by-pass the containment altogether and directly enter the environment from the RCS. Such a scenario is possible e.g., in a pressure water reactor (PWR) through a steam generator tube rupture [50] .

2.2 Accident - Fukushima Daiichi

As mentioned in an earlier chapter, the Fukushima Daiichi accident is one of the more relevant accidents from a safety perspective for most existing nuclear power plants. The accident occurred on March 11th in 2011 and was the result of the combined effects of an earthquake, resulting in loss of all off-site power, and the consequential tsunami flooding the site, resulting in a station blackout. The end consequences of these were a severe damage to three (units 1-3) out of six reactors with the subsequent release of radionuclides.

The radionuclides released to the environment consisted of several different radioactive isotopes. Initially, the noble gases ^{85}Kr and ^{133}Xe were the main constituents of the released atmospheric plume. As the accident progressed, other radionuclides appeared in the plume, such as ^{131}I, ^{134}Cs, and ^{137}Cs. These three are of particular concern as iodine can contribute, in the short-term, to relatively high doses, and cesium is capable of contributing to both internal and external equivalent and effective doses over a longer period. Other radionuclides such as strontium, ruthenium, and some actinides were eventually also observed in the plume. These releases spread both overlands and in the ocean [26].

At Tsukuba (Japan), 170 km southwestward from the Fukushima nuclear power plant, the aerosols in the atmosphere were collected and analyzed for short-lived radionuclides over a

longer period. Specifically, ^{110m}Ag, ^{134}Cs, ^{136}Cs, ^{131}I, ^{95}Nb, ^{129m}Te, and ^{132}Te were investigated in relation to ^{137}Cs. Among these, only ^{95}Nb diverged from the expected activity based on the physical decay from the modeling. Unlike the other radionuclides, for which the activity decreased with time, the ^{95}Nb increased as time progressed; hence indicating not only a single release occurrence but a continuing release as well. A suggested explanation by the author [51], was the formation of halides of ^{95}Nb itself or/and its parent ^{95}Zr (possibly inside the containment), which would results in species of the two with a much lower boiling point than their metallic states.

A specific action taken during the Fukushima accident that could have resulted in the formation of different halides was the use of seawater for emergency cooling [26]. The main constituents of seawater are chloride (19.33 g/kg$_{Seawater}$, salinity at 35) and sodium (10.53 g/kg$_{Seawater}$, salinity at 35) [52]. Of these, the former could interact and form halide complexes. Thus, comparing the boiling point of the chloride with the metallic and oxide state of both the niobium and zirconium, it is clear that the transition from metallic and/or oxide to chloride would increase the volatility of these. It is also possible that other radionuclides may be affected by the use of seawater, as the boiling points of the halides are typically lower than for e.g., the metallic and oxide forms. The boiling points for some radionuclides as metallic and as different halides are presented in Figure 3.

Table 3. The boiling point of some elements in the metallic state and a chloride state [53].

Element/Compound	Melting point	Boiling point
Mo	2895	4912
MoO_2	≈ 2073 dec.	
MoO_3	1075	1428
$MoCl_2$	773 dec.	
$MoCl_3$	673 dec.	
$MoCl_4$	554	
Nb	2750	5014
NbO_2	2174	
Nb_2O_5	1785	
$NbCl_4$	1073 dec.	821 subl.
$NbCl_5$	478.95	520.55
Te	722.66	1261
TeO_2	1006	1518
TeO_3	703	
$TeCl_2$	481	601
$TeCl_4$	497	660
Zr	2127	4679
ZrO_2	2983	4573
$ZrCl_2$	995	
$ZrCl_3$	864	
$ZrCl_4$	710 tp	604 sp

dec.: decomposes; sp: sublimation point; subl.: sublimes; tp.: triple point

Research on the specific interactions between seawater and radionuclide under nuclear accident conditions are very scarce in the literature and further investigations is needed. Lacking the knowledge necessary, the use of seawater may have enhanced several of the radionuclides source terms during the Fukushima Daiichi accident through the formation of more volatilize species. Specifically, for the fission products that have chlorides with lower melting and boiling points than their metallic and/or oxide counterparts.

2.3 Radionuclides

The main source of the radionuclides in a nuclear power plant is the fuel, in which they are mainly formed through thermal-neutron induced fission of fissile material. Thus, these specific radionuclides are referred to as fission products. Consequently, the more important and dictating factors for what quantities of the different radionuclides could be released from the fuel is the type and state of the fuel at the moment of the accident. Today, the most common fuel is the cylindrical pressed UO_2, which uses ^{235}U to act as the main fissile material. The fuel may either be natural (0.7%) or enriched (typically to 3.5-5%) in ^{235}U [54]. Another oxide fuel used is the mixed oxide fuel, in which plutonium has been mixed with uranium [55]. Aside from the fuel type, the burn-up of the fuel itself is directly correlated to how much of the fissile material has undergone fission. Consequently, this describes the concentration of the different fission products [55]. Additionally, the burn-up also affects the oxygen potential of the fuel (oxygen/metal-ration increases during operation [56]), which is highly relevant e.g., the release of molybdenum, niobium, and strontium [43]. Furthermore, the temperature gradient, both axial and radial, will also affect the composition through the transport of material and thermal diffusion processes [56]. All of these considerations will affect the release of radionuclides both quantitatively and speciation wise at the onset of the accident. According to Kleykamp [56], there are four classifications of the different states that the radionuclides can exist in nuclear fuel, these are as follows:

1. Fission gases, including other volatile fission products
    - Kr, Xe, Br, I
2. Metallic precipitates
    - Mo, Tc, Ru, Rh, Pd, Ag, Cd, In, Sn, Sb, Te
3. Oxide precipitates
    - Rb, Cs, Ba, Zr, Nb, Mo, Te
4. Oxides dissolved in the fuel matrix
    - Sr, Zr, Nb, Y, La, Ce, Pr, Nd, Pm, Sm

This classification does not necessarily provide the full knowledge needed to identify what radionuclide will be of the most concern in the event of a severe nuclear power plant accident. Instead, additional research has been performed [5] to better understand what the more volatile radionuclides are.

2.4 Fission Products

Generally, the most concerning radionuclides/fission products are those that are easily volatilized, as they are the most likely to be released during an accident and thus may reach the general public. A classification based on the volatility is needed, which has been achieved through the VERCORS experiments [5]. This have classifies the fission products volatility into four groups: volatile, semi-volatile, low-volatile, and non-volatile fission products. This classification was also supported by the VERDON experiments [8]. The different fission products that can be found in each group are shown in Table 4.

Table 4. Classification of the fission products, according to volatility in the context of a nuclear accident scenario [5].

Group	Fission product or gas
Volatile	Kr, Xe, I, Cs, Sb, Te, Cd, Rb, Ag
Semi-volatile	Mo, Rh, Ba, Pd, Tc
Low volatile	Ru, Nb, Sr, Y, La, Ce, Eu
Non-volatile	Zr, Nd, Pr

It is not only the specific volatility of a fission product that determines its severity. There still needs to be a considerable amount of the fission product for it to be of special concern. One way of attaining such quantifiable information is to determine the fission yield of different fissile material. The values for the yields of different fission products can be found in the literature [57].

Based on volatility and quantification by fission yield, a possible estimate of the most problematic fission products can be made. From this, one fission products that can be identified is tellurium, which will be the limitation and the continued focus of this work.

2.5 Tellurium - Radioactivity and Fission yield

The four main isotopes of tellurium under normal operation are ^{131}Te, ^{132}Te, ^{133m}Te, and ^{134}Te. These correspond to 60% of the total tellurium inventory [58]. All four of these tellurium isotopes decay to iodine, with a slight variation giving rise to different decay chains [59]. The fission yields of these tellurium isotopes are also in the upper part of the fission yields curve and the specific fission yield of each of these four tellurium isotopes from ^{235}U and ^{239}Pu can be seen in Table 5, alongside, the individual decay modes, corresponding half-lives, and the corresponding decay product have been added.

Table 5. The thermal fission yield of different tellurium isotopes from ^{235}U and ^{239}Pu. In addition, the relevant tellurium isotope mass number (A), their decay modes, half-life ($t_{1/2}$), and parent (P) to daughter (D) products are included [59].

A	^{235}U [%]	^{239}Pu [%]	DM 1 ($t_{1/2}$)	DM 2 ($t_{1/2}$)	P/D
131	2.878	3.724	m, β^- (33.25 h)	β^- (25 m)	^{131}Te/^{131}I
132	4.296	5.274	β^- (76.3 h)		^{132}Te/^{132}I
133	6.6	6.99	m, β^- (55.4 m)	β^- (12.5 m)	^{133}Te/^{133}I
134	7.79	6.87	β^- (41.8 m)		^{134}Te/^{134}I

A - mass number; m - metastable; DM - decay mode

The actual accumulated amount of tellurium has been determined and can be found in the literature for the Peach Bottom [60] BWR at shutdown and calculated for a 900 MWe PWR using DARWIN-PEPIN [41] code at the end-of-life. For this BWR the estimated masses (calculated using the values from the nuclide chart [59] from the activity in reference [60]) of tellurium was 0.7 kg, which can be compared to the iodine mass at 0.98 kg and cesium mass at 124 kg. For the PWR, the amounts were estimated for the specific configuration of the PWR mentioned in the literature [41] to be 26.2 kg of tellurium compared to 12.7 kg iodine and 161 kg cesium.

Thus, already by observing the produced amount and the corresponding decay product (iodine) of tellurium, there is strong evidence for the issues that tellurium may create, especially considering that the iodine will be adding its consequences to the tellurium releases [58]. Iodine, being considered an issue due to accumulation in the thyroid, therefore poses a well-known health threat [61, 62]. Considering the relatively short half-lives of these tellurium isotopes, as seen in Table 5, it can be concluded that the issue of tellurium will be in the shorter term of a severe nuclear power plant accident. However, considering that iodine is a decay daughter, the consequences of tellurium may be extended longer into the progression of an accident.

2.6 Tellurium - Health Concerns

Aside from the health concerns stemming from the decay product iodine, tellurium itself can enter the body and cause health-related concerns. However, the knowledge of tellurium related to the biological and health effect on the human body is limited, mainly as tellurium is rare in the environment and as such is not commonly utilized by any organisms or a common research topic. The research that does exist has shown that once tellurium has entered the body, it will participate in different biological functions. From the study of different tellurium compounds in rats, affected parts were found to be red blood cells and selenium-related proteins and enzymes [63]. Research by Taylor [64] has also shown, that exposure of tellurium in rats resulted in high levels of tellurium in the heart, kidney, bone, spleen, and lungs. These organs could then be exposed to dose in the case of radioactive tellurium ingestion. Still, the body is capable of emitting the tellurium via urine and breathing. The latter causes so-called ”garlic breath”, due to the distinct odor of garlic from the breath [63].

3 Theory

Several aspects of tellurium chemistry concerning severe nuclear power accidents are important. For this work, the main interests are the chemistry concerning the interaction between sea-water and tellurium, as well as the tellurium in the gas phase of the RCS and the containment. Thus, the following chapters aim to describe the evolution of the tellurium source term from the fuel to the containment. This is done by indicating which species are relevant in the different stages and how they may change in each stage.

3.1 Reactiveness and Expected Chemical Species

The reactiveness of tellurium has been indicated in the literature to be of concern in the context of nuclear accidents. As tellurium is likely to react with e.g., other fission products, structural materials, and different species in the gas phase in all stages (e.g., fuel, cladding, RCS, containment) of an accident [58]. Additionally, the prevailing conditions will have a great impact on the source term of tellurium. The conditions will vary depending on location and accident type, but some examples are oxidizing conditions via an air ingress scenario [65], inert conditions by the injection of inert gas for prevention of hydrogen explosion [66], and reducing conditions by a combination of a steam-starved upper core region and an accelerated oxidation of the zircaloy located in the bottom part [67].

3.1.1 State of Tellurium in the Fuel

Starting with the chemical state of tellurium in the fuel, a range of tellurium species are possible. These species may be classified according to two general groups; oxides and metallic phases (e.g., with uranium, palladium, tin) [56]. Some specific species of tellurium that can be observed in oxide uranium fuel are; metallic-Te (in metallic precipitates) [68], BaTe [69], Cs_2Te [70, 71, 72, 73], Cs_2TeO_3[58], PdTe [69], TeO_2 [58, 71], and TeI_x [74]. Imoto and Tanabe [69] have also performed equilibrium calculations using SOLGASMIX-PV code to acquire the chemical state of tellurium in UO_2. The result of their work [69] can be seen in Figure 1.

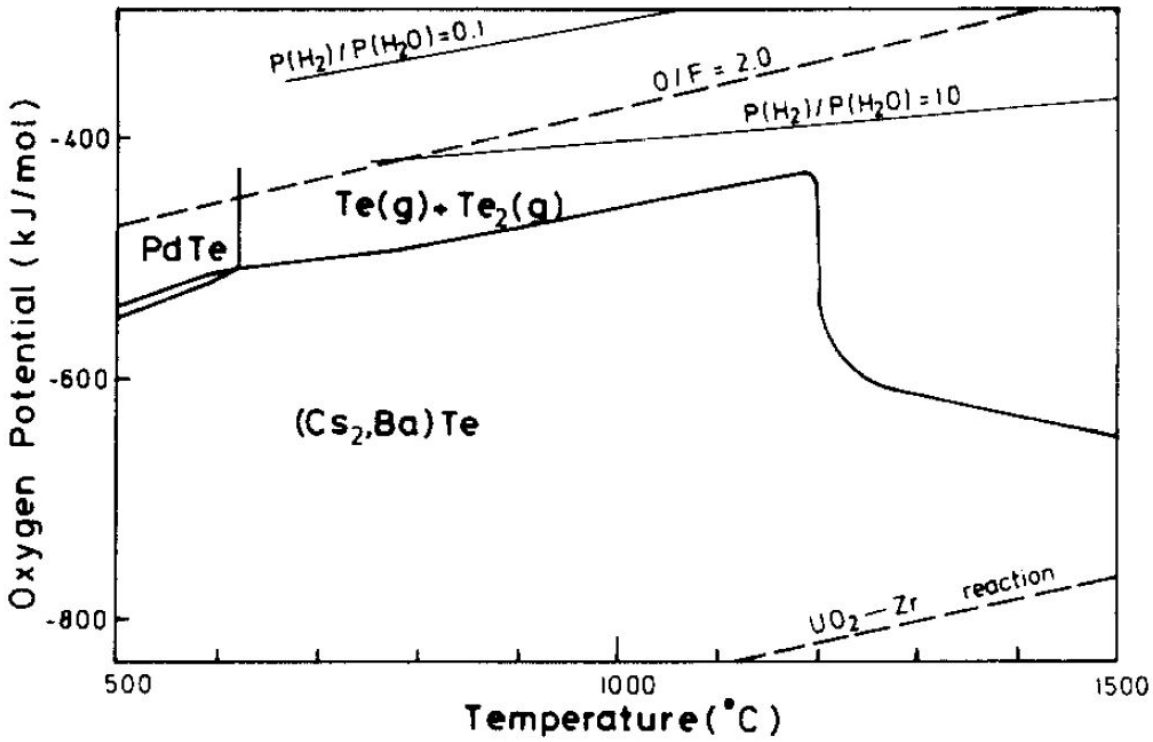

Figure 1. "Oxygen potentials versus temperature diagram for tellurium and its compounds in UO_2." Source: "Chemical State of Tellurium in a Degraded LWR Core" [69].

Aside from being present in the fuel during normal operation, tellurium will also be released to the fuel-cladding gap as Te/Te_2 [58, 69], TeO_2 [58] and Cs_2Te [58, 69, 71] (other cesium-tellurium species are possible as well [75]). In the case of cladding made from zircaloy, it has been observed that tellurium will react with this, forming different zirconium tellurides [68, 76, 77, 78] possibly already at 673 K [78] (as a comparison the water temperature surrounding the cladding: for a BWR is 558 K and for a PWR is 598 K [79]). Consequently, little of the tellurium would remain in the gap under normal operation. The reaction with the cladding is highly relevant for the tellurium source term evaluation as it delays any substantial release of tellurium. Furthermore, once the release does start it is rapid either reaching above or to the same levels as other volatile fission products being released [6].

3.1.2 Cladding Interaction with Tellurium

Interaction with the zircaloy cladding has been investigated and this phenomenon is fairly well known [68, 75, 76, 77]. The tellurium species formed in the cladding have been suggested to be $ZrTe_2$ [69] as well as $Zr_{1+x}Te_2$ and Zr_5Te_4 [76]. One important consequence of the formation of these species is the mentioned delay in the release of tellurium from the cladding. Consequently, little tellurium is released until either sufficiently high temperature (2620 K [5]) has been reached or the cladding has oxidized [14, 15]. The latter, as oxidation of zirconium is favored over tellurium and, hence the tellurium-zirconium species would dissociate. According to the literature [78], this can occur above an oxygen potential of -171 kcal/mol O_2, potentially as shown in Reaction 1 [69].

$$ZrTe_2(s) + 2H_2O(g) \rightleftarrows ZrO_2(s) + 2H_2(g) + Te_2(g) \quad (1)$$

When the tellurium release from the cladding occurs, the tellurium species will either be as metallic or tin telluride [75, 80]. The release of tin telluride occurs if pockets of tin in the cladding (formed by solubility differences of tin in zirconium and zirconium oxide [80]) overlaps with pockets of tellurium at the moment of release. However, depending on the oxygen potential, the tin telluride may dissociate into tin dioxide and tellurium, as shown in Reaction 2 [68].

$$SnTe(s,l) + O_2(g) \rightleftarrows SnO_2(s) + Te(l,g) \quad (2)$$

Alternatively, if steam is present Reaction 3 may also take place at a temperature above 1273 K [69].

$$SnTe(g) + 2H_2O(g) \rightleftarrows SnO_2(s) + 2H_2(g) + Te(g) \quad (3)$$

Should, the oxygen potential be sufficiently high, the tellurium may also oxidize as shown in Reaction 4 [68].

$$SnTe(s,l) + 2O_2(g) \rightleftarrows SnO_2(s) + TeO_2(g) \quad (4)$$

According to Boer and Cordfunke [68], Reaction 4 will shift to the right under oxidizing conditions with an oxygen partial pressure between 20 kPa and 50 kPa. At these levels, little metallic tellurium would be expected. Furthermore, when Boer and Cordfunke [68] investigated the effect by steam they observed that a ratio of 100/1 of steam/hydrogen resulted in the vaporization of tin dioxide and tellurium from the cladding. However, at lower steam/hydrogen-ratios of 1/1 or 1/100, the release occurred as tin telluride.

3.1.3 Tellurium within the Reactor Coolant System

The next stage of the tellurium release after the fuel and cladding is the RCS (i.e., early in-vessel phase) if the reactor vessel remains undamaged. At this stage, further factors will be affecting the source term of tellurium. Some of these are different temperatures, changes in total pressure, the composition of the gas (hydrogen/steam), radiation, impurities, the release rate of radionuclide, and condition of the structural surfaces [58]. The possible tellurium species that may enter the RCS will depend on the preceding conditions (e.g., oxidizing, reducing) as well as the progression of the accident. According to the literature [73, 81], possible species are: Te/Te_2, TeO, TeO_2, Cs_2Te, and H_2Te. Furthermore, SnTe [75, 81] may also reach the RCS. Once inside the RCS, the changes that these may undergo due to the conditions in the RCS could result in the formation of either new permanent or transient species. Thus, further changing the speciation.

Starting with Te/Te_2 in the gas phase both of these may undergo oxidation forming different oxides such as TeO and TeO_2 [58, 82]. For gaseous Te, a possible reaction with oxygen can be seen in Reactions 5 [83] and 6 (combustion in air [83]) for the formation of TeO and TeO_2 respectively.

$$Te + \frac{1}{2}O_2(g) \rightleftarrows TeO(g) \quad (5)$$

$$Te(s) + O_2(g) \rightleftarrows TeO_2(s) \quad (6)$$

Furthermore, at increased temperatures, the dissociation of Te_2 is enhanced. This is suggested [58, 84] to increase the TeO content as the equilibrium in Reaction 7 is shifted towards the right.

As well in the distribution diagram of tellurium under humid conditions shown in Figure 3 a) [84]

$$Te_2(g) + H_2O(g) \rightleftarrows TeO(g) + Te(g) + H_2(g) \tag{7}$$

Alternatively, the Te(g) could interact with water, forming tellurium hydroxides (e.g., TeOH or $Te(OH)_2$). This could occur as Reaction 8 shows [84].

$$Te(g) + H_2O(g) \rightleftarrows TeOH(g) + \frac{1}{2}H_2(g) \tag{8}$$

Specifically, studies [58, 83, 85, 86] have shown that the presence of steam at high temperatures will increase the volatility of TeO_2. One suggested explanation [58, 83, 85] for this is the formation of the transient species $TeO(OH)_2$, which could form as shown in Reaction 9. An alternative species could be $Te(OH)_2$, which is formed according to Reaction 10 [86]. Should either of these form, they would then be more volatile than the TeO_2 itself. This, has been experimentally observed [85] and thermodynamically supported [84].

$$TeO_2(g) + H_2O(g) \rightleftarrows TeO(OH)_2(g) \tag{9}$$

$$TeO_2(g) + H_2O(g) \rightleftarrows Te(OH)_2(g) + \frac{1}{2}O_2(g) \tag{10}$$

As indicated by Konings et al. [86] it is also a possibility that both $TeO(OH)_2$ and $Te(OH)_2$ exist concurrently. Based on thermodynamics calculations performed by Garisto [84], the distribution diagram of tellurium shows that including $TeO(OH)_2$ to the calculation shows it is possible that it can coexist with other oxides of tellurium, hence it may very well exist under oxidizing conditions with steam.

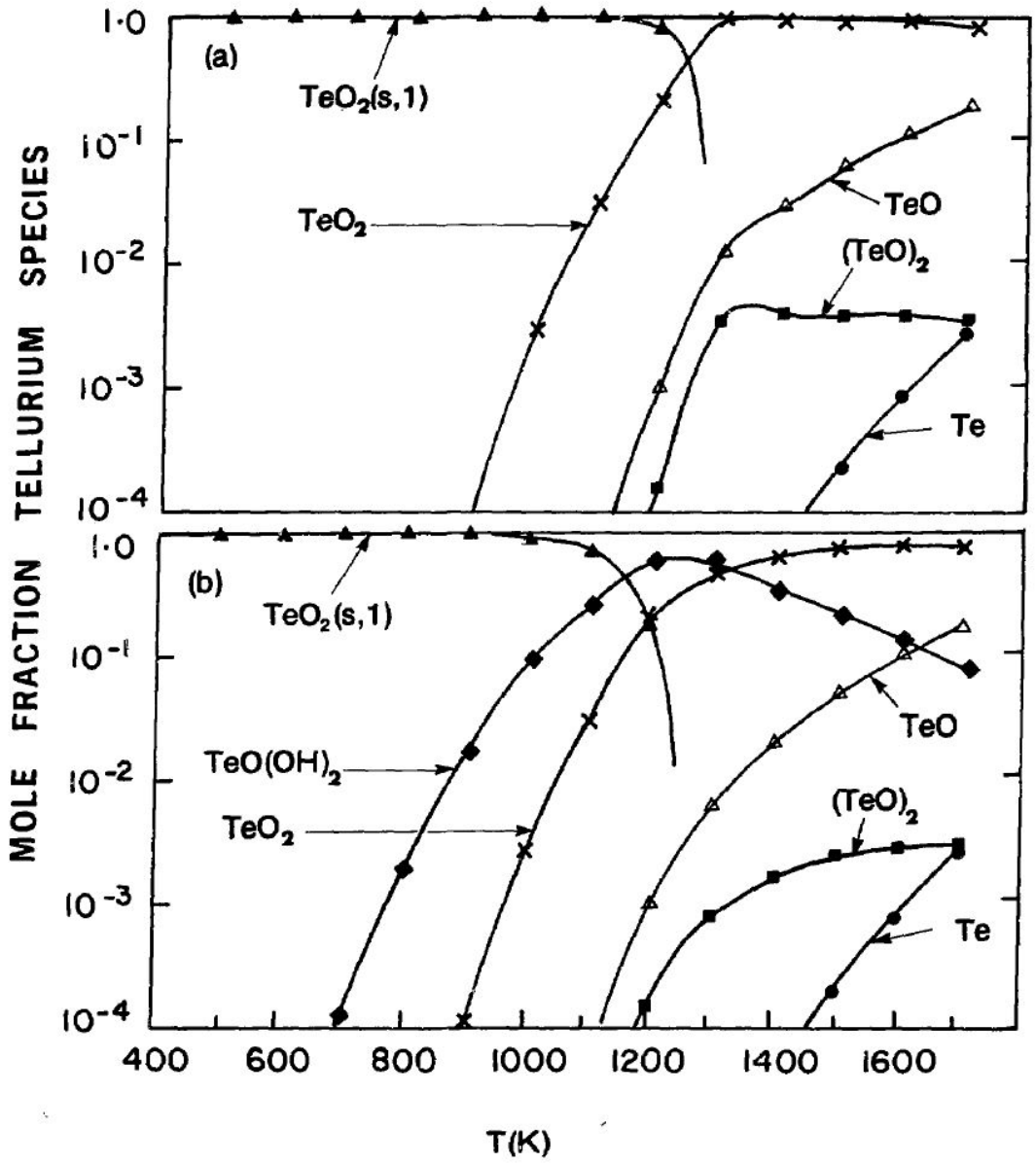

Figure 2. Distribution diagram of tellurium (0.02 mole), oxygen (0.5 mole), and steam (4 mole). Top image (a) lacking and bottom image (b) including the species $TeO(OH)_2$ in the database used. Source: "Thermodynamics of Iodine, Cesium and Tellurium in the Primary Heat Transport System Under Accident Conditions" [84].

Another tellurium species that may be affected by steam in the RCS is Cs_2Te. It is formed at high concentrations of cesium (i.e., cesium/iodine-ratio is larger than one) and possibly as shown in Reaction 11. This reaction is thermodynamically favorable at low pressures and/or when the partial pressure of hydrogen is high [58].

$$2CsOH(s,l) + H_2(g) + Te(s,l) \rightleftarrows Cs_2Te(s) + 2H_2O(g) \tag{11}$$

When Cs_2Te does interact with steam, both H_2Te and CsOH can form as shown by Reaction 12 [81].

$$Cs_2Te(g) + 2H_2O(g) \rightleftarrows H_2Te(g) + 2CsOH(g) \tag{12}$$

Alternatively, at steam pressures above 10^5 Pa of partial steam pressure interaction with steam may instead result in Reaction 13 occurring [72].

$$Cs_2Te(s) + 2H_2O(g) \rightleftarrows 2CsOH(g) + H_2(g) + \frac{1}{2}Te_2(g) \tag{13}$$

Another suggested reaction by Garisto [84] that is thermodynamically favored at 1.2 MPa (calculations was performed at this pressure) is shown in Reaction 14.

$$Cs_2Te(s) + 2H_2O(g) \rightleftarrows 2CsOH(s) + H_2(g) + Te(s) \tag{14}$$

As temperatures rise (above 1400-1600 K) or the conditions becomes sufficiently oxidizing, the Cs_2Te would dissociate [71]. However, not only is Cs_2Te possible but also other cesium-tellurium complexes may exist that could be altered by steam. One such possible species would be CsTe, which according to the literature [77] is formed between temperatures of 873 to 1073 K under steam atmosphere (hydrogen-steam ratio of 0.1). The interaction between steam and CsTe could occur as Reaction 15 shows [81].

$$2CsTe(g) + 2H_2O(g) \rightleftarrows Te_2(g) + 2CsOH(g) + H_2(g) \tag{15}$$

Consequently, the interaction between these two previously mentioned cesium tellurides and steam may both aid in the formation and dissociation of them depending on the prevailing conditions.

An observed connection between tellurium and cesium has not only been shown in calculations and bench-scale experiments but also in the context of nuclear accident research fission product programs (e.g., VERCORS, PHÉBUS). In the VERORCS experiments [6], it was seen that tellurium deposition coincided with that of cesium, hence indicating a possible correlation between them. However, no identification of any new species was attained. Furthermore, in the latter PHÉBUS program [14, 15] it was also seen that the tellurium did not behave as expected, i.e., by forming and depositing as SnTe. This observation was true for both FPT-0 (Fission Product Test) and FPT-1 [14], as well as the FPT-2 [15]. In the latter test, a possible explanation was that a cesium-tellurium species had formed instead of SnTe.

Moving on to the next tellurium species, H_2Te, this is most relevant under reducing conditions with steam [58, 71] at higher temperatures (above 500 K, according to existing distribution diagram [58] shown in Figure 3 b)). The H_2Te may form between hydrogen and tellurium as shown by Reaction 16 [58, 84].

$$H_2(g) + Te_2(g) \rightleftarrows H_2Te(g) + Te(g) \tag{16}$$

The amount of H_2Te would consequently depend on the ratio of hydrogen/tellurium, as an increasing ratio would result in a shift to the right in Reaction 16 [84]. If oxygen is available for interaction with H_2T, a reaction between these could occur, as shown in Reaction 17 above 423 K [81] or Reaction 18 [87].

$$2H_2Te(g) + O_2(g) \rightleftarrows Te_2(g) + 2H_2O(g) \tag{17}$$

$$H_2Te(g) + \frac{1}{2}O_2(g) \rightleftarrows Te(g) + H_2O(g) \tag{18}$$

Observing the distribution diagram established by Garisto [84], it is seen that for the investigated parameters, H_2Te will be present already at 500 K and start to decrease at roughly 1200 K. Alongside H_2Te, other tellurium species e.g., Te/Te_2 and TeO will also be present. The distribution diagram itself has been included as found in the literature [84] in Figure 3.

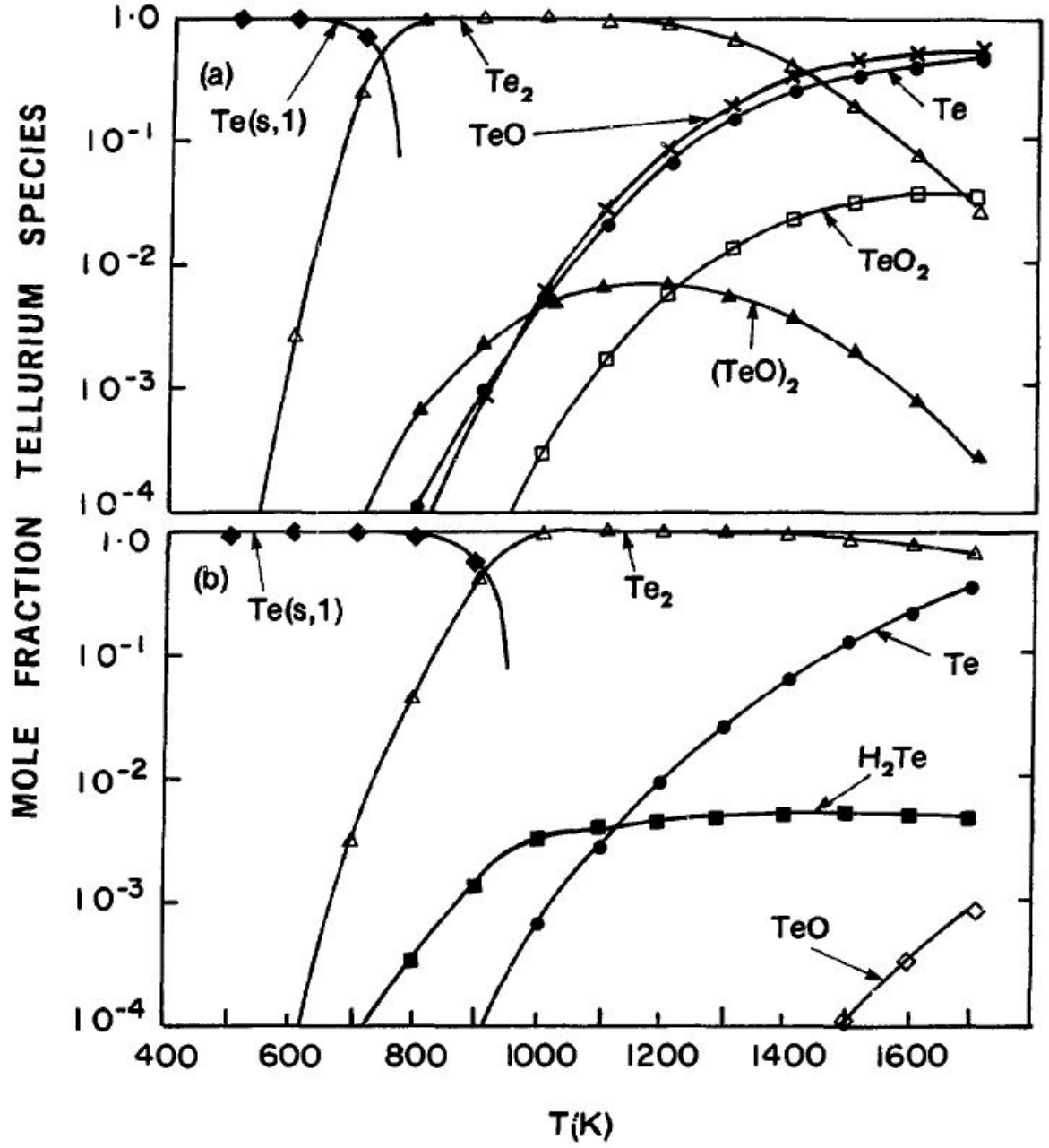

Figure 3. Distribution diagram of a) steam (0.533 moles) and tellurium (0.0002 moles) and b) steam (0.33 moles), hydrogen (0.17 moles), and tellurium (0.02 moles). Source: "Thermodynamics of Iodine, Cesium and Tellurium in the Primary Heat Transport System Under Accident Conditions" [84].

A summary of expected tellurium species under different conditions can be found in Table 6.

Table 6. A summary of possible tellurium species that have been mentioned in this thesis, that may exist in the gaseous phase under different accident conditions. Tin related compound have been excluded as they are not part of this work. At what temperature these are expected to exist, the distribution diagram can be consulted in Figures 2 and 3.

Accident conditions	No steam	With steam	With humid and cesium
Oxidizing	TeO, TeO_2, Te[a]	$TeO(OH)_2$/$Te(OH)_2$	Non
Inert	Te, Te_2	TeO[a], TeO_2[a]	Cs_2Te (below 1400 K), CsTe
Reducing	Te, Te_2	H_2Te, TeO[a]	Cs_2Te (below 1400 K), CsTe

[a] At high temperature.

Besides the changes that new conditions may induce, interactions with different surfaces in the RCS and other structural material (e.g., control rod material) may also affect the tellurium source term. Such investigations have been performed by Sallach et. al. [88], who studied the interaction of different surfaces with tellurium. Specifically, the surfaces investigated were 304 stainless steel and Inconel-600, both non-oxidized and pre-oxidized. Similarly, the control rod material silver was also investigated. It was found that all three of these materials interacted with tellurium vapor. For the 304 stainless steel and Inconel-600 lacking an oxide layer, tellurium reacted with iron and nickel, forming $Fe_{2.25}Te_2$ and $Ni_{2.86}Te_2$. However, when the oxide layer was present on the surfaces the formed compounds detected were $FeTe_2$ and $NiTe_2$. When a silver coupon was exposed to tellurium vapor a considerable coating of silver telluride was observed.

Another species investigated by Elrick and Ouellette [89] in steam was tin telluride. In this work, the metal surfaces investigated were 304 stainless steel, Inconel 600, silver, and nickel. Additionally, the effect of CsOH was also investigated. They observed that the tin telluride dissociated under the steam conditions. As it was observed separately on the metal surfaces and also that the tellurium reacted rapidly with the surfaces. When tin was present, it hindered the tellurium reaction with the nickel surface. For all other surfaces, tellurium was observed to interact with them. Finally, they did not observe any cesium telluride in their work.

3.1.4 Containment Enclosure Aspects of Tellurium

Once the corium has breached the reactor vessel or if a break occurs somewhere else in the RCS that allows the radionuclides to be released, the next physical barrier is the containment enclosure. The expected tellurium species to reach the containment enclosure are e.g. Te/Te_2, H_2Te, Cs_2Te, and SnTe [58, 90]. However, depending on the conditions in the preceding location, other species may also be relevant.

For those species that would reach the containment, the following factors have been suggested [58] to be of concern and potentially affect the speciation: fission products material from the RCS, aerosols made up of structural and control rod material from the core, air, steam, liquid water, complexation with organics, and concrete and metal surfaces. Of these factors, the metal surfaces found in the containment are the most relevant for the work presented in this thesis and thus some knowledge relevant for this work will be included. However, it could also be possible that the safety features (e.g., catalytic hydrogen recombiners or CSS) that are put in place to mitigate the effects of an accident can also alter the tellurium speciation.

Inside the containment, a wide range of surfaces are present that may have an effect on the different radionuclides entering the containment in addition to tellurium. In the Swedish BWR and PWR containments, both concrete and steel surfaces are mostly covered by epoxy paint. Besides the concrete surfaces, other relevant surfaces are those made from aluminum and zinc [16, 17, 18, 91] as well as surfaces covered by copper aerosols originating from copper cables [16]. Values from the nuclear power plants of Ringhals unit 2 (metals) and Forsmark unit 3 (paint) have been provided in Table 7.

Table 7. The areas of different surfaces found at Ringhals unit 2 (metals) and Forsmark unit 3 (paint).

	Area [m^2]	Location	Reference
Aluminum[b]	11 930	Sheets, fans	[16, 18]
Copper[b]	1 350	Bars and gratings[c]	[16, 18]
Paint[a]	6 340	Floors	[20]
Paint[a]	5 100	Walls	[20]
Zinc[b]	6 300	Floor gratings ventilation tubes	[16, 18]

Values of [a]Forsmark nuclear power plant unit 3 and from [b]Ringhals nuclear power plant unit 2; [c]Aerosol covered surfaces, assumed size of particles: 10 μm

Furthermore, possible species formed between the surfaces in Table 7 and tellurium can be found in Table 8. In the latter table data for other relevant tellurium species are included.

Table 8. Some different tellurium compounds relevant for containment chemistry and some corresponding relevant characteristics. The main source of data was "CRC Handbook of Chemistry and Physics" [53], when other sources were used it have been indicated.

Compund/Element	Color	MP [K]	BP [K]
Te	Gray-white	722.66	1261
TeO_2	White[a]/yellow[b]	1006	1518
TeO_3	Yellow-orange	703	
H_2Te		224	271
H_2TeO_3	White	313, dis.	
H_6TeO_6	White	409	
Te_3Cl_2 [92]	Silver-gray	511	
$TeCl_2$	Black eutectic	481	601
$TeCl_4$	White	497	660
Te_4Cl_16 [92]	Pale-yellow solid, maroon liquid	496	663
Al_2Te_3	Gray-black	$\approx$ 1168	
CuTe	Yellow	trans. $\approx$ 673	
Cu_2Te	Blue	1400	
$CuTeO_3$	Black, glassy		
SnTe	Gray	1079	
ZnTe	Red	1568	

MP: melting point; BP: boiling point; dis.: dissociation; trans.: transition;[a]Paratellurite; [b]Orthorhombic[92]

The use of CSS to remove radionuclides from the containment atmosphere may also alter their chemical speciation, more specifically, by the additives used in the spray solutions. Regarding tellurium in the literature, little research has been conducted on the removal efficiency of airborne tellurium. However, observations were made from the PHÉBUS experiments showing that removal of airborne tellurium species occurred primarily by gravitational settling and to some degree diffusiophoresis [93]. More recently, some work has been performed by Pasi et. al. [94] with tellurium in the containment sump. In this work, the complexity of the tellurium behavior in the containment sump due to added chemicals originating from the spray solution, as well as the γ-radiation, was shown. Thus, the solution used in the CSS may under certain conditions alter the tellurium speciation in the formed sump.

The main constituting parts of the solutions used in the CSS are a base (e.g., sodium hydroxide, trisodium phosphate), boric acid, and additional additives (e.g., sodium thiosulphate) [95]. These are used at concentrations that enhance the mitigation and dissociation of iodine species [96]. This is usually done by ensuring an alkaline containment sump solution at a pH around 9.3 [96]. In the formed containment sump, more material may be present, such as debris materials and possible corrosion products. This, provides a pathway for

4 Experimental

The following chapters are intended to provide an overview of the different facilities used during all the experimental work. Following these methods, the analytical equipment used are presented.

4.1 Seawater-Tellurium Experiments

To evaluate the effects of seawater on tellurium, triplicates of different mixtures (1:4, 1:1, and 4:1; weight basis) containing tellurium (99.8%, 200 mesh, Sigma Aldric) and sodium chloride (99.5%, Acros Organics) were made. These mixtures were then placed in individual alumina pans (TA instrument) and heated separately under either oxidizing (synthetic air: 79%/21% nitrogen/oxygen, AGA) or inert (99.98%, in-house nitrogen gas) conditions using a TGA (TGAQ500, TA Instrument). The experiments were all carried out by heating (5 K/min) from ambient temperature to isothermal temperature (1173 K). This temperature was then maintained for 20 min. Following the isothermal temperature, the system was left to cool to ambient temperature. Two reference samples were also heated containing only one of the constituting parts of the mixtures.

Additionally, a high-temperature furnace was also used to investigate the 1:1 mixture of tellurium and iodine under oxidizing conditions. The aim was to obtain a visual observation of the sample after being heated to several different temperatures. An overview of the setup used can be seen in Figure 4. However, neither the filter nor the atomizer was used in these experiments.

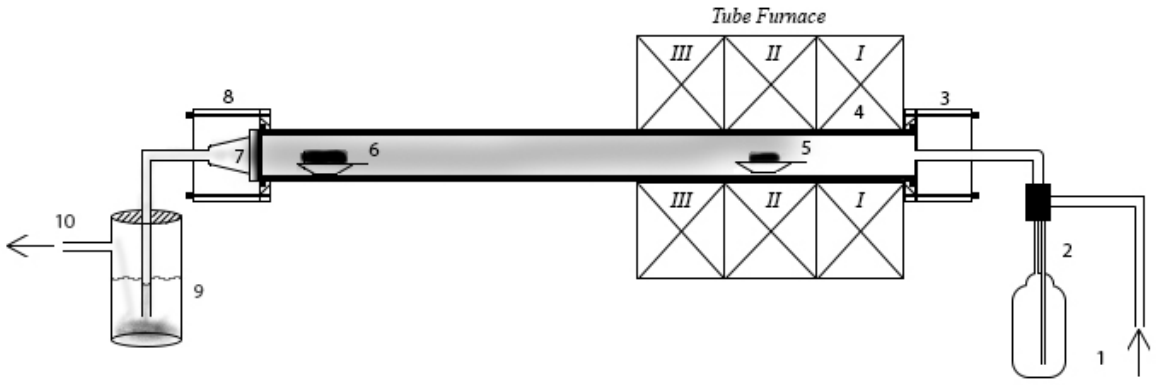

Figure 4. The experimental schematics: (1) gas inlet, (2) atomizer, (3) inlet, (4) Al_2O_3-tube, (5) the precursor location,(6) the metallic coupon, (7) cone-formed outlet, (8) connector, (9) a sodium hydroxide solution trap and a water trap, and (10) the gas outlet.

Using a tube furnace (ETF 30-50-18-S, Entech), the mixture was heated (10 K/min) in a crucible (Boat, Porcelain 85x13x8 mm, VWR) to the isothermal temperature (1073 K, maintained for 20 min), which was located inside an aluminum tube (Al_2O_3, 99.7%, Degussit AL23, Aliaxis). The total weight of each sample mixture was 2 g, using the same supplier and quality as for the TGA part of both tellurium and sodium chloride. To establish the oxidizing conditions, a flow (1.5 l/min, Aalborg gas regulator) of compressed air was used. The isothermal temperatures

investigated were: 473 K, 573 K, 623 K, 673 K, 723 K, 773 K, 823 K, 873 K, 923 K, 973 K, 1023 K, and 1073 K. Once the experiment was done, the system was left to cool with the gas flow on.

4.2 Reactor Coolant System Experiment

To investigate the behavior of tellurium in the RCS, as well as any effect caused by cesium iodide, a dual furnace setup was used. Excluding the additional furnace, the facility used was the "VTT fission product transport facility". The main details of this facility can be found elsewhere [97, 98]. However, a schematic overview can be seen in Figure 5.

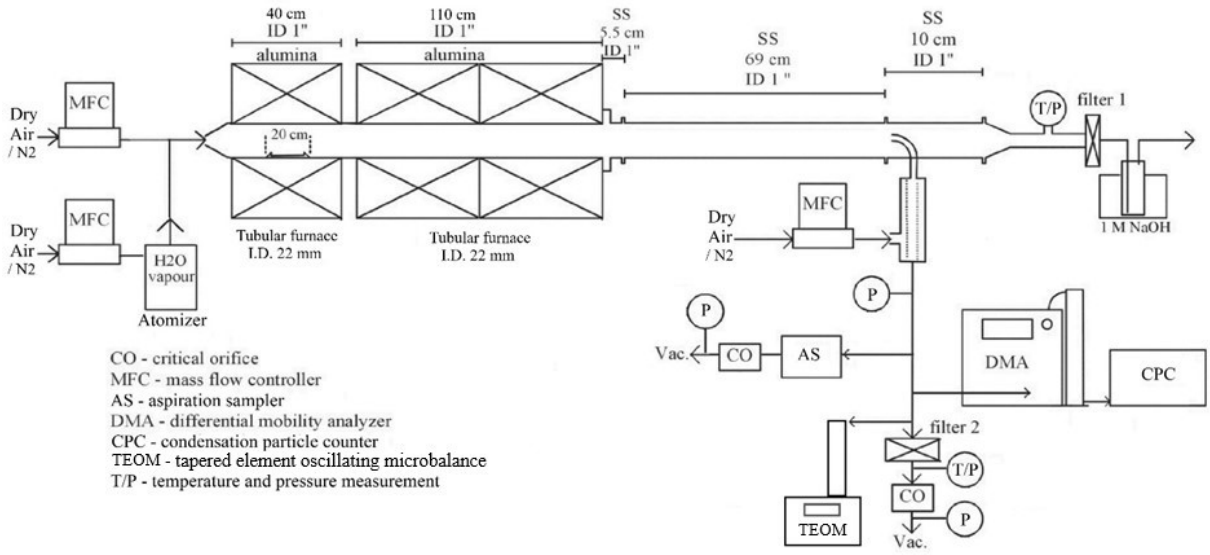

Figure 5. Schematics of the experimental facility for tellurium transport studies [97, 98].

Briefly, two furnaces were used, one of which was the main reaction furnace (Entech, ETF20/18-II-L), with a smaller one (Entech/Vecstar, VCTF 3) located upstream to vaporize the tellurium precursor (approximately 1 g, 99.5%, Sigma Aldrich). Through both furnaces, an aluminum tube (Al_2O_3, 99.7%) with an inner diameter of 22 mm was located in which the experiments were carried out. At the end of the reaction furnace, a stainless steel tube was attached to the aluminum tube to transport the outgoing gas (temperature decreased to ca. 300 K) to either an online measuring device (1/5 of the flow) or a plane polytetrafluoroethylene (PTFE) filter followed by two sodium hydroxide liquid traps (0.1 M) (4/5 of the flow). Towards the end of each experiment, sampling of the gas phase aerosols was done using perforated carbon-coated nickel grid (400 mesh) with the aspiration sampler. Two conditions corresponding to oxidizing and inert were investigated, both without and with humidity. Additionally, one extra run with cesium iodide added to the humid conditions was also performed. The flow through the system was 5 l/min (measured with a Thermal Mass Flowmeter TSI 3063, TSI Incorp). In the two experiments involving humidity and/or cesium iodide (99.999%, Sigma-Aldrich) an atomizer (TSI 3076) was used, which was filled with either only water (Milli-Q, ultrapure water) or cesium iodide (0.15 M) dissolved in water (Milli-Q, Ultrapure water). The outgoing gas from the atomizer was channeled through a heated line (390 K) before entering the smaller furnace.

All experiments were carried out in the same way. First, the reaction furnace was heated (10 K/min) to the isothermal temperature (1500 K). Once the temperature was reached, the tellurium precursor located inside an alumina crucible was positioned inside the small furnace. Heating (10 K/min) was then started off the small furnace to the set-point temperature (810 K). Concurrently, a nitrogen gas flow (0.5 l/min) was maintained until reaching the temperature set-point of the small furnace and then stopped. Following this, the main gas corresponding to the investigated experimental condition was started. An overview of the experiments can be found in Table 9.

Table 9. Experimental matrix for the reactor coolant system.

Experiment	Condition	Temperature[a] [K]	Humidity [ppmV]	Cesium iodide solution [M]
RCS-1	Oxidizing	1500	Dry	
RCS-2	Oxidizing	1500	$2.1 \cdot 10^4$	
RCS-3	Oxidizing	1500	$2.1 \cdot 10^4$	0.15
RCS-4	Inert	1500	Dry	
RCS-5	Inert	1500	$2.1 \cdot 10^4$	
RCS-6	Inert	1500	$2.1 \cdot 10^4$	0.15

*Inside the reaction furnace

4.3 Containment Experiments

To evaluate the behavior of tellurium and reaction with or deposition on surfaces in a BWR containment, a single furnace (ETF 30-50-18-8, Entech) setup was used. Positioned inside the furnace was the tellurium (1 g, 99.8%, 200 mesh, Sigma Aldrich) precursor in either a porcelain (boat, porcelain 85x13x8 mm, VWR) or alumina (Al_2O_3-material) crucible. The latter was used only during reducing conditions, due to heavy corrosion of the porcelain crucible under reducing conditions. Using a sufficiently long (130 cm) alumina tube (Al_2O_3, 99.7%, Degussit AL23, Aliaxis), which extended far enough out from the furnace to ensure room temperature at the end of it. At this location and temperature, three metal surfaces representing parts of a BWR containment were located. These metals consisted of copper, zinc, and aluminum (positioned in a row in the mentioned) and were cut from a copper sheet (thickness: 3 mm, 99.5% Alfa Aesar), a zinc rod (⊘: 13 mm, 99.5% Alfa Aesar), and an alumina rod (⊘: 19 mm, 99.5% Alfa Aesar). Following the metal coupons, a filter and a sodium hydroxide (≥ 97%, Sigma Aldrich) liquid trap (0.1 M, 250 ml) was located. In subsection 4.1 a schematic of the system used can be found in Figure 4.

During the containment experiments, three different conditions (oxidizing, inert, and reducing) both dry and humid were investigated. In the case of humid experiments, an atomizer was located before the furnace and filled with water (500 ml, Millipore 18 MΩ). To establish the different conditions and transport the volatilized precursor, three carrier gases were used: compressed air (oxidizing, Porter gas regulator), argon (inert, 99.999%, Air liquid, Aalborg gas regulator), and argon with 5% hydrogen (reducing, Air liquid, Aalborg gas regulator). An overview of these experiments with some of the parameters used can be found in Table 10.

Table 10. Overview of the containment experiments. The relative humidity (RH) determined at the outlet with the furnace heated to 1273°C and a temperature of 300°C at the measuring location, using a Fisherbrand™Traceable™humidity meter.

Experiment	Atmosphere	Gas type	RH [%]	Surfaces
C-1	Oxidizing	Compressed air	0.1	Cu, Zn, Al
C-2	Oxidizing	Compressed air	99	Cu, Zn, Al
C-3	Inert	Argon	0.1	Cu, Zn, Al
C-4	Inert	Argon	99	Cu, Zn, Al
C-5	Reducing	Argon with 5% hydrogen	0.1	Cu, Zn, Al
C-6	Reducing	Argon with 5% hydrogen	99	Cu, Zn, Al

Once the tellurium precursor and the surfaces were in position, a nitrogen (in-house gas [2] flow was maintained under the initial heating phase (to 673 K, 10 K/min) to establish pre-accident conditions. After this phase, the gas was stopped and heating (10 K/min) continued until isothermal temperature (1273 K) was reached. At this temperature, and after a ten-minute delay (ensuring a stable temperature), the experimental gas was initiated (1-2 l/min[3]) and maintained for fifty minutes. Furthermore, reference experiments without tellurium were carried out under all conditions to determine if the atmosphere itself had any effect on the metal coupons.

4.4 Containment Spray Experiments

To determine the efficiency at which the CSS removes the tellurium from the gas phase of the containment, the ”VTT spray chamber” experimental setup was used. This consisted of a single furnace (Entech/Vecstar, VCTF 3) with a stainless-steel tube (AISI 316L) inside it, which was then connected to a cylindrical chamber with a spray nozzle (Lechler, 136.330.xx.16, ⊘ of 60 mm and ⊘ 120 mm at the distances of 150 mm and 300 m from the nozzle) in the upper part with walls covered by Teflon. The chamber was used to simulate a containment with a CSS. From the nozzle, droplets (ca. 10 μm) made of the different solutions investigated were generated and the feed rate of the droplets was controlled using pressurized (ca. 300 kPa) air or nitrogen. On the bottom of the spray chamber, the collected droplets accumulated and formed the ”sump”. The temperature inside the containment was 293 K. An overview of the setup is shown in Figure 6.

[2] According to responsible personnel, 99.9% purity. However, this was not certified nor verified.

[3] Slightly lower under humid conditions, due to the atomizer.

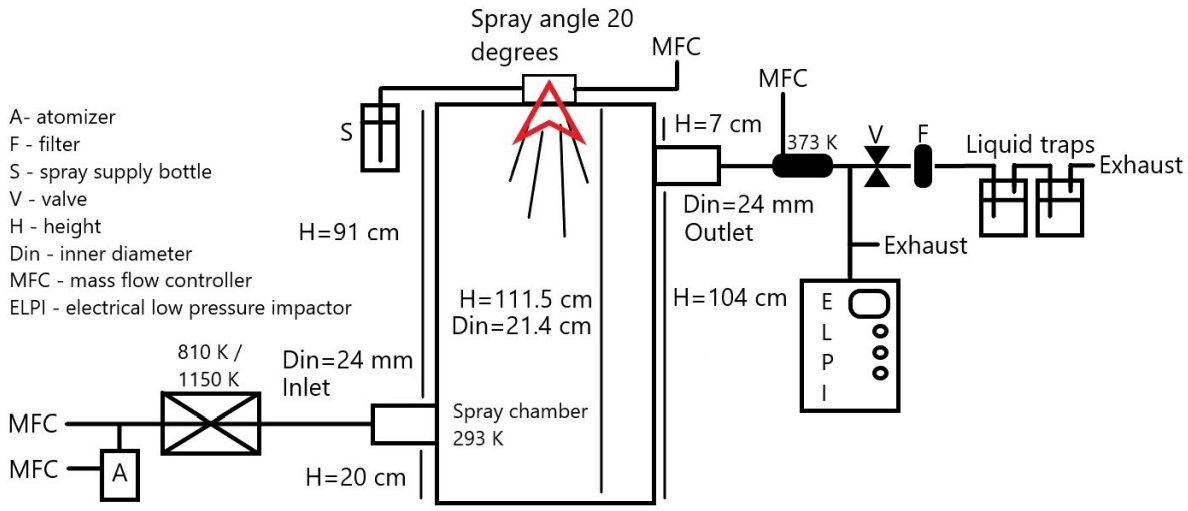

Figure 6. Schematics of the experimental facility for tellurium spray experiments. Source is paper IV.

Two types of precursors were investigated, corresponding to metallic tellurium (99.5% purity, supplied by Sigma Aldrich) and tellurium dioxide (≥ 97% purity, supplied by Sigma Aldrich). Of these, 1 g of the metallic tellurium and 1.2 g tellurium dioxide (corresponds to 1 g of pure tellurium) were individually heated to 810 K and 1150 K, respectively. Furthermore, two conditions (oxidizing and inert) were investigated for metallic tellurium and one condition (oxidizing) for the tellurium dioxide (as it is unlikely to form under inert conditions). Additionally, both humidity and humidity with added cesium iodide was also investigated. To establish the different conditions of oxidizing (air) and inert (nitrogen), a gas flow of 5 l/min was injected into the furnace once the isothermal temperature had been established. However, when humidity or humidity with added cesium iodide were investigated, an atomizer (TSI 3076) was located before the small furnace, filled with either water (Milli-Q, ultrapure water) or cesium iodide (99.999%, Sigma-Aldrich) solution (0.15 M). Through the atomizer a partial flow of 2.5 l/min was directed. This outgoing flow was then mixed with 2.5 l/min of the same gas type as the one injected into the atomizer. The total flow injected into the furnace then became 5 l/min. Additionally, the outgoing gas from the atomizer was channeled through a heated line (390 K) before mixing and entering the furnace. Passing through the furnace and reaching the containment chamber, the temperature of the gas had dropped to 293 K. Following the furnace, the flow was separated into two flows one going to online measurements and a filter followed by two sodium hydroxide (≥ 97%, Sigma Aldrich) liquid traps (0.1 M). The spray solutions investigated were water, alkaline borate solution (0.23 M H_3BO_3, 0.15 M NaOH), and alkaline borate solution with sodium thiosulphate (0.23 M H_3BO_3, 0.15 M NaOH, 0.064 M $Na_2S_2O_3$) [99, 100]. Additionally, one run without any spray solution was performed to represent a reference. An experimental matrix can be seen showing all experiments performed in this part in Table 11.

Table 11. The experimental overview matrix with the main parameters of the containment spray experiments.

Experiment	Spray solution	Precursor	Condition	Additive	Furnace temperature [K]
D-1	Non Water ABS w/o ABS w	TeO_2	Oxidizing	Non	1150
D-2	Non Water ABS w/o ABS w	TeO_2	Oxidizing	Humidity	1150
D-3	Non Water ABS w/o ABS w	TeO_2	Oxidizing	Humidity with CsI	1150
D-4	Non Water ABS w/o ABS w	Te	Oxidizing	Non	810
D-5	Non Water ABS w/o ABS w	Te	Oxidizing	Humidity	810
D-6	Non Water ABS w/o ABS w	Te	Oxidizing	Humidity with CsI	810
D-7	Non Water ABS w/o ABS w	Te	Inert	Non	810
D-8	Non Water ABS w/o ABS w	Te	Inert	Humidity	810
D-9	Non Water ABS w/o ABS w	Te	Inert	Humidity with CsI	810

ABS: Alkaline borate solution; w/o: without; w: with

4.5 Analytical Methods

Several analytical methods were used to investigate the samples acquired from the different experiments. The following sections contain the different methods and a short description of each.

4.5.1 Quantification - Morphology, Elemental, Speciation

To determine the morphology and elemental composition, two different scanning electron microscopes (SEM) and a transmission electron microscopy (TEM) were used, which depended on what facility was utilized. The work performed at Chalmers (i.e., Containment Experiments), a Phenom ProX (Thermo Fisher Scientific, Phenom-World B.V.) SEM with Phenom ProSuite (Thermo Fisher Scientific, Phenom-World B.V.) software and an Element Identification module at 15 kV was used. For the work that was done at VTT (i.e., Reactor Coolant System Experiments), both an SEM with energy-dispersive X-ray spectroscopy (EDX) and TEM were used. This SEM was a Zeiss Crossbeam 540 with EDX using a silicon drift detector (SDD, EDAX 30 cm^2 Octane Elite™) and the SEM was operated at 2-3 kV with a probe current of 100-200 pA. The EDX collected the spectra using 8-10 kV high voltage. Finally, the TEM used was a TALOS™F200X (S)TEM with a 200 kV field emission.

X-ray diffraction (XRD) spectroscopy (Siemens Diffraktometer D5000, CuK-α characteristic radiation wavelength) was used to determine the crystal structure of different samples. The glancing angle XRD approach, as described by B.A. van Brussel and J.Th.M. De Hosson [101], and a coupled beam-detector analysis was used. The advantage of the former is that thinner deposits become clearer in contrast to the underlying bulk material. This methods was only used for the work when the deposits formed on the metal surfaces were investigated (i.e., from Containment Experiments). The coupled approach was mainly used for the filters (i.e., from Containment Experiments). The peaks in the diffractograms were identified using the software (DIFFRAC.SUITE EVA, Bruker AXS version 4.1.1) and database (The International Centre for Diffraction Data, PDF-4+2019 RDB) used in conjunction with the XRD.

For the XRD analysis of the Containment Experiments, the angle used for each sample was adjusted individually (due to manual leveling of the surface level in relation to the X-ray beam). Therefore, the angled used for the different samples are not known relative to the surface of the different objects. Still, for the metal surfaces (i.e., from the experiments referred to as C-1, C-2, C-3, C-4, C-5, and C-6 in Table 10) two angles relative to the sample placeholder (5° and 1°) were chosen, based on trial and error. The one resulting in the clearest diffraction peaks was included. During the analyzes, the sample placeholder was rotating (360°/min) and the detector itself was moving from 10° to 90°.

These XRD-diffractograms were processed post-analysis by reducing the intensity of the whole diffractogram (when deemed needed) and processing according to the ”Chromatogram baseline estimation and denoising using sparsity (BEADS)”-method [102] using the code [103]. None of the diffractograms were altered to the point that any distinct diffraction peak disappeared.

The chemical speciation of the aerosols collected on the filters was determined using a PHI 5000 X-ray photoelectron spectrometer (XPS). This was equipped with a monochromatic AlKα-source (E_{photon}=1486.8 eV), generating the X-rays. All analysis used the binding energy spectra

of Au-$4f_{7/2}$ (83.96 eV), Ag-$3d_{5/2}$ (368.21 eV) and Cu-$2p_{3/2}$ (932.62 eV) for alignment. To enable analysis, a small part of each filter used in the Reactor Coolant System Experiment was cut away. These parts were analyzed, both with a survey scan (1 eV/step in the range 0-1300 eV) using a passing energy of 280 eV and selected ranges (0.1 eV/step) using a passing energy of 26 eV (all performed in the same location). The choice of the selected ranges was chosen to correspond to the following elements: Te-$3d_{5/2}$, O-1s, Cs-$3d_{5/2}$, and I-$3d_{5/2}$, The one chosen depended on what was relevant for each sample. Alongside these, the carbon peak (C1s) was used as an internal standard. Furthermore, the identification was done by the fitting of the curves using the PHI Multipak software (V.9.7.0.1. 2016, Ulvac-Phi inc.).

The reference values needed for the XPS evaluation have been provided in Table 12.

Table 12. Different tellurium related compounds and corresponding binding energies of these.

Te-$3d_{5/2}$	Binding energy [eV]	Reference	Cs-$3d_{5/2}$	Binding energy [eV]	Reference
Te-metal	573.1 (± 0.2)	[104]	Cs	726.0 (± 0.2)	[105]
Te	572.9 (± 0.2)	[106]	Cs	726.3 (± 0.2)	[107]
Te	572.95	[108]	Cs_2O	725.1 (± 0.5)	[107]
TeO_2	576.1 (± 0.2)	[104]	CsI	724.1 (± 0.2)	[109]
TeO_2	576.21 (± 0.1)	[110]	CsOH	724.5	[111]
TeO_2	575.8	[112]	$Cs_{0.78}Te$	724.57	[113]
TeO_3	577.3 (± 0.2)	[104]	$Cs_{0.90}Te$	724.62	[113]
TeO_3	576.8 (± 0.2)	[106]	$Cs_{2.4}Te$	726.36	[113]
$Te(OH)_6$	576.7 (± 0.2)	[104]	$Cs_{2.60}Te+Te^o$	726.33	[113]
TeI_4	575.9 (± 0.2)	[104]	$Cs_{2.69}Te+Te^o$	726.28	[113]
∅TeI_3	575.4 (± 0.2)	[104]			
∅TeI_2	575.0 (± 0.2)	[104]	I-$3d_{5/2}$		
∅Te_2	583.9 (± 0.2)	[104]	I_2	619.09	[114]
$Cs_{0.78}Te$	572.53	[113]	CsI	618.45, 619.65	[114]
$Cs_{0.90}Te$	572.47	[113]	I_2O_5	623.3	[114]
$Cs_{2.4}Te$	572.72	[113]			
$Cs_{2.60}Te+Te^o$	572.48, 574.25	[113]	O 1s		
$Cs_{2.69}Te+Te^o$	572.27, 574.30	[113]	TeO_2	530.6	[112]

4.5.2 Quantification - Amounts on Filters and Traps, Online Monitoring during Experiments

To determine the amounts of the different elements in the sodium hydroxide liquid traps used in the different experiments, an inductively coupled plasma mass spectrometer (ICP-MS) was used. The type was a Thermo Scientific ™iCap Q ICP-MS. All the samples were treated in the same way, by dilution using nitric acid (0.5 M, ultra-pure HNO_3, Sigma Aldrich) with a rhodium internal standard (10 μg/l, element standard for atomic spectroscopy 1000 ±5 mg/ml, 20°C, Spectrascan). Depending on what was sought after in the trap, relevant elements were used in the standards (the same quality as the rhodium). The evaluation of the data was performed using Qtegra™Intelligent Scientific data solution (v.2.21465.44).

To quantify the amounts of the different elements in the different samples produced (only from Reactor Coolant System Experiments), instrumental neutron activation analysis (INAA) was

used. Two types of samples were investigated; filter and aliquot of the sodium hydroxide liquid traps. Each type of sample was investigated to determine the amount of cesium, iodine, and tellurium. The pre-analysis preparation was performed for the filter by folding and pressing. The liquid aliquot samples (volume: 100 μl) were added to a Whatman 1 cellulose chromatography disc-shaped paper that was then dried (320 K, heating bulb), and both types of samples were heat-sealed inside polyethylene (PE) capsules (0.15 mm thick). Additionally, calibrators were used made from tellurium (99.9%, Merck) in diluted HNO_3. These were made using 50 μl of the dissolved tellurium, which was then prepared in the same way as the aforementioned liquid samples. Similarly, both cesium and iodine calibrators were also prepared from solutions with certified concentrations (Analytika, Ltd., Czech Republic). The three different calibrators contained 14.7 ± 0.15 μg, 2.01 ± 0.02 μg, or 103.0 ± 0.5 μg of cesium, iodine, and tellurium, respectively.

The samples were irradiated using the experimental reactor LVR-15 at Řež (Research Centre Řež, Ltd., Czech Republic) to produce the neutrons required for the INAA. Two types of irradiation were used, a short-term (1 min) and a long-term (2.5 h), to acquire the content of iodine and tellurium (short-term) as well as cesium (long-term). Different types of encapsulations were needed for the two types of irradiation as well as different containers for transportation to the irradiation location inside the reactor. The details of these are presented elsewhere [115]. Once the samples reached the locations for the irradiation, they were exposed to thermal, epithermal, and fast neutron fluence rates of $2.9{\cdot}10^{13}$ $cm^{-2}{\cdot}s^{-1}$, $1.0{\cdot}10^{13}$ $cm^{-2}{\cdot}s^{-1}$, and $1.0{\cdot}10^{13}$ $cm^{-2}{\cdot}s^{-1}$ respectively. The samples used for the long-term irradiation were the same as the ones used during the short-term irradiation after sufficient decay.

Following the short-term irradiation and a 10 min decay time, the samples and calibrators were counted for 10 min to determine the amounts of tellurium (^{131}Te, $t_{1/2}$ = 25.0 min, γ-line 159.0 keV [116]), and iodine (^{128}I, $t_{1/2}$ = 24.99 min, γ-line 442.9 keV [116]). This, using a coaxial high purity germanium (HPGe) detector (Princeton Gamma-Tech) with a 20.3% relative efficiency and a full width at half maximum (FWHM) resolution of 1.75 keV (for both the photons at 1332.5 keV of ^{60}Co). A Canberra Genie 2000 gamma-ray spectrometer was connected to the detector with associated linear electronics to acquire the data.

For the long-term irradiation, as previously mentioned, the samples used were the same as for the short-term irradiation. Therefore, these samples were left to sufficiently decay after the short-term irradiation and were then rewrapped before the next irradiation. After irradiation, the samples were left to decay for 6-7 days, which was followed by a counting time of 40-60 min. The main focus was to determine the cesium (^{134}Cs $t_{1/2}$=2.065 y, γ-lines 604.7 keV, and 795.9 keV [116]) amount in the different samples, but the content of tellurium was determined as well. However, this determination was redundant for this work, as the short-term was enough to determine the tellurium content. Thus, the former of these mentioned result is presented elsewhere [115]. The counting of cesium was performed using a Canberra Genie 2000 gamma-ray spectrometer using a Canberra HPGe-detector with a relative efficiency of 77.8% and an FWHM resolution of 1.87 keV at 1332.5 keV.

A special feature of the facility at VTT was the possibility to measure aerosols online during the experiments (for the Reactor Coolant System Experiments) performed there. Two characteristics were determined, the total mass concentration and the size distribution. The former was monitored using a Tapered Element Oscillating Microbalance (TEOM, Rupprecht Patashnick Co., Inc. Series 1400A), which was used with a 10 s time resolution and a sampling-flow rate

of 1.07 ± 0.01 l/min. Entering the TEOM, the particles were collected in a replaceable filter. To reduce the effect by condensation of water on the result, the inlet line, sampling flow, and filter were heated (300 K). The software used to monitor the measurements and the functionality of the instrument was ROComm software version 2.1.0. The size distribution was determined using a combination of a differential mobility analyzer (DMA, TSI 3080/3081) and a condensation particle counter (CPC, TSI 3775, counting efficiency $\geq$ 96%) using a time resolution of 3 min and a flow rate of 0.3 ± 0.01 l/min of the particle sizes was done according to their electrical mobility and counting was according to the determined size classes by the DMA and the CPS, respectively. For spherical particles, the electrical mobility diameter was equal to the geometric diameter [117]. A pre-impactor was located at the inlet of the DMA, to remove particles larger than 615 nm. The size range measured was from 15 to 670 nm (64 size channels per decade). The software used to control the measuring system was Aerosol Instrument Manager software version 9.0 (TSI).

5 Results and Discussion

The results of the work presented herein are kept together according to the experiment in which the results were obtained in (i.e., one chapter for each paper).

5.1 Seawater-Tellurium Experiment

The outcome of the TGA analysis performed under inert and oxidizing conditions was performed with three different mixture ratios of tellurium and sodium chloride as well as two references with only one of each part. Using the values obtained, the average weight values using the three replicates were calculated and normalized towards the first average value. The results are presented in Figure 7 for the inert conditions and Figure 8 contains the results of the oxidizing conditions. To differentiate the results, different colors and symbols have been assigned to the different ratios investigated (S1 red pluses, S2 pink stars, and S3 black boxes) and references (Ref1 green crosses and Ref2 blue diamonds).

5.1.1 Inert Conditions

For all samples under inert conditions, two distinct different mass loss phases were observed from the TGA results. Both of these phases for all samples started at roughly the same temperatures, 690-710 K for the first mass loss phase and 920-1080 for the second mass loss phase. The TGA results are provided in Figure 7. Observing the pure tellurium reference (Reference 1), similar mass loss phases were observed. However, the pure sodium chloride reference (Reference 2) had only one mass loss phase, which started at roughly 1000 K.

By observing the behavior of the samples during heating, seemingly a higher ratio of tellurium resulted in a longer first mass loss phase. Once the first mass loss phase stopped, the gradient slowed down significantly. The degree that this occurred to, seemingly depended on the fraction of the tellurium in the sample, as more of it resulted in a lower remaining total mass. The second mass loss phase start varied slightly between the different samples, as well as how the gradient of mass loss evolved. Following the second mass loss phase, the experiment continued until the end, ending at normalized masses of 7.6%, 12%, and 2.5% for samples 1, 2, and 3 as well as 5% and close to zero for Reference 1 and Reference 2, respectively. A summary of when the mass losses occurred and at what temperatures can be seen in Table 13.

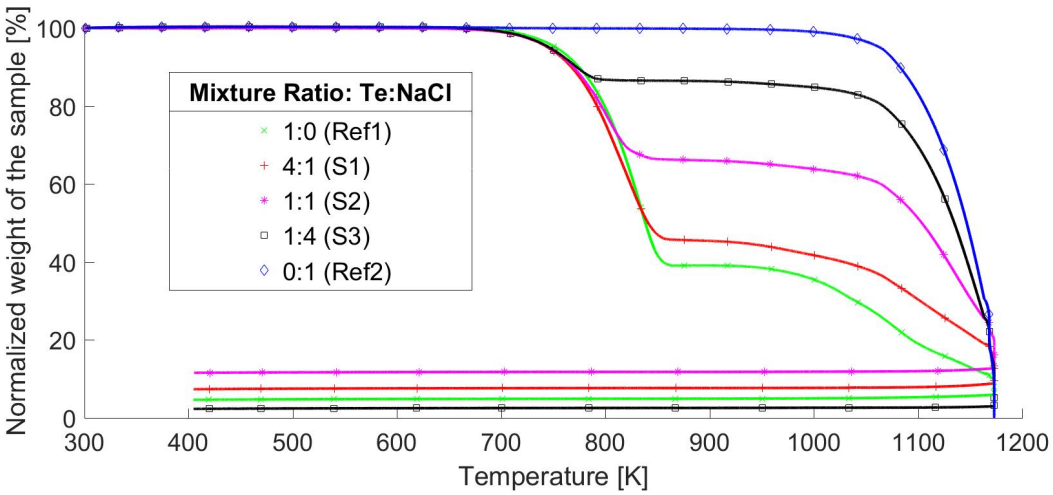

Figure 7. Thermogravimetric analysis results for the different Te:NaCl-ratios (weight basis) heated in inert conditions. The different lines represent the average of three replicates of 1:0 (Ref1, green crosses), 4:1 (S1, red pluses), 1:1 (S2, pink stars), 1:4 (S3, black boxes), and 0:1 (Ref2, blue diamonds) of tellurium and sodium chloride respectively. All weights have been normalized towards the first measured weight (8-9 mg) by thermogravimetric analysis. The measuring interval was one second.

Comparing the different sample ratios to that of the pure tellurium reference, the temperature for when the different mass loss phases occur are similar. Thus, it is reasonable that similar volatilization of species is occurring, as the initial behavior is very similar. The first mass loss also starts close to the melting point of tellurium (722 K [53]) and thus a phase change is occurring for tellurium. Based on the literature, it is likely that the species leaving is Te_2 or possibly Te [71]. Furthermore, after the first mass loss phase the weights of the different sample levels out at different values. This difference is reasonable as the leveling out increases with the content of sodium chloride and is, hence correlated to it. Regarding the second mass loss of the samples, this starts roughly at the melting point of sodium chloride (1074 K [92]) and thus most likely is correlated to it. Similarly, at the same temperatures the pure sodium chloride reference is also seen to experience a mass loss, which also supports this idea. Considering the tellurium part of the sample, it would also be volatilized at these temperatures as the pure tellurium reference is also loosing mass. However, little evidence can be seen that sodium chloride affected the tellurium from this data.

Table 13. The start and end of the different mass loss phases, as well as the final normalized mass for the samples and references under inert conditions. The samples corresponded to ratios of 1:4 (Sample 1), 1:1 (Sample 2), 4:1 (Sample 3) of tellurium and sodium chloride. The reference consisted of either pure tellurium (Reference 1) or sodium chloride (Reference 2).

	Temperature range First Mass Loss [K]	Temperature range Second Mass Loss [K]	Final Normalized Mass [$\%_{wt}$]
Reference 1	690-870	920-end	≈ 5
Reference 2	1000-end	-	≈ 0
Sample 1	620-865	925-end	≈ 8
Sample 2	680-850	920-end	≈ 12
Sample 3	670-805	920-end	≈ 3

Based on the similarities observed in Figure 7 between the different samples, it can be concluded

that little occurred between tellurium and sodium chloride under inert conditions inside the pan. This is also supported by the observation that the main constituting part of the sample dictated the behavior of the mixture. However, these observations do not exclude a gas phase interaction between the two compounds, or a potentially very rapid interaction at high temperatures, as this would not be apparent in the TGA results.

5.1.2 Oxidizing Conditions

The TGA experiment under oxidizing conditions also clearly indicates two distinct different mass loss phases. However, the mass loss never completely stops, and minor releases occur between the two main mass loss phases. The beginning of the two main mass loss phases for all samples were at temperatures of 690-710 K and 1000-1030 K for the first and second phases, respectively. At a higher fraction of tellurium, the final normalized mass was decreasingly lower and the time between the two mass loss phases were shorter. Comparing these to the references, noticeable differences can be observed. Both samples and references are shown in Figure 8. The pure sodium chloride reference (Reference 2) had only one mass loss phase (similar to the inert conditions reference) at circa 1000 K. Compared with the pure tellurium reference (Reference 1), it had two main mass loss phases. That had between them a mass increase phase occurring, which was not observable at all for any of the samples. Similar to the samples, the first mass loss phase started roughly at similar temperatures (around 700 K), whereas the second mass loss phase started earlier then the samples at roughly 900 K. At the end of the experiments, the normalized mass reached levels of 14%, 18%, and 8% for samples 1, 2, and 3 as well as 30% and close to zero for Reference 1 and Reference 2, respectively. A summary of when the mass losses occurred and at what temperatures can be found in Table 14.

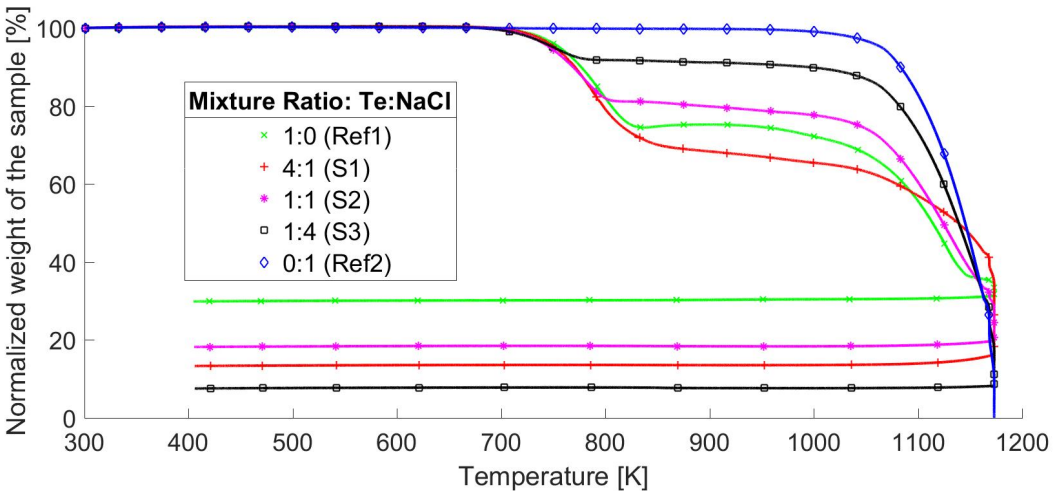

Figure 8. Thermogravimetric analysis results for the different Te:NaCl-ratios (weight basis) heated in oxidizing conditions. The different lines represent the average of three replicates 1:0 (Ref1, green crosses), 4:1 (S1, red pluses), 1:1 (S2, pink stars), 1:4 (S3, black boxes), and 0:1 (Ref2, blue diamonds) of tellurium and sodium chloride respectively. All weights have been normalized towards the first measured weight (8-9 mg) by thermogravimetric analysis. The measuring interval was one second.

Considering at what temperature the first main mass loss phases of the samples start at, this is close to the melting point of tellurium (722.66 K [53]) and may be connected to it. The pure

tellurium reference behaves in the same way and it is reasonable that the first mass loss phase of each sample is only due to the melting and volatilization of the tellurium. After the initial mass loss phases of the samples, the mass loss trend leveled out for all samples, but the pure tellurium reference mass loss did not. Instead, it started to increase in mass and thus diverged from the behavior of the samples. This mass increase could be correlated to the oxidation of tellurium to the α-TeO_2 according to the O-Te phase diagram [118] or as Reaction 6 shows. However, this mass increase did not occur for the different samples or the sodium chloride reference. Thus, the addition of sodium chloride either prevented or counteracted the mass increase. The final mass loss of all the different samples occurred around 920 K, which is close to the melting point of TeO_2 (1006 K [53]). Meaning that a phase change likely occurred and observing the phase diagram for the Te-O system [118], both liquid and gaseous state of the TeO_2 may exist above this temperature. The second mass loss phase could be explained by the volatilization of TeO_2. For the pure sodium chloride reference, the only mass loss phase observed was at around 1000 K.

Table 14. The start and end of the different mass loss phases and the final normalized mass for the samples and references of the oxidizing condition. The samples corresponded to ratios of 1:4 (Sample 1), 1:1 (Sample 2), 4:1 (Sample 3) of tellurium and sodium chloride. The reference consisted of either pure tellurium (Reference 1) or sodium chloride (Reference 2).

	Temperature range First Mass Loss [K]	Temperature range Second Mass Loss [K]	Final Normalized Mass [$\%_{wt}$]
Reference 1	700-840	900-end	≈ 30
Reference 2	1000-end	-	≈ 0
Sample 1	700-870	1030-end	≈ 14
Sample 2	695-815	1020-end	≈ 18
Sample 3	680-785	1000-end	≈ 8

Considering these results, the sodium chloride did affect the volatilization of tellurium as the observed mass increase for the pure tellurium reference, did not occur for any of the samples. This could be explained by the sodium chloride simply preventing the oxidation of the tellurium in the pan by physically covering the tellurium, and therefore preventing the mass increase. Alternatively, a chemical reaction may have occurred between the tellurium and sodium chloride. This could also prevent the oxidation of the tellurium or could form a more volatile species that offsets the mass increase through the increased volatilization. Possible tellurium species could be with chloride, as these would be more volatile based on melting and boiling points and possibilities of chlorides can be observed in Table 3.

Regardless of what occurred, comparing the different samples the differences are minor and seem related to the content of sodium chloride, as increasing the ratio of sodium chloride increased the similarity of the samples to the pure sodium chloride reference. This means that even a small (relative to these experiments) amount of sodium chloride affects the tellurium volatility.

5.1.3 Visualization of Samples through Furnace Experiments

To gain insight into what occurred during the oxidizing experiments, a mixture of 1-1 of tellurium and sodium chloride was heated to several temperatures, followed by rapid cooling. This

was mainly done to obtain a visual observation of the mixture after being heated to the different temperatures. The different samples produced for each temperature can be observed in Figure 9. The first image (A), resembles the initial appearance of the state of the samples; the black part is tellurium (black powder) and the white part is sodium chloride (white powder).

The eight individual samples were heated to temperatures starting at 473 K and reaching 1073 K, with an initial temperatures step of 100 K, followed by a temperature step of 50 K. Observing the images in Figure 9, it was first at 673 K (D) that the sample changed as sodium chloride became more apparent. These continued to emerge as the temperature continued to increase, most likely due to the disappearance of the tellurium. However, at 873 K (H) the second main change was observed. This was that a yellow phase started to emerge, which covered both the mixture and the crucible. Reaching 923 K (I), the yellow color became more prominent and the integrity of the sample starts to decrease. At 973 K (J), the sample as a whole started to melt and a noticeable loss of volume had occurred after the experiment. Finally, at 1023 K (K) and onward only the yellow phase remained as well as a glaze covering the crucible.

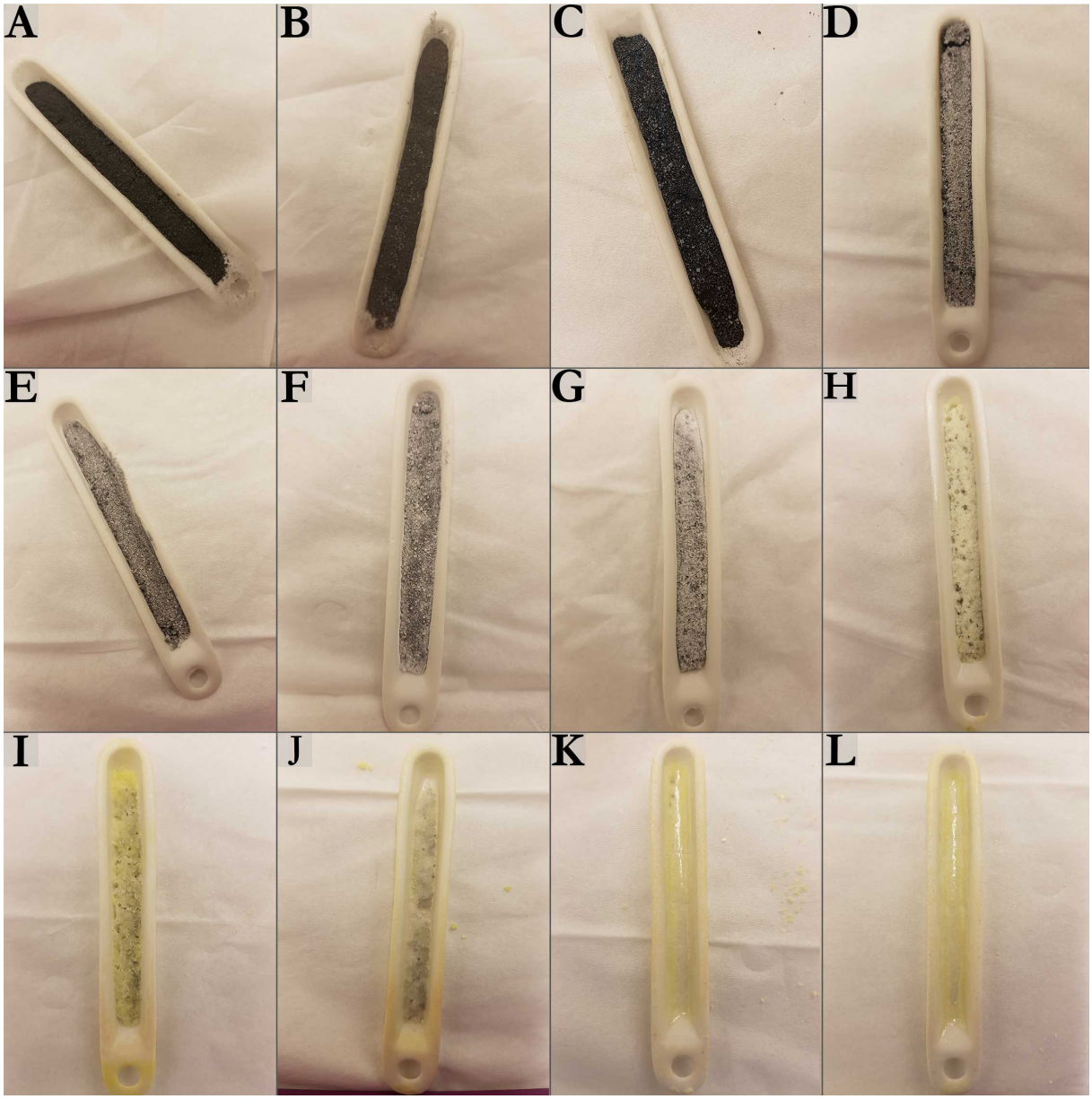

Figure 9. Crucibles containing the sample, as seen after the furnace experiment. The initial composition of the samples was 1:1 of tellurium and sodium chloride (2 g). In total eight, temperatures were investigated: (A) 473 K, (B) 573 K, (C) 623 K, (D) 673 K, (E) 723 K, (F) 773 K, (G) 823 K, (H) 873 K, (I) 923 K, (J) 973 K, (K) 1023 K, and (L) 1073 K.

The first three samples (A, B, C) seen in Figure 9 show only minor changes, whereas those following (D to L) all show noticeable change from the initial state. Considering the temperatures, this trend is reasonable as the melting point of tellurium (722.66 K [53]) is close to the fifth sample (E) and the melting point of sodium chloride (1075.2 K [53]) is close to the eleventh sample (K). The reason for increasing visibility of the sodium chloride already at 600 K is not clear. As previously mentioned, the sample reaching 723 K (E) should have less tellurium, and therefore makes the sodium chloride more visible. This, considering that the melting point of tellurium has been exceeded. Reaching 873 K (H), a yellow phase did appear. Considering the coloration and the elements involved, two possible yellow species are; Te_4Cl_{16} or the orthorhombic-TeO_2 [92]. Of these, only the first has a melting point below 1000 K. At a temperature of 1023 K

(K), little remains of the samples. As the melting (1075.2 K [53]) and boiling (1738 K [53]) points of sodium chloride, some should remain at such a temperature, indicating that something has occurred which has resulted in more volatile species of the sodium chloride. Alternatively, a sodium-tellurium complex may have formed, a possibility for which is Na_2TeO_3. However, this is less likely as it is reported to have a white color [53]. Nevertheless, from these results, no definite conclusion can be made about what species may have formed. However, it is clear that the sodium chloride did have an effect on the tellurium.

Comparing the two methods used for oxidizing conditions, a consistency between the results exists. The observed decrease in tellurium from the furnace experiments occurs at the same time as the first major mass-loss phase of the TGA experiment. In the period between the two major mass loss phases, the TGA shows as slow mass loss and concurrently for the furnace samples the yellow phase appears. This indicates a correlation between the slow mass loss phase and the build-up of the yellow phase. The second major mass-loss phase of the TGA experiment coincides with the significant reduction of the mass of the furnace sample. Simultaneously to this mass loss phase, the pure sodium chloride reference shows at best, minor amounts of mass released. This is an indication that something is occurring at these temperatures that results in the mass loss, which could be the formation of a more volatile species such as Te_4Cl_{16}. Considering both the TGA and furnace experiments it is a possibility that the sodium chloride affected the tellurium volatility during these experiments under oxidizing conditions. Thus, the use of seawater may enhance the volatility of tellurium under oxidizing conditions.

5.2 Reactor Coolant System experiment

The investigation of the tellurium behavior in the RCS to determine the effect of cesium iodide on tellurium was performed under oxidizing and inert conditions both dry, humid, and humid with added cesium iodide. All of these experiments were carried out as singlets and the experimental uncertainties of these results are unknown.

5.2.1 Initial Observations and Quantification

After each experiment the samples and the remaining precursor were visually inspected and weighed using a balance.

Following the experiments, the precursors used under the oxidizing conditions (RCS-1, RCS-2, and RCS-3) all had a slight gray color, while from the inert experiments (RCS-4, RCS-5, and RCS-6) all the precursors remained black. The filters located after the reaction furnace had white deposits under dry (RCS-1) and humid (RCS-2) oxidizing conditions. An initial yellow color was observed on the filter from the experiments (RCS-3) performed under humid oxidizing conditions with added cesium iodide. After storage and transport to the INAA location the yellow color had faded significantly and a white color remained. A black deposit with a white tone to it had formed on all filters from all three inert experiments. The liquid sodium hydroxide traps located after the filters from both the three oxidizing and three inert conditions showed no visible change after each experiment. The weights of the remaining precursor (i.e., released mass) and species trapped on the filter (i.e., transported mass) from each experiment were determined with the balance and are shown in Table 15.

Table 15. The released amounts of the precursor and the amounts reaching the filter.

		Released Mass	Transported Mass[a]
Oxidizing Conditions	RCS-1	56	50
	RCS-2	44	40
	RCS-3	25	20
Inert Conditions	RCS-4	283	63
	RCS-5	296	35
	RCS-6	275	53

[a]Reaching the filter

From the color change of the precursors and the color of the deposit on the filter, an initial speciation can be obtained. For the oxidizing conditions, the gray color of the precursor indicates that the black tellurium has most likely undergone a slight oxidization during the oxidizing conditions to e.g., tellurium dioxide as indicated in Reaction 6. The white color on the filter indicates tellurium dioxide [53]. The yellow color observed could be explained by several species but considering that it faded during storage and transport it most likely is iodine. An alternative could be the yellow orthorhombic-tellurium dioxide [92]. The tellurium dioxide is unlikely as it is not as volatile as iodine and would not result in the yellow color fading away.

The weights from the balance provides an initial estimate of the transported amounts in under oxidizing and inert conditions. From these results alone, the highest transported mass occurred under inert conditions. However, under oxidizing conditions the precursor oxidized (e.g., as Reaction 6). This would add mass to the precursor and therefore appear as less of the precursor was volatilized. For the oxidizing experiment with cesium iodide (RCS-3), the released mass and transported mass were noticeably lower than the other two (RCS-1 and RCS-2). This indicates a decrease in the transported mass but provides little evidence of anything else. Thus, from these results alone it is not clear what occurred under these conditions.

5.2.2 Detailed Quantification

To provide a more detailed mass determination as well as the individual distribution of the elements in the samples, INAA was performed on the filters and liquid sodium hydroxide traps. The elements determined were cesium, iodine, and tellurium, of which the amounts of the two first were only determined from the samples of two experiments (RCS-3 and RCS-6). The tellurium INAA-values were also compared to the released amounts presented in Table 15. For the values of the liquid traps, they correspond to the original solution volume (i.e., 250 ml) used in each experiment.

Table 16. The amount of tellurium, cesium, and iodine that was determined in the filter was located after reaction furnace and in the liquid sodium hydroxide trap following it. The fraction within parenthesis is the data from the INAA divided from the mass released determine by the balance measurement presented in Table 15.

	Te [mg] (^{131}I)		Cs [mg] (^{134}Cs)		I [mg] (^{128}I)	
	Filter	Trap	Filter	Trap	Filter	Trap
RCS-1	32 (58%)	1.1 (2.0%)				
RCS-2	28 (63%)	0.95 (2.2%)				
RCS-3	13 (50%)	0.71 (2.8%)	1.7	<0.01	0.5	<0.003
RCS-4	46 (16%)	0.99 (0.3%)				
RCS-5	40 (13%)	0.57 (0.2%)				
RCS-6	42 (15%)	0.94 (0.3%)	1.6	0.04	1.1	0.03

From the INAA data, it can be seen that the largest transport occurred under oxidizing conditions compared to inert conditions for both the filter and trap. This was only when comparing the tellurium amounts from the filter with the released amounts from the precursor. Otherwise, actual determined amounts were higher under inert conditions for the filters. This indicates that under inert conditions most of the tellurium was deposited throughout the tube. It should be noted that the precursor under oxidizing conditions was most likely oxidized, as it turned from black to slightly gray. This resulted in an uncertainty of the released amounts, as the oxygen would add mass to the precursor. Still, during the handling of the precursors from the three oxidizing conditions it seemed that it was mainly the surface of the remaining precursors that was oxidized. Therefore, the remaining precursor would still be largely tellurium.

These results showed that under oxidizing conditions the increased humidity increased the amount of tellurium transported through the reaction furnace, as the existing literature would suggest [41, 83, 85, 86]. Adding cesium iodide to the system resulted in a decrease of transported tellurium. Comparing the molar amounts of cesium to iodine on the filters, showed a divergence from one. Specifically, more cesium was observed, indicating an excess of cesium, which could be due to a chemical change of the cesium iodide by the prevailing conditions, through the formation of I_2 and some cesium compounds. Alternatively, a reaction with tellurium may have occurred, possibly as Reaction 11. This would require that cesium iodide had formed cesium hydroxide and that hydrogen was available. The presence of hydrogen is questionable under oxidizing conditions as it would not prevail. Considering that the tellurium amount is significantly lower, this suggests that tellurium was in some way affected by the addition of cesium iodide.

Under the different inert conditions, dry and humid with added cesium iodide had the most transported tellurium through the reaction furnace. This means that increasing the humidity of the inert atmosphere decreased the amount of transported tellurium. The addition of cesium iodide to the humidity did increase it back to the same levels transported under the dry inert conditions indicating an effect on the transported tellurium. The molar ratio of cesium and iodine was again different from one (i.e., excess of cesium), which indicates that something occurred to the cesium iodide.

Both the decrease and increase in the tellurium amounts on the filters during inert humid and humid with cesium iodide additive conditions can be explained by the formation of new species. In the former case, slight oxidization may have occurred of the gaseous tellurium, possibly as Reaction 7 shows to TeO. This species would then have been less mobile than other species

or deposit as temperatures decreased. The increase of the tellurium amounts in the second scenario can be explained by the formation of a tellurium-cesium complex, similar to what has been suggested in the literature [15] and as shown in Reaction 11 or the reverse of Reaction 13. However, this would require both cesium hydroxide and hydrogen to have formed. The hydrogen could be available through Reaction 7. This would then also explain the ratio between cesium and iodine, as the iodine could have escaped during the experiment or the transport to the INAA-analysis as I_2, increasing the amount of cesium on the filter in comparison to iodine.

Comparing the contents of the filters to the liquid sodium hydroxide traps, it is clear that the filters captured most of the transported particles. This indicates that at these temperatures the main transport mode was as aerosols. As for the filters, the highest tellurium fraction reaching the traps was under oxidizing conditions. This fraction was increasing, first when humidity was added and again when cesium iodide was added. For the three inert conditions, the values were very similar, and should a difference exist it may be too small to observe in these results. The additionally used method of ICP-MS did not detect any amount of cesium or tellurium in any of the traps.

5.2.3 Chemical Speciation

To determine the chemical speciation of what was trapped on the different filters, a small part of each was cut away and analyzed using XPS. Specifically, the aim was to identify species related to cesium, iodine, and tellurium. Reference data is therefore needed and such data, relevant for this part, is presented in Table 12.

The outcome of the identification of each XPS spectra is presented in Tables 17 and 18 for the samples from the oxidizing and inert conditions, respectively.

Table 17. Identified species by XPS on the filter acquired under oxidizing conditions.

	RCS-1		RCS-2		RCS-3			
Element	O	Te	O	Te	O	Te	Cs	I
Shell	1s	$3d_{3/2}$	1s	$3d_{3/2}$	1s	$3d_{3/2}$	$3d_{3/2}$	$3d_{3/2}$
Binding	530.5	576.3	530.4	576.3	529.8	575.6	723.8	618.3
energies	532.0		531.6	574.3[a]	531.7	577.5		
Chemical state	TeO_2	TeO_2	TeO_2	TeO_2	TeO_2	TeO_2	CsI	CsI
of element				NN		TeO_3[b]		

NN: not identified; [a] very weak; [b] possible alternative $Te(OH)_6$, Te(VI): 577.0 eV according to the operator. The measurement uncertainty for the electron energy was ± 0.1 eV.

For oxidizing conditions, all three samples show clear indications for the species TeO_2. When the humid oxidizing condition was investigated a new, but very weak peak emerged. This peak was not successfully identified. When cesium iodide was added to the humid atmosphere, again a new peak emerged. This peak was correlated to tellurium in oxidation state +6. According to the binding energy, possible species were either TeO_3 or $Te(OH)_6$. Those peaks detected for both cesium and iodine were both identified as cesium iodide.

To observe TeO_2 in these filters is expected at lower temperatures and formed as Reaction 6 shows. Observing new species under humid oxidizing is also possible as the interaction suggested by the literature [41, 83, 85, 86] between the TeO_2 and water at high temperatures could result in a change in the observed speciation at low temperature. Alternatively, Reaction 8 could have occurred forming TeOH. Both of these possibilities could also be true for the humid conditions with added cesium iodide as well. As in the latter case, the observed peak was different and more intense compared to the one observed from the humid oxidizing conditions. This indicates a possible interaction between tellurium bearing species and cesium iodide. According to the literature [71], this is be unlikely as cesium telluride has been reported to be unstable in oxidizing conditions.

Table 18. Identified species by XPS on the filter acquired under inert conditions.

	RCS-4		RCS-5		RCS-6			
Element	O	Te	O	Te	O	Te	Cs	I
Shell	1s	$3d_{3/2}$	1s	$3d_{3/2}$	1s	$3d_{3/2}$	$3d_{3/2}$	$3d_{3/2}$
Binding energies	530.6 532.3	576.3 573.2	530.4 532.0	576.3 573.2	530.1 532.4	575.9 572.9 578.3	723.7 725.9	618.5 620.6
Chemical state of element	TeO_2	TeO_2 Te	TeO_2	TeO_2 Te	TeO_2	TeO_2 Te NN	CsI Cs	CsI I_2

NN: not identified; The measurement uncertainty for the electron energy was ± 0.1 eV.

The outcome of the inert experiments showed the presence of both Te and TeO_2 in all of the samples. Observing metallic Te is reasonable considering the conditions as the potential for oxidation of tellurium is rather low under the dry inert conditions. First when the humidity is increased of the system, should any oxidization occur. As Reaction 7 shows from Te_2 to TeO, which then would have formed TeO_2 at lower temperature. It is also possible that some air may have leaked in during the experiment or slight oxidation occurred during storage. Still, the consequences were small, as comparing the inert conditions samples visually to the oxidizing conditions sample showed a considerable difference (i.e., no oxidization of the precursor). Instead, the reason might be that the tellurium oxidized during storage and/or transport to the XPS. When investigating the effect of cesium iodide, a new tellurium peak emerged. However, this peak was not positively identified using the reference data. For both cesium and iodine new peaks were detected and suggested species were Cs and I_2, respectively.

From the speciation of the inert conditions filter samples, the main difference was that new peaks emerged for all the elements when humid inert condition with added cesium iodide was investigated. Of these, only one connected to tellurium was not positively identified. However, the identification attained for cesium is questionable, especially since metallic cesium is very unlikely to remain during the storage in air. It is possible that what is observed for cesium may be correlated to the unidentified tellurium peak. Indicating a new tellurium-cesium species had formed, which is possible according to the literature [15]. A possibility for this to occur is through either Reaction 11 or the reverse of Reaction 13. This supports the INAA measurements if the volatility of the cesium-tellurium complex is greater than those existing under humid inert conditions.

5.2.4 Online Measurements

For the experiments, both the mass concentration of suspended particulate matter (all diameters) and the number size distribution were determined. In total, six of each were acquired and are presented in Figures 10 and 11. However, for the experiment with humid oxidizing conditions with added cesium iodide (Experiment 3 in Figure 10, elsewhere called RCS-3) only the result for the later part of the experiment is available. This due to an initial malfunctioning of the measuring equipment.

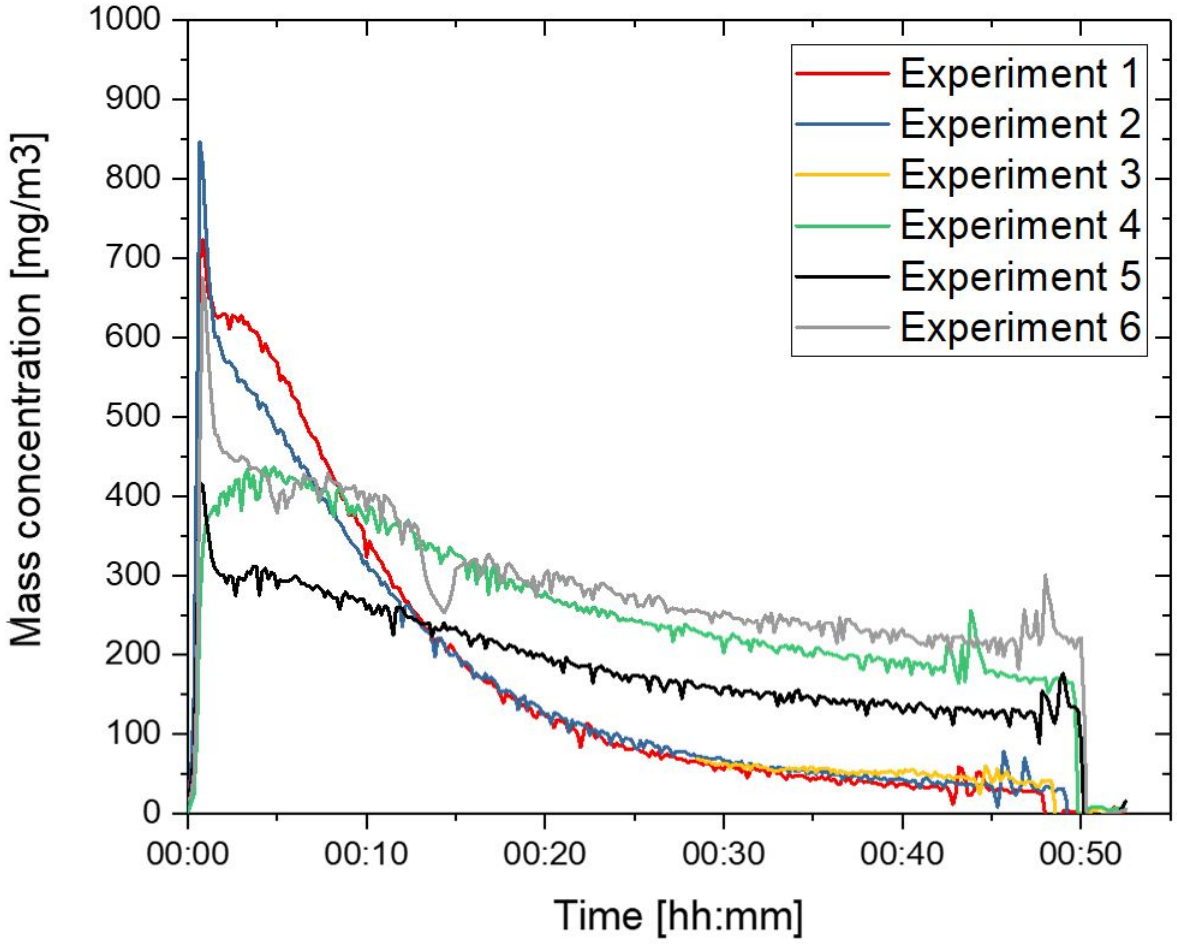

Figure 10. Evolution of the mass concentration of tellurium containing aerosol in the experiments. Experiment 1:RCS-1;Experiment 2:RCS-2;Experiment 3:RCS-3;Experiment 4:RCS-4;Experiment 5:RCS-5;Experiment 6:RCS-6

Observing these mass concentrations, the experiments performed under both oxidizing and inert conditions had an initial surge of mass concentration as the flow was started. Of these surges, the once occurring under inert conditions were the highest. Following the surge for all experiments, there was a decrease in the mass concentrations that eventually stabilized. The experiments performed under oxidizing conditions, these had generally a lower mass concentration when stabilized, compared to the inert conditions. This was likely due to the oxidation of the precursor, which slowed down the release rate.

The experiments performed under oxidizing conditions showed only a small increase in the

aerosol mass concentration when humid oxidizing condition with added cesium iodide were used. The slight increase can be attributed to the addition of cesium iodide to the aerosols. For the experiments under inert conditions, a slight decrease was observed under the humid inert condition, and an increase when cesium iodide was added. The decrease may be due to added humidity resulting in tellurium oxide, as Reaction 7 shows. The formed TeO would then deposit before reaching the TEOM, as TeO is only stable at high temperatures. It could form tellurium dioxide as it was approaching room temperature, which would explain the observed tellurium dioxide on the filter. The increase observed when cesium iodide was present, could be explained by the already suggested possibility in the literature [15] of a cesium-tellurium complex. This means that cesium iodide either increased the volatility of tellurium under humid inert conditions or added mass to the tellurium aerosol.

The number size distribution of tellurium bearing aerosols were also determined (particles diameter < 1 μm). The results for both oxidizing and inert conditions are presented in Figure 11.

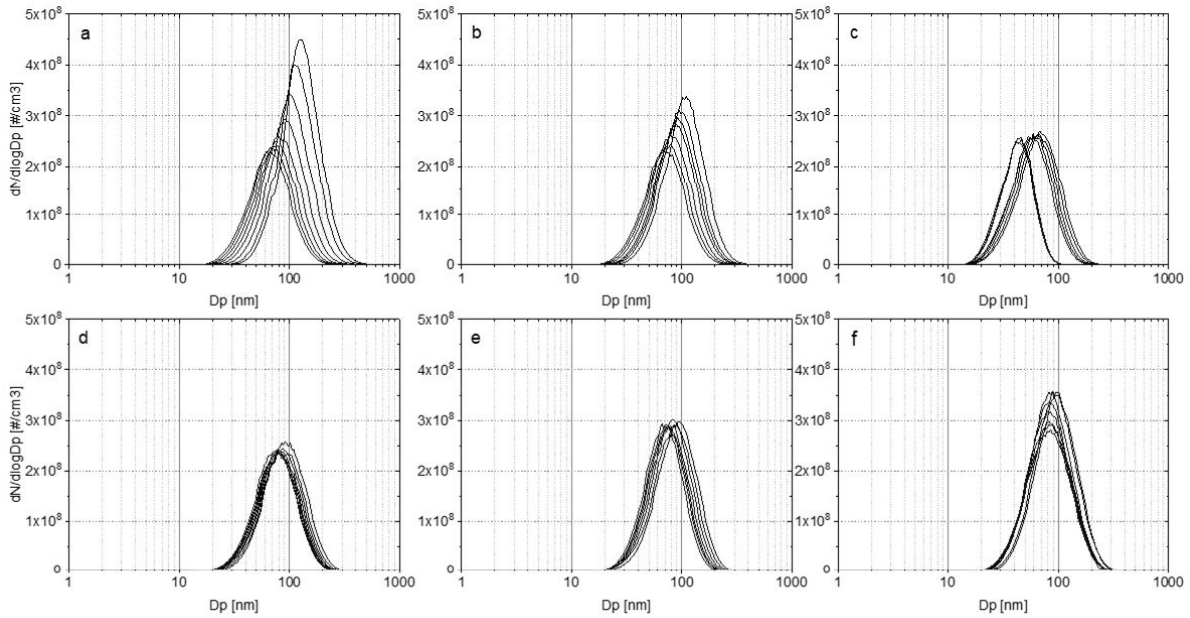

Figure 11. Evolution of the number size distribution of tellurium containing aerosol in the experiments. The diameter and number concentration of particles decreased in the course of experiments: a) RCS-1, b) RCS-2, c) RCS-3, d) RCS-4, e) RCS-5, and f) RCS-6.

The number size distribution of tellurium bearing aerosols under both oxidizing and inert conditions, showed decreasing trends of both the number and diameter during the experiments. For oxidizing conditions, the distribution remained unchanged when going from dry to humid conditions, even if the former had initially a higher number concentration. When adding cesium iodide to the system, a continuous decrease of the size distribution was observed, while the number concentration of the particles remained stable. The count median diameter (CMD) of tellurium-bearing particles for the experiments was estimated to decrease from 100 nm to 60 nm for both the dry and humid experiments, whereas the addition of cesium iodide measured a CMD decreasing from 70 nm to 40 nm. The size distribution from the three inert conditions was similar to one another. The number concentration increased when going from dry to humid

conditions and became even higher when cesium iodide was added. The CMD for the inert conditions, changed from 100 nm to 70 nm and with the addition of cesium iodide the CMD range was from 100 nm to 85 nm.

In these results, a change in the particle distributions was observable from all the investigated conditions (oxidizing, inert) as well as a change in the particle distribution due to the addition of cesium iodide. Under oxidizing conditions, the size distribution decreases at a whole due to the addition of cesium iodide, whereas under the inert conditions the size distribution ended slightly higher (i.e., the CMD) compared to dry and humid inert conditions. The continuous decrease observed in all experiments is most likely related to the decrease in the mass being transported after the initial surge, and therefore less agglomeration of the tellurium aerosols occurs towards the end, due to less material in the gas. Under oxidizing conditions, the decrease observed when cesium iodide was investigated could be related to the cesium iodide particles reducing the agglomeration of the tellurium aerosols. This either by reaction with tellurium or oxygen (preventing tellurium from reacting with it). Another possibility, could be instead that the cesium iodide increase the size of tellurium aerosols and therefore increase the tellurium deposition before the reaching the measuring location. However, under inert conditions, the addition of cesium iodide slightly increased the final size of the distribution (i.e., CMD). Considering, that the initial surge of tellurium had faded towards the end of the experiment it is likely that the cesium iodide was ensuring larger tellurium particles. This could occur by either reaction that forms larger particles (e.g., Cs_2Te) or an enhanced agglomeration due to the cesium iodide.

5.2.5 Morphology and Elemental Composition

At the end of each of the experiment, particles were collected on TEM grids and analyzed using an SEM coupled with an EDX. From all experiments, long agglomerate chains (oxidizing > 100 nm; inert: > 50 nm) were collected from the gas phase. These agglomerates consisted of primary particles smaller than < 100 nm. The micrographs produced of these are shown in Figure 12.

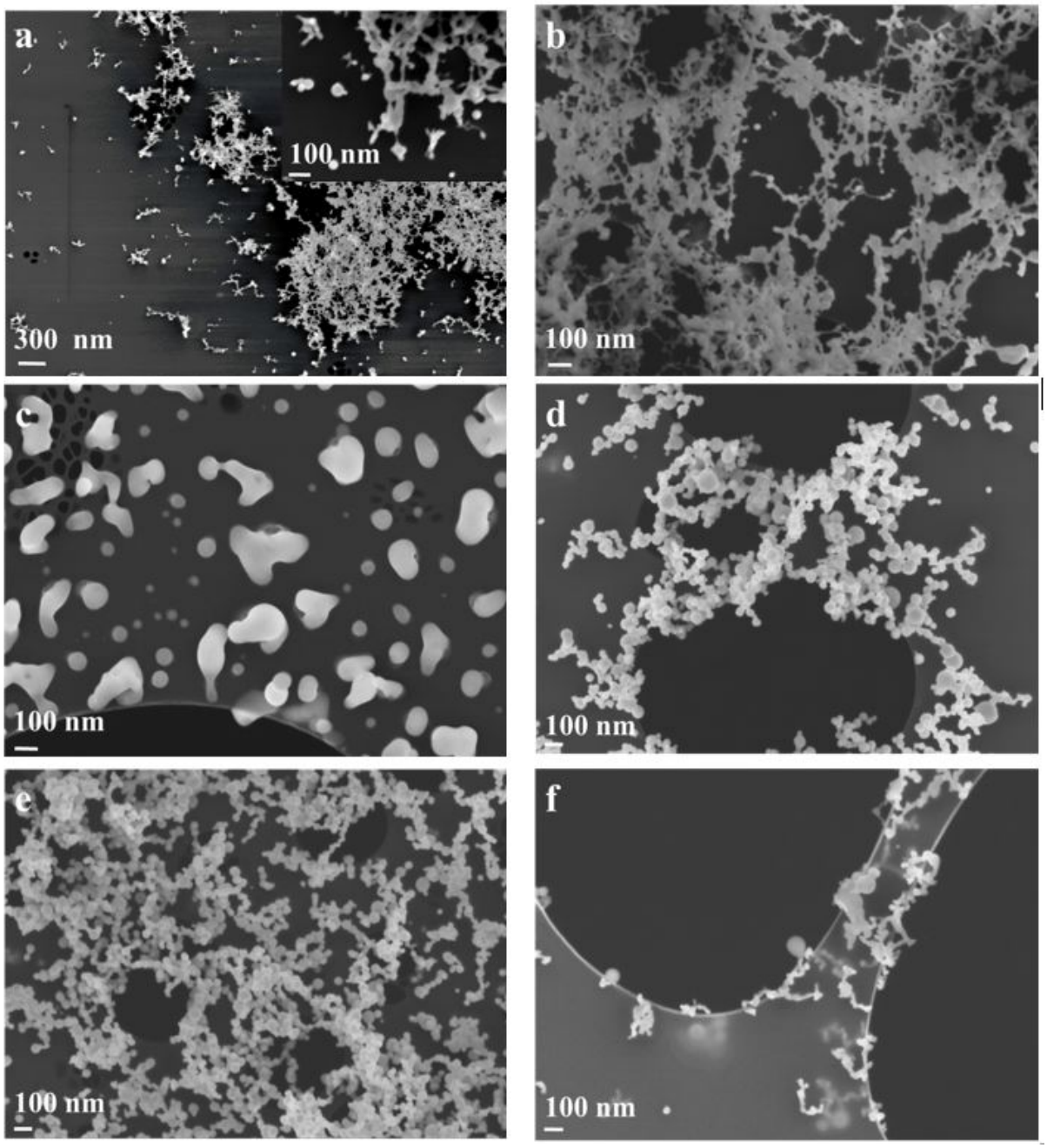

Figure 12. SEM micrographs of the experiments conducted in air: a) RCS-1, b) RCS-2 and c) RCS-3 and in nitrogen d) RCS-4, e) RCS-5 and f) RCS-6. The scale bar is 100 nm except in a, where the scale bar is 300 nm. The inset in a) has a scale bar of 100 nm.

Under oxidizing conditions, the agglomerate chains were of thin dendritic structures. With the addition of cesium iodide, the primary particles of the agglomerate chains fused with the cesium iodide related particles, resulting in irregularly shaped large particles. The appearance of the agglomerated chains from the inert conditions were similar to the oxidizing conditions (except the size).

From X-ray spectra acquired from the micrographs, the presence of tellurium was seen in all experiments, but in the experiments involving cesium iodide (RCS-3 and RCS-6) neither cesium nor iodine were detected. Using the TEM, it was possible to detect cesium. However,

no indication of iodine was found, possibly due to overlapping peaks of cesium, iodine, and tellurium.

The micrographs showed little changes between the different experimental conditions, aside from an increase in the fusions of primary particles. Besides this, the elemental composition of the particles detected was as expected, namely, tellurium and cesium (from the relevant experiments). Not observing iodine was attributed to possible overlap. These elemental observations are therefore in line with previous methods used.

5.3 Containment Experiment

To explore the behavior of tellurium in the containment, several experiments under three different conditions (oxidizing, inert, reducing) were investigated both dry and with increased humidity. The main aim was to observe any reaction or deposition on the surfaces found in a BWR containment. However, these experiments were only carried out as singlets and the experimental uncertainties of these results are unknown.

From a purely visual standpoint, the initial observations revealed little signs of any interaction between the tellurium and the surfaces located at room temperature. Only a thin (possible to see through the deposits) deposit had formed on each of the three surfaces with similar colors (i.e., within one experimental condition) under each condition. For the two oxidizing conditions, the appearance of the deposits was white, and for the deposits from the two inert and two reducing conditions they were black. To enable the SEM investigation, all of the deposits had a small part removed with the adhesive side of a carbon tape. In doing so, revealed little visual change for the underlying surface. Considering the coloration and the preluding conditions, a possible candidate species under oxidizing conditions is tellurium dioxide and for inert and reducing conditions, metallic tellurium. However, from these observations no definite conclusion can be made of either speciation or if an interaction of sorts occurred.

During the experiments, particles were trapped on the filters. In the case of oxidizing conditions, mainly white-colored deposit with some hint of black had formed on the two filters. For the filters from both the two inert and the two reducing conditions, a back deposit with some white/gray coloration to it was observed. Based on the observed colors alone, the black under all conditions would be metallic tellurium and the white likely tellurium dioxide. In the case of inert and reducing conditions, it is not clear why oxidation occurred.

After each experiment, the mass of the crucible, metal coupons, and filters was weighed using a balance. Of these objects, only the filters had a noticeable mass difference using the balance. Indicating, that the weight of the deposits was small and most of the precursor was volatilized. Thus, the weights of the metal coupons and crucible were excluded. However, it should be clarified that there was minor residue left in the crucibles used. The weight of the filter before and after each experiment is shown in Table 19.

Table 19. The weight of the filters before and after they were used in the BWR containment experiments.

	m_{before} [mg]	m_{after} [mg]
C-1	0.15	0.26
C-2	0.15	0.29
C-3	0.15	0.33
C-4	0.15	0.3
C-5	0.15	0.3
C-6	0.15	0.32

Observing the weights of all the filters used in the experiments, the amounts trapped on the filters were similar at around 0.15 mg. However, under oxidizing conditions the oxidization of the tellurium would add to the mass. Meaning that the mass increase observed of the filter will be a combination of tellurium and oxygen. Unlike the inert and reducing conditions, where the main species reaching the filter would be metallic tellurium. This assuming, that no interaction occurred with any of the surfaces. Thus, indicating that more tellurium was trapped by the filters under inert and reducing conditions.

5.3.1 Oxidizing Conditions

The morphology of the particles observed in the deposits from all metal surfaces deposited during oxidizing conditions were smooth round spheres of different sizes. No apparent differences were noticeable, between dry and humid conditions. Micrographs of all deposits from oxidizing conditions are shown in Figure 13. In these micrographs, some locations have been indicated. These locations are where the element compositions were determined using the EDX. The acquired spectra indicated tellurium, but also oxygen and carbon (likely source: carbon tape). Only in the deposit from the zinc surface under humid oxidizing conditions was something else detected, which was zinc.

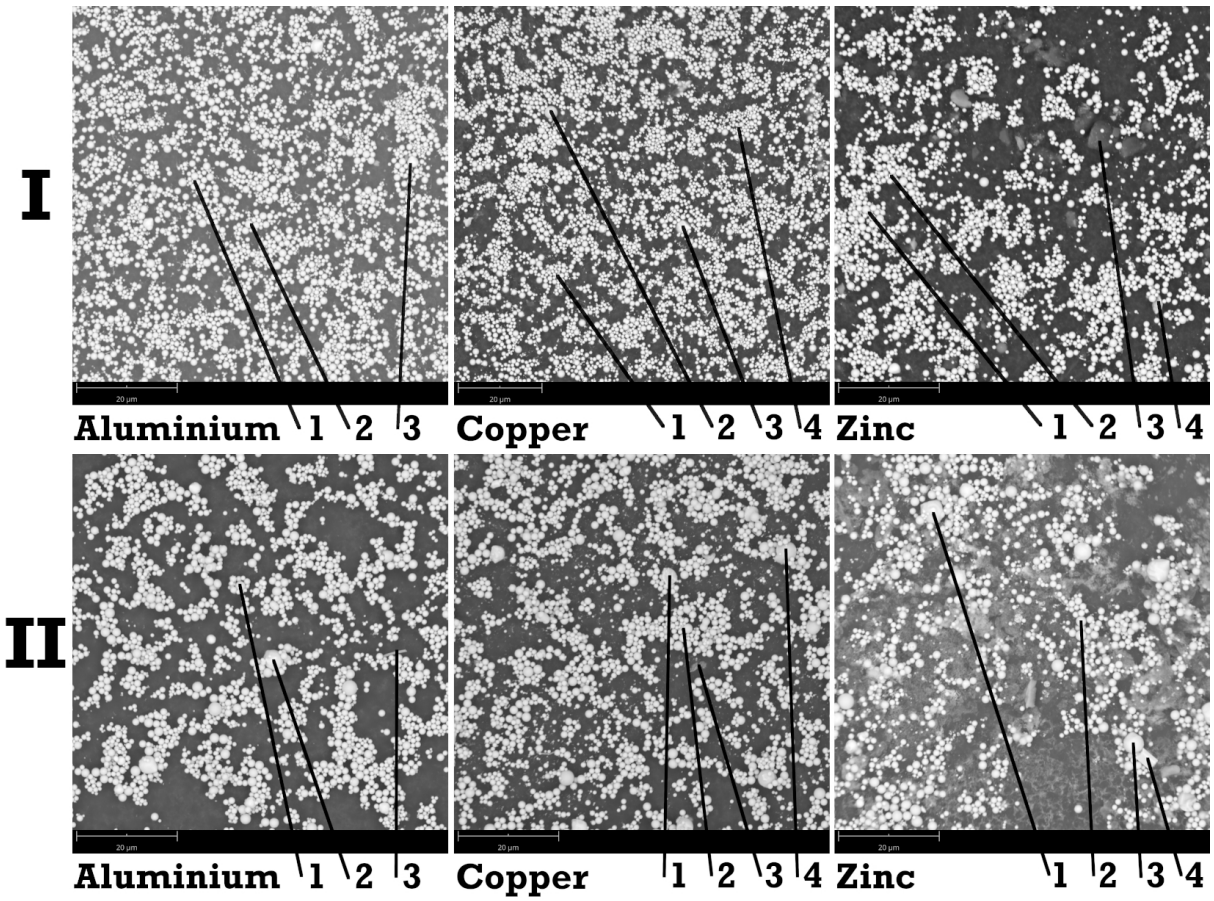

Figure 13. Six micrographs from dry (I) and humid (II) oxidizing conditions experiments, each showing the deposits from the aluminum (left), copper (middle), and zinc (right) surfaces.

The elemental composition of the different deposits is to some degree as expected, meaning that both tellurium and oxygen were present considering the precursor and oxidizing conditions at high temperature. However, the fact that zinc was observed is not as expected, as the temperature where the zinc surface was located should not readily result in any reaction. Thus, finding zinc in the deposit would mean that something did occurred during this experiment. This could be due to the condition itself (i.e., humid oxidizing condition), the formation of a thin water film or the tellurium species existing under this condition interacted with the surface. According to the literature [58, 83, 85], a transient tellurium species (e.g., $TeO(OH)_2$) exists at high temperatures when humidity is high under oxidizing conditions. This new species may be a possible reason for the observation of zinc in the deposits if it remains in the gas phase at the location of the zinc surface. However, little research exists on the potential reactiveness of this transient species.

The species in the deposits on all metal surfaces and on the filters were determined. In all produced diffractograms, TeO_2 was identified. In the deposits, under humid oxidizing conditions, two different crystal structures were detected: paratelluride and orthorhombic, of which only the latter was detected under dry oxidizing conditions. The species trapped by the filters from both dry and humid conditions, had both crystal structure detected on them.

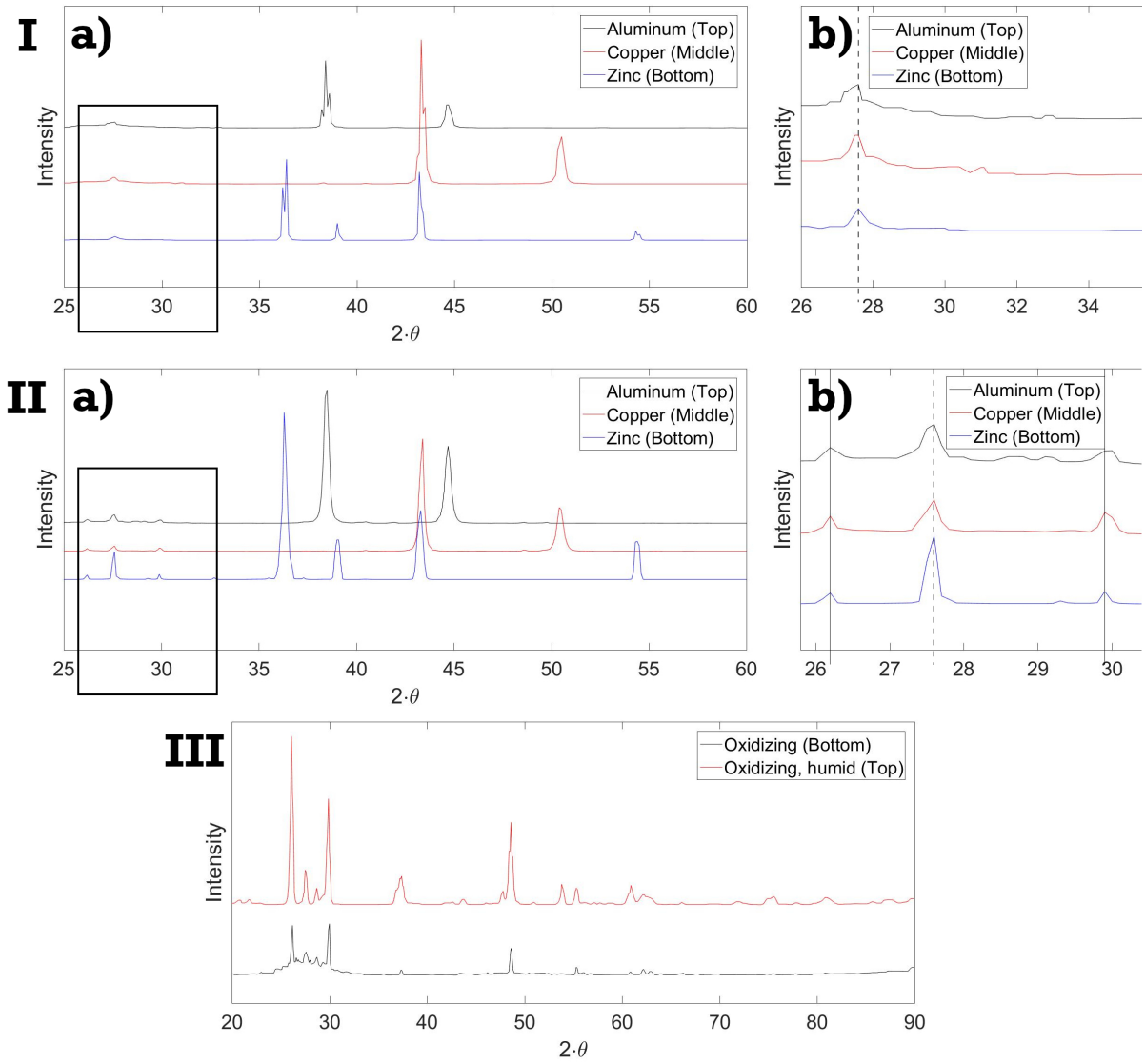

Figure 14. The X-ray diffraction analyzes of the depositions formed on the metal surfaces from dry (I) and humid (II) oxidizing conditions experiments. Areas highlighted by boxes (I.a and II.a) are shown to the right (I.b and II.b). Diffractograms for the filter used during these experiments are also shown (III).

The main difference observed between the dry and humid conditions was the presence of two different crystal structures of the tellurium dioxide in the deposits on all metal surfaces. Observing the filters, both of the crystal structures were detected in the trapped particles under both conditions. This indicates that the humidity may have increased the amount of the species resulted in the formation of the paratelluride-TeO_2 (above that of the XRD-detection limit). Therethrough, more of it was able to deposit on the surface. This could be the result of the formation of a water film. A species that could be responsible for the alternative crystal structure is tellurium oxide (TeO). This is only stable at high temperatures and is formed under oxidizing conditions at high temperatures [58]. It would then form the tellurium dioxide observed in these experiments as the temperature decreased, then with paratelluride crystal structure. Alternatively, the transient species formed under humid oxidizing conditions at high temperatures could have a higher tendency for deposition on the surfaces. It would then also have formed the TeO_2-paratelluride on the surfaces.

The liquid sodium hydroxide traps were also investigated for any amount of tellurium and the metals (aluminum, copper, zinc). For the two oxidizing conditions, tellurium was detected in the traps from both dry and humid conditions at roughly: $0.008\%_{wt}$ and $0.65\%_{wt}$ of the original precursor amount, respectively. The only metal detected in either trap was under humid oxidizing conditions, where around 0.3 mg of zinc was measured.

These values, which are consistent with the literature [58, 83, 85], indicate a higher amount of tellurium transported to the liquid sodium hydroxide trap under humid oxidizing condition. However, detecting zinc in the trap was not expected, indicating that something did occur with the zinc surface under humid oxidizing conditions. This was already seen by the SEM/EDX. From the reference experiments carried out, no signs of zinc in the trap was observed, which strengthen the idea that the tellurium species existing under humid oxidizing conditions affected the zinc surface. Additionally, literature [88, 89] have shown that tellurium does react with different surfaces in the RCS (e.g., 304 stainless steel and Inconel-600, both with and without an oxide layer), therefore it is possible that other surfaces such as zinc may also react with tellurium.

5.3.2 Inert Conditions

Under inert conditions, the morphology of the particles under both dry and humid inert conditions were a mixture of smooth spheres, clusters of smaller round particles, spike-shaped, and rectangular objects. When comparing the morphology of the two depositions from the dry and humid inert conditions, little differences were noticeable. The relevant micrographs are shown in Figure 15, in which some locations have been highlighted. In these locations, the elemental composition was determined. Essentially, only tellurium and carbon were detected, with the occasional oxygen observed. The carbon most likely came from the carbon tapes used to remove the deposits from the metal surfaces.

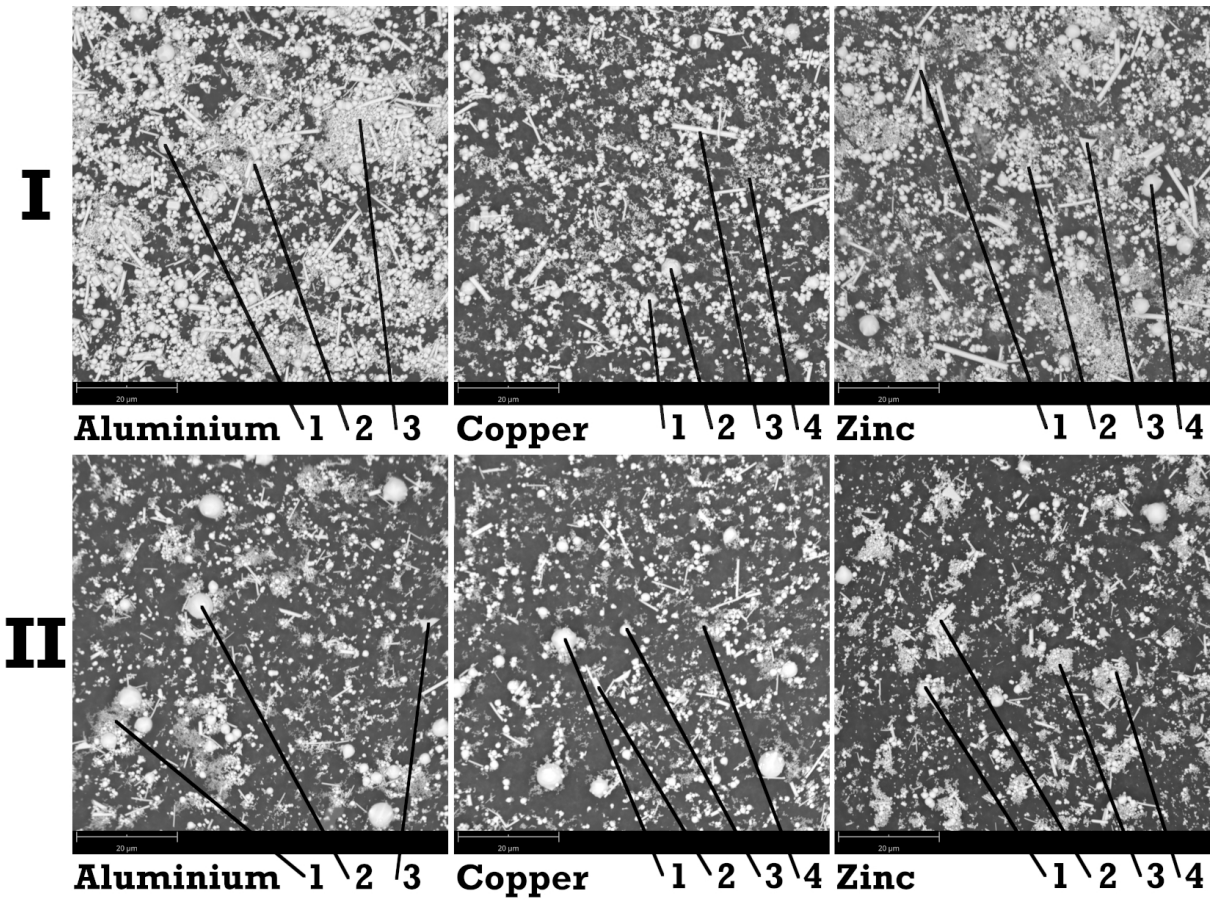

Figure 15. Six micrographs from dry (I) and humid (II) inert conditions experiments, each showing the deposits from the aluminum (left), copper (middle), and zinc (right) surfaces.

The presence of tellurium is expected, considering the inert conditions at high temperatures. That oxygen was present in the samole, can be explained by oxidation of tellurium during storage/transport to the SEM/EDX or slight oxidation of tellurium due to the humidity in the humid inert condition. Alternatively, some air may have leaked in during the experiment.

Determining the species of the deposits from the metal surfaces and the filters, showed that Te was the only species present. The diffractograms can be found in Figure 16.

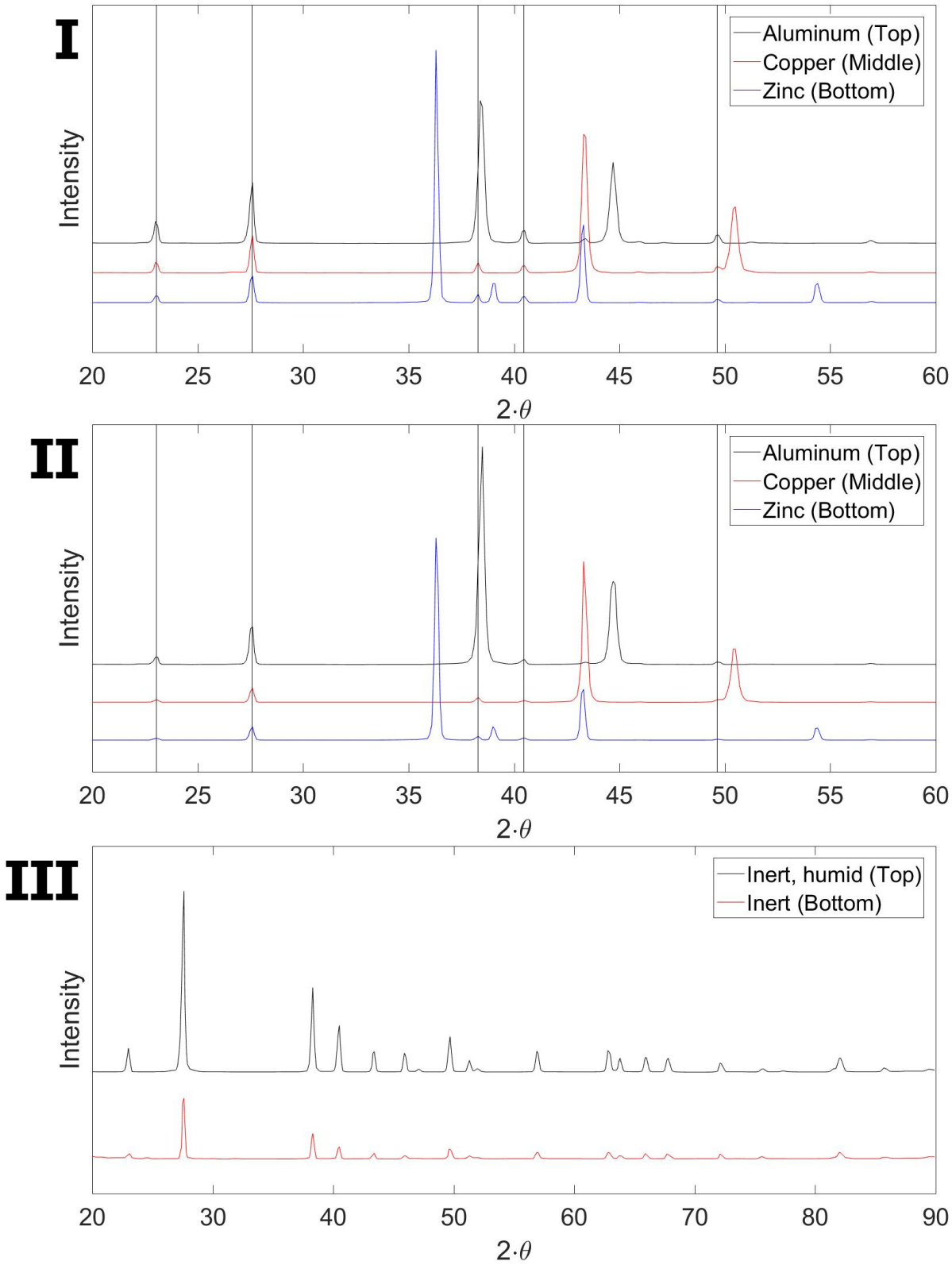

Figure 16. The X-ray diffraction analyzes of the depositions formed on the metal surfaces from dry (I) and humid (II) inert conditions experiments. Diffractograms for the filter used during these experiments are also shown (III).

The results shown in Figure 16 indicates that the addition of humidity to inert conditions had little effect (or at least to the detection limit of the XRD) on the species of tellurium that deposits and is stable at room temperature.

In the liquid sodium hydroxide traps, no detectable amounts of tellurium were measured. However, 0.2 mg of aluminum was observed in the trap from the humid inert condition.

Considering the weights of the filters, located just before the liquid sodium hydroxide traps, no significant increase in the mass was observed compared to the other two conditions. This indicates that the tellurium species formed are less volatile and not as capable of reaching either the trap or necessarily the filter. As little remained in the crucible, it could however be that under both inert conditions larger particles formed that resulted in enhanced deposition on the tube walls. The presence of aluminum in the trap could be due to the tube itself being made from Al_2O_3 and small amounts being released from it.

5.3.3 Reducing Conditions

Investigating dry and humid reducing conditions resulted in deposits on the metal surfaces with a morphology consisting of smooth spheres, spike-shaped, and rectangular objects. Little differences were seen between the deposits acquired under the two reducing conditions. The micrographs of the deposits from the reducing conditions are shown in Figure 17 and some locations have been highlighted. The chemical composition of these locations were determined and only tellurium and carbon, with the occasional oxygen, was detected. The observed carbon most likely originates from the carbon tapes used to remove the deposits from the metal surfaces.

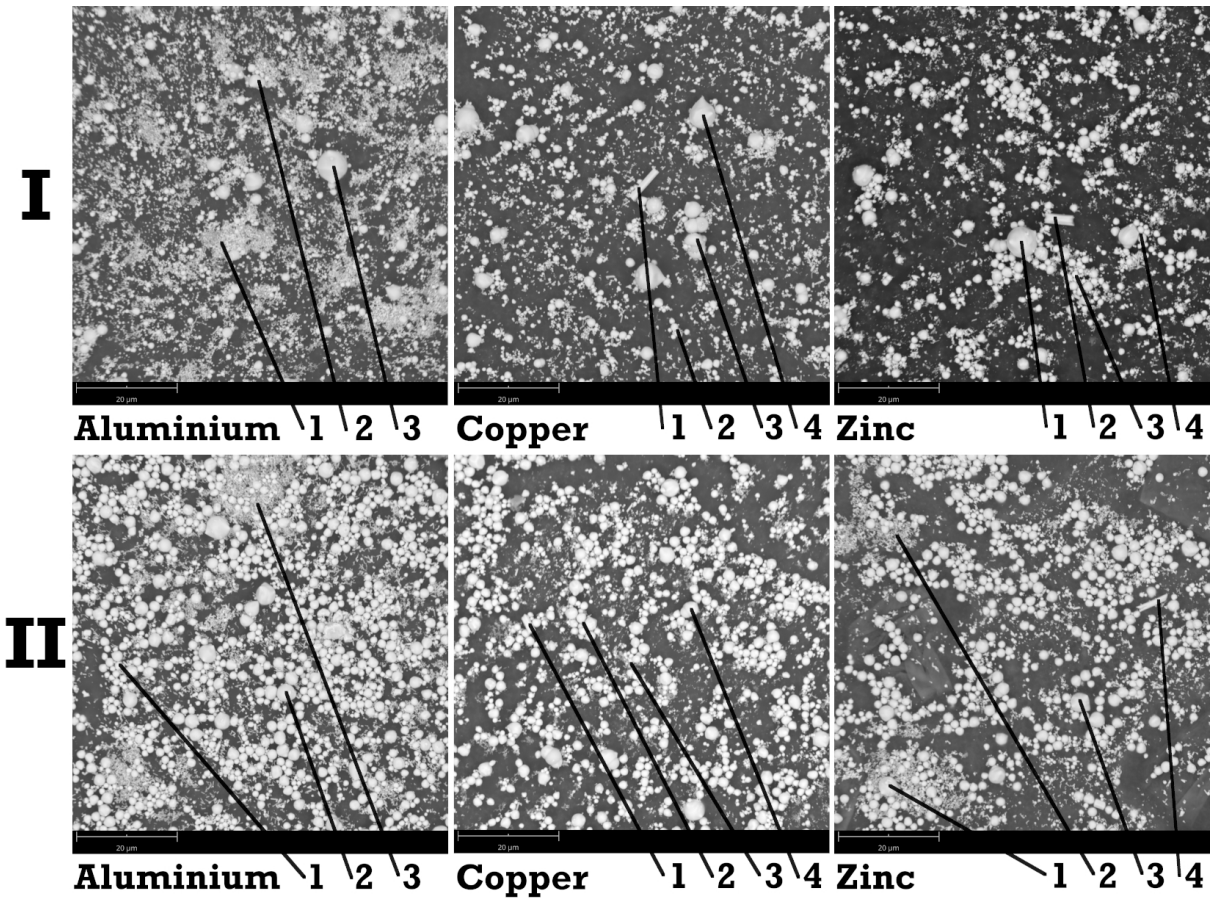

Figure 17. Six micrographs from dry (I) and humid (II) reducing conditions experiments, each showing the deposits from the aluminum (left), copper (middle), and zinc (right) surfaces.

Tellurium is expected considering the temperature and reducing conditions at higher temperature. Similar to the inert conditions the presence of oxygen may come from slight oxidation during storage/transport to the SEM/EDX analysis, or that air leaked in during the experiment.

In the diffractograms produced from the deposits from the metals surfaces and filters under both reducing conditions, only metallic Te was detected. The corresponding diffractograms are shown in Figure 18.

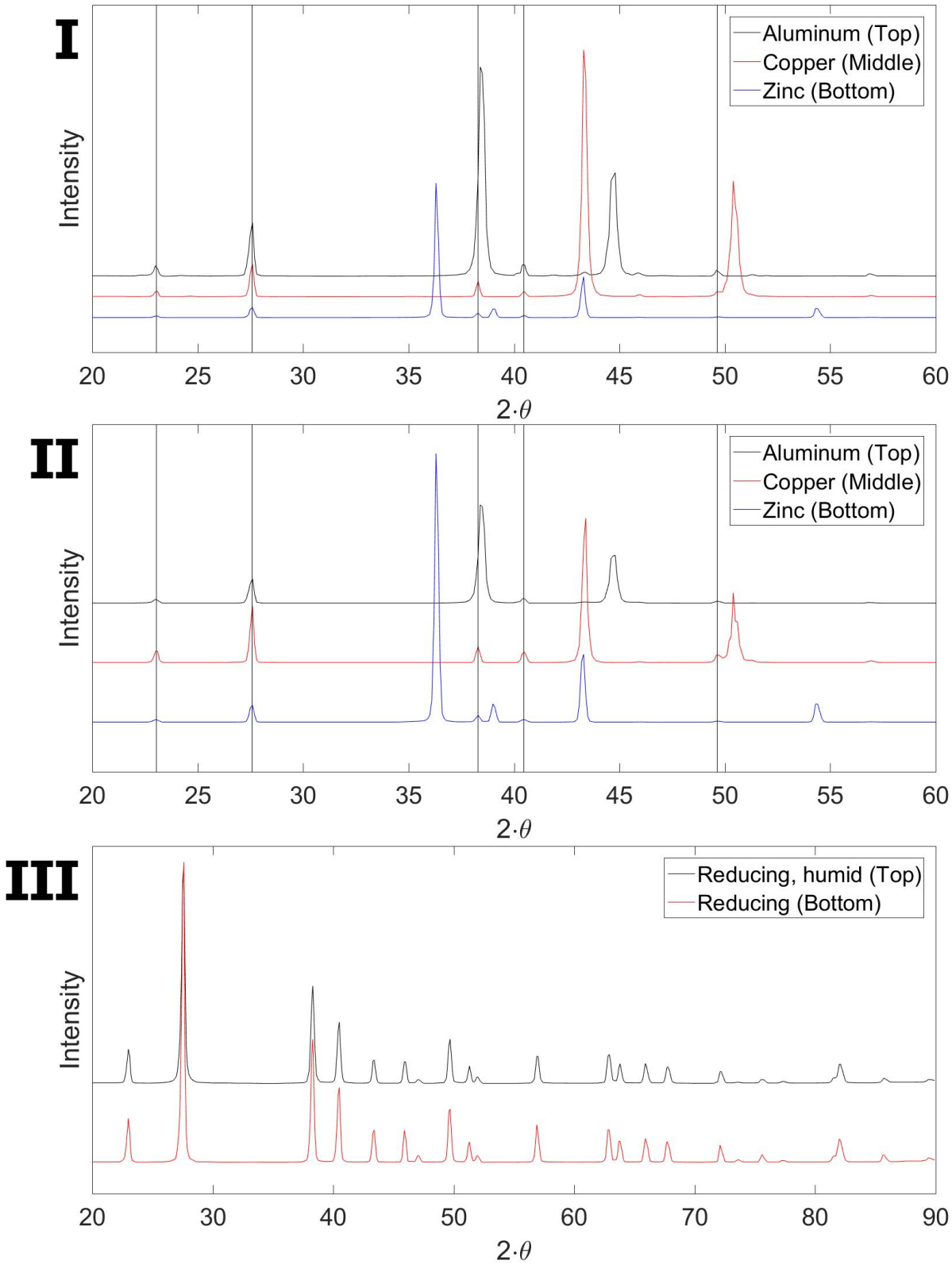

Figure 18. The X-ray diffraction analyzes of the depositions formed on the metal surfaces from the dry (I) and humid (II) inert conditions experiments. Diffractograms for the filter used during these experiments are also shown (III).

Little difference between dry and humid reducing conditions can be seen in these diffractograms. These results are also similar to the result obtained for inert conditions. This indicates that neither the inert nor the reducing conditions or increasing the humidity of the two, had any effect on the speciation of tellurium at room temperature.

The content of the liquid sodium hydroxide traps under the two reducing conditions only showed detectable amounts of tellurium and aluminum under humid conditions. Around $1.1\%_{wt}$ of tellurium compared to the orignal precursor amount and 0.2 mg of aluminum were measured.

Similar to the observed aluminum under humid inert conditions, the source may be the tube itself as no aluminum was detect in the deposits from the aluminum surface. Under reducing conditions, a possible species that could have reacted with the tube is H_2Te [58]. Additionally, the formation of this species may also have promoted the transport of tellurium to the liquid sodium hydroxide trap.

5.4 Spray Experiment

To determine the efficiency of the CSS with regards to tellurium-bearing species, experiments were carried out under two conditions (oxidizing or inert) with two different precursors (metallic tellurium or tellurium dioxide) and three different spray solutions (water, alkaline borate solution with and without sodium thiosulphate). For this work, only the experimental part of paper IV is considered. Only singlets of the samples were acquired and the experimental uncertainties of these results are unknown.

For the three locations consisting of the crucible, the sump, and the filter, weights from each experiment were determined with a balance (crucible), ICP-MS (sump), or INAA (filter). The results of these are summaries are shown in Table 20. In this table, the efficiencies of the spray solutions used has been given. This has been calculated using the tellurium value from the experiments without any spray used as a reference.

Table 20. The outcome of the experiments from the spray experiments. Values referred to as "Released" are how much mass left the crucible. The efficiency is determined by comparing the filter with spray solutions to the case without any solution.

Experiment	Released [mg]	Spray solution	Sump [mg]	Filter [mg]	Efficiency [%]
D-1	199	a: Non		0.240	
		b: Water	6.2	0.042	83
		c: ABS w/o	2.0	0.001	99.5
		d: ABS w	1.4	0.008	97
D-2	255	a: Non		0.570	
		b: Water	14	0.069	88
		c: ABS w/o	2.6	0.016	97
		d: ABS w	1.9	0.016	97
D-3	295	a: Non		0.588	
		b: Water	27	0.047	92
		c: ABS w/o	2.8	0.013	98
		d: ABS w	2.4	0.013	98
D-4	51	a: Non		0.373	
		b: Water	5.2	0.063	83
		c: ABS w/o	1.0	0.002	99.5
		d: ABS w	0.64	0.002	99.5
D-5	-51	a: Non		0.023	
		b: Water	2.0	0.006	74
		c: ABS w/o	0.74	0.007	70
		d: ABS w	0.43	0.003	86
D-6	-7	a: Non		0.283	
		b: Water	5.3	0.020	93
		c: ABS w/o	0.8	0.002	99
		d: ABS w	0.3	0.002	99
D-7	789	a: Non		0.497	
		b: Water	9.7	0.180	64
		c: ABS w/o	9.0	0.138	72
		d: ABS w	7.4	0.125	75
D-8	883	a: Non		0.348	
		b: Water	24	0.150	57
		c: ABS w/o	22	0.128	63
		d: ABS w	13	0.107	69
D-9	[a]	a: Non		0.177	
		b: Water	5.6	0.017	90
		c: ABS w/o	4.6	0.009	95
		d: ABS w	1.0	0.007	96

ABS: Alkaline borate solution; w/o: without sodium thiosulfate; w: with sodium thiosulfate; [a]The same as for D-8

In all of these experiments, the heating of the precursor resulted in vaporization. This can be observed for most experiments by the released amounts. However, the values of the metallic tellurium under oxidizing conditions show a very small release and even negative values. This can be explained by the oxidization of the precursor, which resulted in a mass increase of the precursor, to such an extent that it offsets the occurred mass loss. Therefore, these specific results are not only showing the released amounts, but also mass increase due to the oxidation.

Almost all experimental conditions and precursor types, showed an increase in the removal efficiency when adding the chemicals to the spray solution. The only exception was under humid oxidizing conditions using metallic tellurium as a precursor (D-5:c); then a slight decrease was observed of the removal efficiency when using alkaline borate solution without sodium thiosulfate. However, the addition of sodium thiosulfate (D-5:d) increased the efficiency again to above that of the pure water. Furthermore, generally, the highest efficiencies were attained under oxidizing conditions with both of the precursors. The only exception was under humid oxidizing conditions with metallic tellurium as a precursor (D-5), where the efficiency was noticeably lower (for all spray solution types) compared to all other oxidizing conditions (regardless of precursor). The experiments performed under inert conditions (D-7, D-8, D-9), revealed that humid inert conditions (D-8) had the lowest efficiencies of tellurium removal, whereas humid inert with added cesium iodide (D-9) showed the highest efficiencies. Aside from the latter experiments, the removal efficiencies were generally lowest under inert conditions. Additionally, the experiments performed under humid oxidizing with metallic tellurium as the precursor (D-5) may have had low efficiencies for tellurium removal. However, a possible artifact from the experiments under oxidizing conditions with metallic tellurium could be the previously mentioned oxidization of the precursor. This may have affected these results, but the effect should have been minimal as the experiments were performed consequently. Another artifact that may have affected the result attained from the sump may have been the deposition of tellurium on the wall from the preceding reference experiment. The sumps formed when the first spray solution was used (i.e., the pure water spray) most likely contain extra tellurium from the preceding reference experiment. These values are therefore not necessarily representative of the actual experiment. However, this effect on the consecutive experiments with solutions containing added chemicals should be minimal.

The effectiveness of using a spray for removing tellurium has been shown through these results, as well as the enhanced effect of the use of chemicals. In general, more than half of the airborne tellurium was removed under all conditions using only water as the spray solution. This was then improved further, almost fully removing all airborne tellurium once the investigated chemicals were used for the oxidizing conditions (D-5 being an exception) with both precursors (tellurium dioxide and metallic tellurium). However, under inert conditions using metallic tellurium as a precursor, the removal efficiency was noticeably lower under dry and humid conditions. However, when cesium iodide was added to the experiment the removal efficiency reached almost full removal of airborne tellurium, indicating a possible change in the speciation of the gaseous tellurium. Observing existing literature [58], the species could be a cesium telluride as it has been suggested to be highly soluble in water and the tellurium dioxide is only slightly soluble in water [92].

Comparing the two conditions, it is clear that the speciation prevailing under the oxidizing conditions (regardless of precursor) will be efficiently reduced. However, under inert conditions the effectiveness of the spray was noticeable lower, with the exception when cesium iodide was part of the experiment. An explanation to this may be the difference in solubility between the

oxides of tellurium (e.g., TeO_2) and metallic tellurium. As e.g., tellurium dioxide is soluble [83] and metallic tellurium would not dissolve as it is stable in water [119]. This is further supported by a slight increase under oxidizing conditions when the investigated chemicals were added, i.e., higher pH of the solution. Consequently, this will increase the solubility of tellurium dioxide and therefore more would be removed from the gas. The increase in pH could also explain the increase removal efficiency observed under inert conditions. However, if it is the solubility that is the main reason for these observation requires further investigation.

6 Summary

This work has investigated the effect of several aspects concerning the chemistry of the tellurium source term in terms of volatility under oxidizing and inert conditions. These conditions are possible, either under an accident with air ingress or if an inert gas would be injected to prevent a hydrogen explosion. The topics that have been discussed in this work were the use of seawater as an emergency cooling medium, the effect by cesium iodide, and surfaces found in a BWR containment. The effectiveness of the CSS on airborne tellurium was also determined. Following paragraphs contains a summary of each experiment dedicated to each aspect.

From the seawater experiments, evidence was found that under oxidizing conditions the sodium chloride increased the release of tellurium. This as a mass increase observed for the pure tellurium reference was lacking in all the samples. Furthermore, samples acquired through the furnace experiments showed an unexpected mass loss and disappearance of the precursor residue at lower temperatures than the melting point of sodium chloride. Thus, it is possible that under these investigated conditions the presence of sodium chloride will increase the released tellurium. Under inert conditions, these results provided no evidence that sodium chloride had any effect on tellurium. However, it also not possible to exclude pure gas-phase interaction or interaction at the high end of the temperatures scale investigated from these results.

During the RCS experiments, tellurium was affected both by the presence of cesium iodide and due to the conditions investigated. Under oxidizing conditions, the amount of tellurium transported was decreased when cesium iodide was investigated, and a new unidentified species appeared on the filter. A new species was also observed under humid oxidizing conditions, which was different from the species observed under humid oxidizing conditions with cesium iodide. This indicates that a change in speciation due to the presence of humidity as well as cesium iodide occurred, which for the latter was not possible to correlate to cesium. Under inert conditions, the addition of cesium iodide enhanced the transported amount of tellurium, and a new species related to tellurium was observed. Moreover, a new species related cesium was also seen that was identified as metallic cesium, which unlikely considering that it is unstable in air. Thus, a cesium-tellurium species may have formed.

From the experiments involving tellurium deposition inside a BWR containment, deposits were formed under all investigated conditions (oxidizing, inert, reducing) on all three surfaces (aluminum, copper, zinc). Under oxidizing conditions, tellurium dioxide was found in all deposits and filters. When the humidity was increased one more crystal structure of the tellurium dioxide was seen in the deposits and the highest amount of tellurium was transported. This could be explained by the formation of transient species ($TeO(OH)_2$) formed under humid oxidizing conditions, which as temperature drops could form the alternative crystal structure of tellurium dioxide. An alternative explanation could be that a water film formed on the surfaces, enabling more of the tellurium dioxide with the different crystal structure to be trapped. Of the surface investigated, only the zinc was found to be affecting the tellurium under humid oxidizing conditions. As the deposit from the zinc surface contained zinc as well as the sodium hydroxide liquid trap, located after the filter. This indicates that the zinc left the surface and likely due to the tellurium as the reference without tellurium did not have any zinc in the trap. The reason for this may be related to either the reactiveness of the transient species or the water film formed on the zinc surface enabling a reaction. Under inert and reducing conditions, only metallic tellurium was observed in the deposits from the metal surfaces and on the filters. Thus, the humidity

had little effect on the speciation on the formed deposits. Additionally, under humid reducing conditions the second-highest amount of tellurium was observed. This can be explained by the formation of H_2Te. From these experiments, it is clear that tellurium will react with zinc surfaces in the containment under humid oxidizing conditions.

Investigating the removal effectiveness of the CSS was done using two conditions (oxidizing, inert), that was dry and humid with either without or with cesium iodide. Furthermore, either one (inert conditions) or two (oxidizing conditions) tellurium precursor (tellurium, tellurium dioxide) with three different spray solutions (water and alkaline borate solution, without and with sodium thiosulfate) were used. Under oxidizing conditions, the removal efficiencies using both precursors were high using only pure water. The result was a removal efficiency of airborne tellurium above a least 70%, which was higher when more chemicals were added to the spray solutions. One exception was the experiment with metallic tellurium under humid oxidizing conditions, where a decrease occurred with the alkaline borate solution without thiosulfate and then an increase for the alkaline borate solution with sodium thiosulfate). This may have been an experimental error. For the dry and humid inert conditions, a generally lower efficiencies were observed. With only using water, the spray removal efficiencies were notably lower than under oxidizing conditions, at a minimum of 50%. This percentage increased when the chemicals were added, but still lower than most oxidizing conditions. However, when cesium iodide was added to the experiment the removal efficiency became almost equal to that of the oxidizing conditions at 90% with only water as the spray solution. This was further enhanced with the addition of the chemicals. Comparing the oxidizing to the inert conditions, one explanation to the decrease removal efficiencies could be the difference in speciation. As under oxidizing conditions, tellurium dioxide is present at the lower temperatures (e.g., the temperatures that exist in the volume related to the spray) and is slightly more soluble than metallic tellurium. This could also explain high efficiency observed for the humid inert conditions with added cesium iodide as if Cs_2Te had formed it is also more soluble then metallic tellurium.

7 Conclusions

In this work, the volatility of the tellurium source term under oxidizing condition representing an air ingress accident and inert condition as a result if injection of inert gas have been explored. This in the context of using seawater as an emergency cooling, by the effect of cesium iodide in the RCS, and with the different metallic surface found inside a BWR. This was followed by determining the CSS effectiveness in removing airborne tellurium.

The volatility of the tellurium source term under oxidizing conditions has been shown to be affected in the experiments. Using seawater as an emergency coolant was shown to enhance it. As the sodium chloride was shown to possibly increase the volatility of tellurium. The effect on volatility from cesium iodide was also demonstrated, as less tellurium was transported when it was part of the gas flow. However, no species were found to be correlated to a cesium-tellurium compound. Additionally, the volatility was also enhanced by humidity as the literate had suggested. Of the surfaces found in a BWR containment, only zinc was found to interact under high humidity with the airborne tellurium. However, determining if this enhanced or reduced the volatility was not possible nor what species was formed. The effectiveness of the CSS was also demonstrated as more than 80% of the tellurium was removed using only water and even higher when adding chemicals to the solution. This possibly related to the solubility of species formed.

The investigation into the volatility of the tellurium source term under inert conditions showed that not all considered topics changed the volatility. Using seawater as an emergency coolant was shown to have minimal effect on the volatility. However, cesium iodide did as more tellurium was transported when cesium iodide was part of the gas. Additionally, this effect was further supported by observing unidentified tellurium species that were possibly correlated to cesium. Indicating an enhanced volatility of tellurium due the formation of new tellurium species. Contrary, the metallic surfaces found in the BWR containment were shown not to notably change the volatility nor altering the tellurium speciation. Additionally, the increased humidity did not either change the speciation. Exploring the effectiveness of the CSS, it was noticeable lower than oxidizing conditions, still above 50% with pure water, and increase slightly with added chemicals to the solution. Noticeably, the addition of cesium iodide to the gas resulted in a significant improvement to above 80%. Possibly, explained by very low solubility of metallic tellurium and a high solubility of cesium telluride.

As seen in this work, there are several possible factors during a nuclear accident that could increase the volatility of tellurium. However, with a maintained CSS, most of the tellurium will end-up in the containment sump.

8 Future Work

Several possible pathways are possible for the continued work with the chemistry of tellurium source term. One way to continue the investigation with tellurium in the gas phase of the RCS, is by further exploring the effect by cesium iodide, to determine the species that may have formed under the conditions investigated in this work. Additionally, more conditions could be explored such as reducing conditions and the already investigated conditions but without humidity. However, other species may also be added to the gas phase to see the effect of them on the airborne tellurium (e.g., air radiolysis product such as N_2O, NO_2 or different material from the control rod, such as silver). Another aspect that would merit further research effort is the effect of different organic on tellurium. This could be done by the addition of relevant organic gases to the atmosphere or interaction with different objects that contain relevant organic sources (e.g., paint, cables). Finally, considering the effectiveness of the spray on the airborne tellurium in the containment, it would also be relevant to investigate the tellurium chemistry of the sump with cesium iodide.

9 Acknowledgments

A great deal of thanks to:

Christian Ekberg, my supervisor. For all the help given during this time as a PhD-student. For the discussions, comments, and the better understanding of science.

Henrik Glänneskog, for instilling the reality to the work and pushing the work forward with structure and questions.

Mark Foreman, for the inspiring effort towards scientific progress and showing the thrill of it.

Britt-Marie Steenari, my examiner.

Gabriele Lombardo, for enduring me the longest of all the Phd-students and being a GoodFella.

PhD-students, old and new that I meet at the department for without you the place would have been less.

All the other colleagues, for answering questions and creating a workplace that is both interesting and fun.

Min familj och vänner, för utan er så hade detta slutat tidigare.

This work was founded by the APRI-9 and APRI-10 (Accident Phenomena of Risk Importance). NKS (Nordic Nuclear Safety Research) is acknowledge in there funding of the part of tellurium experiments at VTT.

References

[1] British Petroleum Company. *Bp Statistical Review of World Energy*. 68^{th} Edition. British Petroleum Co., 2018.

[2] V. Masson-Delmotte, P. Zhai, H.-O. Pörtner, D. Roberts, J. Skea, P.R. Shukla, A. Pirani, W. Moufouma-Okia, C. Péan, R. Pidcock, S. Connors, J.B.R. Matthews, Y. Chen, X. Zhou, M.I. Gomis, E. Lonnoy, T. Maycock, and M. Tignor. *Global Warming of 1.5°C,* Intergovernmental Panel on Climate Change, 2019.

[3] T. Bruckner, I.A. Bashmakov, Y. Mulugetta, H. Chum, A. de la Vega Navarro, J. Edmonds, A. Faaij, B. Fungtammasan, A. Garg, E. Hertwich, D. Honnery, D. Infield, M. Kainuma, S. Khennas, S. Kim, H.B. Nimir, K. Riahi, N. Strachan, R. Wiser, and X. Zhang. *Climate Change 2014: Mitigation of Climate Change. Contribution of Working Group III to the Fifth Assessment Report of the Intergovernmental Panel on Climate Chang*. Intergovernmental Panel on Climate Change, 2014.

[4] European Commission. *Communication From the Commission to the European Parliment and the Council: European Energy Security Strategy*. 2014. URL: http://eur-lex.europa.eu/legal-content/EN/TXT/?uri=CELEX\%3A52014DC0330,2020-01-15.

[5] Y. Pontillon, G. Ducros, and P.P. Malgouyres. "Behaviour of fission products under severe PWR accident conditions VERCORS experimental programme—Part 1: General description of the programme". In: *Nuclear Engineering and Design* 240.7 (2010), pp. 1843 –1852. ISSN: 0029-5493.

[6] Y. Pontillon and G. Ducros. "Behaviour of fission products under severe PWR accident conditions: The VERCORS experimental programme—Part 2: Release and transport of fission gases and volatile fission products". In: *Nuclear Engineering and Design* 240.7 (2010), pp. 1853 –1866. ISSN: 0029-5493.

[7] Y. Pontillon and G. Ducros. "Behaviour of fission products under severe PWR accident conditions. The VERCORS experimental programme—Part 3: Release of low-volatile fission products and actinides". In: *Nuclear Engineering and Design* 240.7 (2010), pp. 1867 –1881. ISSN: 0029-5493.

[8] Y. Pontillon, E. Geiger, C. Le Gall, S. Bernard, A. Gallais-During, P.P. Malgouyres, E. Hanus, and G. Ducros. "Fission products and nuclear fuel behaviour under severe accident conditions part 1: Main lessons learnt from the first VERDON test". In: *Journal of Nuclear Materials* 495 (2017), pp. 363 –384. ISSN: 0022-3115. DOI: 10.1016/j.jnucmat.2017.08.021.

[9] E. Geiger, C. Le Gall, A. Gallais-During, Y. Pontillon, J. Lamontagne, E. Hanus, and G. Ducros. "Fission products and nuclear fuel behaviour under severe accident conditions part 2: Fuel behaviour in the VERDON-1 sample". In: *Journal of Nuclear Materials* 495 (2017), pp. 49 –57. ISSN: 0022-3115. DOI: 10.1016/j.jnucmat.2017.08.002.

[10] C. Le Gall, E. Geiger, A. Gallais-During, Y. Pontillon, J. Lamontagne, E. Hanus, and G. Ducros. "Fission products and nuclear fuel behaviour under severe accident conditions part 3: Speciation of fission products in the VERDON-1 sample". In: *Journal of Nuclear Materials* 495 (2017), pp. 291 –298. ISSN: 0022-3115. DOI: 10.1016/j.jnucmat.2017.08.001.

[11] B. Clément and R. Zeyen. "The objectives of the Phébus FP experimental programme and main findings". In: *Annals of Nuclear Energy* 61 (2013). Special Issue : Phebus FP Final Seminar, pp. 4 –10. ISSN: 0306-4549.

[12] T. Haste, F. Payot, C. Manenc, B. Clément, Ph. March, B. Simondi-Teisseire, and R. Zeyen. "Phébus FPT3: Overview of main results concerning the behaviour of fission products and structural materials in the containment". In: *Nuclear Engineering and Design* 261 (2013), pp. 333 –345. ISSN: 0029-5493.

[13] P. March and B. Simondi-Teisseire. "Overview of the facility and experiments performed in Phlébus FP". In: *Annals of Nuclear Energy* 61 (2013). Special Issue : Phebus FP Final Seminar, pp. 11 –22. ISSN: 0306-4549.

[14] A.V. Jones, R. Zeyen, and M. Sangiorgi. *Circuit and Containment Aspects of PHÉBUS Experiment FPT0 and FPT1*. EUR 27218. Publications Office of the European Union, 2015. DOI: 10.2790/740439.

[15] M. Sangiorgi, A. Grah, and L. Ammirabile. *Circuit and Containment Aspects of PHÉBUS Experiment FPT-2*. EUR 27631. Publications Office of the European Union, 2015. DOI: 10.2790/94418.

[16] H. Glänneskog. "Interactions of I2 and CH3I with reactive metals under BWR severe-accident conditions". In: *Nuclear Engineering and Design* 227.3 (2004), pp. 323 –329. ISSN: 0029-5493. DOI: 10.1016/j.nucengdes.2003.11.008.

[17] H. Glänneskog, J.O. Liljenzin, and L Sihver. "Reactions between reactive metals and iodine in aqueous solutions". In: *Journal of Nuclear Materials* 348.1 (2006), pp. 87 –93. ISSN: 0022-3115. DOI: 10.1016/j.jnucmat.2005.09.004.

[18] J. Holm, H. Glänneskog, and C. Ekberg. "Deposition of RuO_4 on various surfaces in a nuclear reactor containment". In: *Journal of Nuclear Materials* 392.1 (2009), pp. 55 –62. ISSN: 0022-3115. DOI: 10.1016/j.jnucmat.2009.03.047.

[19] S. Tietze, M.R.StJ. Foreman, and C. H. Ekberg. "Formation of organic iodides from containment paint ingredients caused by gamma irradiation". In: *Journal of Nuclear Science and Technology* 50.7 (2013), pp. 689–694. DOI: 10.1080/00223131.2013.799400.

[20] S. Tietze, M.R.StJ. Foreman, C. H. Ekberg, and B.E. van Dongen. "Identification of the chemical inventory of different paint types applied in nuclear facilities". In: *Journal of Radioanalytical Nuclear Chemistry* 295 (2013), 1981–1999. DOI: 10.1007/s10967-012-2190-3.

[21] I Kajan, T. Kärkelä, U. Tapper, L.S. Johansson, M. Gouëllo, H. Ramebäck, S. Holmgren, A. Auvinen, and C. Ekberg. "Impact of Ag and NOx compounds on the transport of ruthenium in the primary circuit of nuclear power plant in a severe accident". In: *Annals of Nuclear Energy* 100 (2017), pp. 9 –19. ISSN: 0306-4549. DOI: 10.1016/j.anucene.2016.10.008.

[22] I. Kajan, T. Kärkelä, A. Auvinen, and C. Ekberg. "Effect of nitrogen compounds on transport of ruthenium through the RCS". In: *Journal of Radioanalytical Nuclear Chemistry* 311 (2017), pp. 2097–2109. DOI: 10.1007/s10967-017-5172-7.

[23] J.T. Smith. *Nuclear Power and the Environment. Nuclear Accidents*. Ed. by R.M. Harrison and R.E. Hester. Issues in Environmental Science and Technology. The Royal Society of Chemistry, 2011, pp. 57–81. ISBN: 978-1-84973-194-2. DOI: 10.1039/9781849732888.

[24] G. Katata, M. Chino, T. Kobayashi, H. Terada, M. Ota, H. Nagai, M. Kajino, R. Draxler, M. C. Hort, A. Malo, T. Torii, and Y. Sanada. "Detailed source term estimation of the atmospheric release for the Fukushima Daiichi Nuclear Power Station accident by coupling simulations of an atmospheric dispersion model with an improved deposition scheme and oceanic dispersion model". In: *Atmospheric Chemistry and Physics* 15.2 (2015), pp. 1029–1070. DOI: 10.5194/acp-15-1029-2015.

[25] N.A. Beresford and J. Smith. *Chernobyl: Catastrophe, Consequences and Solutions*. 1st ed. Environmental Sciences. Berlin Heidelberg: Springer- Verlag, 2005. ISBN: 3-540-23866-2. DOI: 10.1007/3-540-28079-0.

[26] International Atomic Energy Agency IAEA. *The Fukushima Daiichi Accident*. Non-serial Publications. Vienna: IAEA, International Atomic Energy Agency, 2015. ISBN: 978-92-0-107015-9.

[27] R. Wakeford. "The Windscale reactor accident–50 years on." In: *Journal of radiological protection* 27 (2007), pp. 211–215. DOI: 10.1088/0952-4746/27/3/E02.

[28] A. Duchac and M. Noel. "Disturbances in the European Nuclear Power Plant Safety Related Electrical Systems". In: *Journal of Electrical Engineering-Elektrotechnicky Casopis* 62.3 (2011), pp. 173–180. DOI: 10.2478/v10187-011-0029-8.

[29] G. Steinhauser, A. Brandl, and T.E. Johnson. "Comparison of the Chernobyl and Fukushima nuclear accidents: A review of the environmental impacts". In: *Science of The Total Environment* 470-471 (2014), pp. 800 –817. ISSN: 0048-9697. DOI: 10.1016/j.scitotenv.2013.10.029.

[30] World Nuclear Association. *Safety of Nuclear Power Reactors*. 2019-06. URL: https://www.world-nuclear.org/information-library/safety-and-security/safety-of-plants/safety-of-nuclear-power-reactors.aspx (visited on 06/01/2020).

[31] B.R. Sehgal. "Chapter 1 - Light Water Reactor Safety: A Historical Review". In: *Nuclear Safety in Light Water Reactors*. Ed. by Bal Raj Sehgal. Boston: Academic Press, 2012, pp. 1–88. ISBN: 978-0-12-388446-6. DOI: 10.1016/B978-0-12-388446-6.00001-0.

[32] C.R.F. Azevedo. "Selection of fuel cladding material for nuclear fission reactors". In: *Engineering Failure Analysis* 18.8 (2011), pp. 1943 –1962. ISSN: 1350-6307. DOI: 10.1016/j.engfailanal.2011.06.010.

[33] W.L. Server and R.K. Nanstad. "1 - Reactor pressure vessel (RPV) design and fabrication: the case of the USA". In: *Irradiation Embrittlement of Reactor Pressure Vessels (RPVs) in Nuclear Power Plants*. Ed. by N. Soneda. Woodhead Publishing Series in Energy. Woodhead Publishing, 2015, pp. 3 –25. ISBN: 978-1-84569-967-3. DOI: 10.1533/9780857096470.1.3.

[34] *Design of Reactor Containment Systems for Nuclear Power Plants*. Specific Safety Guides NS-G-1.10. Vienna: INTERNATIONAL ATOMIC ENERGY AGENCY, 2004. ISBN: 92-0-103604-3.

[35] H. Pham and W.J. Galyean. "Reliability analysis of nuclear fail-safe redundancy". In: *Reliability Engineering & System Safety* 37.2 (1992), pp. 109–112. ISSN: 0951-8320. DOI: 10.1016/0951-8320(92)90003-4.

[36] M. Lilja, T. Johansen, R.E. Grini, and Ø. Berg. "Development of an Early Fault Detection System for Nuclear Power Plants". In: *IFAC Proceedings Volumes* 21.5 (1988). 3rd IFAC Conference on Analysis, Design and Evaluation of Man-Machine Systems 1988, Oulu, Finland, 14-16 June 1988, pp. 93 –98. ISSN: 1474-6670. DOI: 10.1016/S1474-6670(17)53888-4.

[37] United States Nuclear Regulatroy Commission. *Scram*. 2019-03. URL: https://www.nrc.gov/reading-rm/basic-ref/glossary/scram.html (visited on 06/02/2020).

[38] R.W. Shumway. "GENERAL FEATURES OF EMERGENCY CORE COOLING SYSTEMS". In: *Nuclear Power Safety*. Ed. by J.H. Rust and L.E. Weaver. Oxford: Pergamon, 1976, pp. 281 –302. ISBN: 978-0-08-021744-4. DOI: 10.1016/B978-0-08-021744-4.50014-2.

[39] M. Bal, R.C. Jose, and B.C. Meikap. "Control of accidental discharge of radioactive materials by filtered containment venting system: A review". In: *Nuclear Engineering and Technology* 51.4 (2019), pp. 931 –942. ISSN: 1738-5733. DOI: 10.1016/j.net.2019.01.008.

[40] M. Dehjourian, M Rahgoshay, R. Sayareh, G. Jahanfarnia, and A.S. Shirani. "Effect of Spray System on Fission Product Distribution in Containment During a Severe Accident in a Two-Loop Pressurized Water Reactor". In: *Nuclear Engineering and Technology* 48.4 (2016), pp. 975 –981. ISSN: 1738-5733. DOI: 10.1016/j.net.2016.03.007.

[41] "Fission Product Release and Transport". In: *Nuclear Safety in Light Water Reactors: Severe Accident Phenomenology*. Ed. by B.R. Sehgal. 1st ed. Boston: Academic Press, 2012. Chap. 5, pp. 426–517. ISBN: 978-0-12-388446-6. DOI: 10.1016/B978-0-12-388446-6.00005-8.

[42] L. Soffer, S. B. Burson, C. M. Ferrell, R. Y. Lee, and J. N. & Ridgely. *Accident source terms for Light-Water Nuclear Power Plants*. Report. NUREG-1465. 1995.

[43] A. Bentaïb, H. Bonneville, B. Clèment, M. Cranga, G. Ducros, F. Fichot, C. Journeau, V. Koundy, D. Magallon, R. Meignen, J.M. Seiler, and B. Tourniaire. "Development of the core melt accident". In: *Nuclear Power Reactor Core Melt Accidents*. Ed. by D. Jacquemain. 1st ed. 2015. Chap. 5, pp. 101–300. ISBN: 978-2-7598-1930-0.

[44] "A study on the hydrogen recombination rates of catalytic recombiners and deliberate ignition". In: *Nuclear Engineering and Design* 166.3 (1996). Topical Issue on The Third International Conference on Containment Design and Operation, pp. 481 –494. ISSN: 0029-5493. DOI: 10.1016/S0029-5493(96)01264-2.

[45] M. Fischer, S.V. Bechta, V.V. Bezlepkin, R. Hamazaki, and A. Miassoedov. "Core Melt Stabilization Concepts for Existing and Future LWRs and Associated Research and Development Needs". In: *Nuclear Technology* 196.3 (2016), pp. 524–537. DOI: 10.13182/NT16-19.

[46] J.H.S. Lee and M. Berman. "Hydrogen Combustion and Its Application to Nuclear Reactor Safety". In: *Heat Transfer in Nuclear Reacter Safety*. Ed. by G.A. Greene, J.P. Hartnett, T.F. Irvine, and Y.I. Cho. Vol. 29. Advances in Heat Transfer. Elsevier, 1997, pp. 59 –127. DOI: 10.1016/S0065-2717(08)70184-9.

[47] T.K. Blanchat and M D. Allen. "Experiments to investigate DCH phenomena with large-scale models of the Zion and Surry nuclear power plants". In: *Nuclear Engineering and Design* 164.1 (1996), pp. 147 –174. ISSN: 0029-5493. DOI: 10.1016/0029-5493(96)01218-6.

[48] M.E. Witherspoon and A.K. Postma. *Leakage of fission products from artificial leaks in the Containment Systems Experiment*. BNWL–1582.

[49] G. Berthoud. "Vapor Explosions". In: *Annual Review of Fluid Mechanics* 32.1 (2000), pp. 573–611. DOI: 10.1146/annurev.fluid.32.1.573.

[50] "Steam generator tube rupture (SGTR) scenarios". In: *Nuclear Engineering and Design* 235.2 (2005), pp. 457 –472. ISSN: 0029-5493. DOI: 10.1016/j.nucengdes.2004.08.060.

[51] Y. Kanai. "Geochemical behavior and activity ratios of Fukushima-derived radionuclides in aerosols at the Geological Survey of Japan, Tsukuba, Japan". In: *Journal of Radioanalytical and Nuclear Chemistry* 303.2 (2015), pp. 1405–1408. DOI: 10.1007/s10967-014-3495-1.

[52] "Composition of Seawater and Ionic Strength at Various Salinities". In: *CRC Handbook of Chemistry and Physics*. Ed. by J. R. Rumble. 101st Edition (Internet Version 2020). Boca Raton, FL.: RC Press/Taylor & Francis.

[53] "Physical Constants of Inorganic Compounds". In: *In CRC Handbook of Chemistry and Physics*. Ed. by J.R. Rumble. 100 (Internet Version 2019. CRC Press/Taylor & Francis, Boca Raton, FL. Chap. 5.

[54] World Nuclear Association. *Nuclear Fuel Cycle Overview*. 2020-05. URL: https://www.world-nuclear.org/information-library/nuclear-fuel-cycle/introduction/nuclear-fuel-cycle-overview.aspx (visited on 06/01/2020).

[55] G. Choppin, J.O. Liljenzin, J. Rydberg, and C. Ekberg. "Chapter 21 - The Nuclear Fuel Cycle". In: *Radiochemistry and Nuclear Chemistry*. Ed. by G. Choppin, J.O. Liljenzin, J. Rydberg, and C. Ekberg. Fourth Edition. Oxford: Academic Press, 2013, pp. 685–751. ISBN: 978-0-12-405897-2. DOI: 10.1016/B978-0-12-405897-2.00021-5.

[56] H. Kleykamp. "The Chemical State of the Fission Products in Oxide Fuels". In: *Journal of Nuclear Materials* Vol. 131 (1985), pp. 221–246.

[57] G. Choppin, J.O. Liljenzin, J. Rydberg, and C. Ekberg. "Chapter 11 - Mechanisms and Models of Nuclear Reactions". In: *Radiochemistry and Nuclear Chemistry*. Ed. by G. Choppin, J.O. Liljenzin, J. Rydberg, and C. Ekberg. Fourth Edition. Oxford: Academic Press, 2013, pp. 313 –338. ISBN: 978-0-12-405897-2. DOI: 10.1016/B978-0-12-405897-2.00011-2.

[58] A. Alonso and C González. *Modelling the chemical behaviour of tellurium species in the reactor pressure vessel and the reactor cooling system under severe accident conditions*. Report. EUR–13787. Commission of the European Communities (CEC), The Joint Research Centre, 1991.

[59] J. Magill, G. Pfenning, R. Dreher, and Z. Sòti. *Karlsruher Nuklidkarte, 7th ed.* 2015.

[60] N. Bixler, R. Gauntt, J. Jones, and M. Leonard. *State-of-the-Art Reactor Consequence Analyses Project Volume 1: Peach Bottom Integrated Analysis*. Report. NUREG/CR-7110. Sandia National Laboratories, Albuquerque, New Mexico 87185, 2013.

[61] E. Cardis, A. Kesminiene, V. Ivanov, I. Malakhova, Y. Shibata, V. Khrouch, V. Drozdovitch, E. Maceika, I. Zvonova, O. Vlassov, A. Bouville, G. Goulko, M. Hoshi, A. Abrosimov, J. Anoshko, L. Astakhova, S. Chekin, E. Demidchik, R. Galanti, M. Ito, E. Korobova, E. Lushnikov, M. Maksioutov, V. Masyakin, A. Nerovnia, V. Parshin, E. Parshkov, N. Piliptsevich, A. Pinchera, S. Polyakov, N. Shabeka, E. Suonio, V. Tenet, A. Tsyb, S. Yamashita, and D. Williams. "Risk of Thyroid Cancer After Exposure to 131 I in Childhood". In: *JNCI: Journal of the National Cancer Institute* 97.10 (2005), pp. 724–732. DOI: 10.1093/jnci/dji129.

[62] S. Yoshida, M. Ojino, T. Ozaki, T. Hatanaka, K. Nomura, M. Ishii, K. Koriyama, and M. Akashi. "Guidelines for Iodine Prophylaxis as a Protective Measure: Information for Physicians. In: Japan Medical Association journal". In: *Japan Medical Association Journal* 57.3 (2014), pp. 113–123.

[63] L.A. Ba, M. Döring, V. Jamier, and C. Jacob. "Tellurium: an element with great biological potency and potential". In: *Organic & biomolecular chemistry* 8.19 (2010), 4203-4216. DOI: 10.1039/c0Ob00086h.

[64] A. Taylor. "Biochemistry of tellurium". In: *Biological Trace Element Research* 55.3 (1996), 231–239. DOI: 10.1007/BF02785282.

[65] D.A. Powers, L.N. Kmetyk, and R.C. Schmidt. *A review of the technical issues of air ingression during severe reactor accidents*. NUREG/CR–6218. 1994.

[66] X. Lyu, X. Meng, B. Wang, F. Niu, S. Liu, X. Huang, and H. Yin. "Analysis of different inert gas injection point's influence on hydrogen risk during post-inerting in nuclear power plant". In: *Annals of Nuclear Energy* 129 (2019), pp. 249 –252. ISSN: 0306-4549. DOI: 10.1016/j.anucene.2019.01.055.

[67] B.J. Lewis, F.C. Iglesias, C.E.L. Hunt, and D.S. Cox. "Release Kinetics of Volatile Fission Products Under Severe Accident Conditions". In: *Nuclear Technology* 99.3 (1992), pp. 330–342. DOI: 10.13182/NT92-A34717.

[68] R. de Boer and E.H.P. Cordfunke. "The chemical form of fission product tellurium during reactor accident conditions". In: *Journal of Nuclear Materials* 240.2 (1997), pp. 124 –130. ISSN: 0022-3115. DOI: 10.1016/S0022-3115(96)00600-9.

[69] S. Imoto and T. Tanabe. "Chemical state of tellurium in a degraded LWR core". In: *Journal of Nuclear Materials* 154.1 (1988), pp. 62 –66. ISSN: 0022-3115. DOI: 10.1016/0022-3115(88)90119-5.

[70] E.H.P. Cordfunke and R.J.M. Konings. "Chemical interactions in water-cooled nuclear fuel: A thermochemical approach". In: *Journal of Nuclear Materials* 152 (1988), pp. 301 –309. ISSN: 0022-3115. DOI: 10.1016/0022-3115(88)90341-8.

[71] J. McFarlane. "Fission product tellurium chemistry from fuel to containment". In: *Proceedings of the Fourth CSNI Workshop on the Chemistry of Iodine in Reactor Safety* (1996). (PSI–97-02). Guentay, S. (Ed.). Switzerland, pp. 563–585.

[72] J. Mcfarlane and J.C. Leblanc. "Fission-Product Tellurium and Cesium Telluride Chemistry Revisited". In: *Geochimica et Cosmochimica Acta* (1996). (AECL–11333), Canada., pp. 851–866. ISSN: 0067-0367.

[73] P.E. Potter, M.H. Rand, and C.B. Alcock. "Some chemical eouilibria for accident analysis in pressurised water reactor systems". In: *Journal of Nuclear Materials* 130 (1985), pp. 139 –153. ISSN: 0022-3115. DOI: 10.1016/0022-3115(85)90303-4.

[74] L. Desgranges, Ch. Riglet-Martial, I. Aubrun, B. Pasquet, I. Roure, J. Lamontagne, and T. Blay. "Evidence of tellurium iodide compounds in a power-ramped irradiated UO2 fuel rod". In: *Journal of Nuclear Materials* 437.1 (2013), pp. 409 –414. ISSN: 0022-3115. DOI: 10.1016/j.jnucmat.2013.02.059.

[75] I. Johnson and C.E. Johnson. "Mass spectrometry studies of fission product behavior: I. Fission products released from irradiated LWR fuel". In: *Journal of Nuclear Materials* 154.1 (1988), pp. 67 –73. ISSN: 0022-3115. DOI: 10.1016/0022-3115(88)90120-1.

[76] R. de Boer and E.H.P. Cordfunke. "Reaction of tellurium with Zircaloy-4". In: *Journal of Nuclear Materials* 223.2 (1995), pp. 103 –108. ISSN: 0022-3115. DOI: 10.1016/0022-3115(95)00005-4.

[77] J.L. Collins, M.F. Osborne, and R.A. Lorenz. "Fission Product Tellurium Release Behavior Under Severe Light Water Reactor Accident Conditions". In: *Nuclear Technology* 77.1 (1987), pp. 18–31. DOI: 10.13182/NT87-A33948.

[78] R.A. Lorenz, E.C. Beahm, and R.P. Wichner. "Review of tellurium release rates from LWR fuel elements under accident conditions". In: (1983). Proceedings of the International meeting on light-water reactor severe accident evaluation, Cambridge, Mass., Aug. 28-Sept. 1.

[79] World Nuclear Association. *Nuclear Power Reactors*. 2020-04. URL: https://www.world-nuclear.org/information-library/nuclear-fuel-cycle/nuclear-power-reactors/nuclear-power-reactors.aspx (visited on 07/28/2020).

[80] Y. Matsuda, H. Anada, and H. E. Bishop. "^{18}O tracer study of the oxidation of zircaloy-4 in steam". In: *Surface and Interface Analysis* 21.6-7 (1994), pp. 349–355. DOI: 10.1002/sia.740210605.

[81] B.R. Bowsher, S. Dickinson, A.L. Nichols, R.A. Gomme, and J.S. Ogden. "The chemical form of fission product telluriumin a severe reactor accident". In: *Symposium on chemical phenomena associated with radioactivity releases during severe nuclear plant accidents; Anaheim, CA (USA); 8-12 Sep 1986*. CONF-860938-. Washington DC, Usa: American Chemical Society, Division of Nuclear Chemistry and Technology, 1986.

[82] E.A. Maugeri, J. Neuhausen, R. Eichler, D. Piguet, and D. Schumann. "Thermochromatography study of volatile tellurium species in various gas atmospheres". In: *Journal of Nuclear Materials* 452.1 (2014), pp. 110 –117. ISSN: 0022-3115. DOI: 10.1016/j.jnucmat.2014.04.036.

[83] W.A. Dutton and W.C. Cooper. "The Oxides and Oxyacids of Tellurium". In: *Chemical Reviews* 66.6 (1966), pp. 657–675. DOI: 10.1021/cr60244a003.

[84] F. Garisto. *Thermodynamics of Iodine, Cesium and Tellurium in the Primary Heat Transport System Under Accident Conditions*. Report. AECL-7782. Atomic Energy of Canada Limited, Whiteshell Nuclear Research Establishment, 1982.

[85] A. P. Malinauskas, J. W. Gooch Jr., and J. D. Redman. "The Interaction of Tellurium Dioxide and Water Vapor". In: *Nuclear Applications and Technology* 8.1 (1970), pp. 52–57. DOI: 10.13182/NT70-A28633.

[86] R.J.M. Konings, E.H.P. Cordfunke, and V . Smit-Groen. "The vapour pressures of hydroxides II. $TeO(OH)_2$". In: *The Journal of Chemical Thermodynamics* 22.8 (1990), pp. 751 –756. ISSN: 0021-9614. DOI: 10.1016/0021-9614(90)90066-Y.

[87] E.C. Beahm. "Tellurium Behavior in Containment under Light Water Reactor Accident Conditions". In: *Nuclear Technology* 78.3 (1987), pp. 295–302. DOI: 10.13182/NT87-A15995.

[88] R.A. Sallach, C.J. Greenholt, and A.R. Taig. *Chemical interactions of tellurium vapors with reactor materials*. NUREG/CR–2921. 1984.

[89] R.M. Elrick and A.L. Ouellette. *Interaction of Tin Telluride and Cesium Hydroxide With Reactor Materials in Steam*. SAND-89-2504, UC - 501. 1991.

[90] E.C. Beahm. *Tellurium behavior in containment under light water reactor accident conditions*. Report. NUREG/CR–4338. Oak Ridge National Lab., TN (USA), 1986.

[91] I. Kajan, H. Lasseson, I. Persson, and C. Ekberg. "Interaction of ruthenium tetroxide with surfaces of nuclear reactor containment building". In: *Journal of Nuclear Science and Technology* 53.9 (2016), pp. 1397–1408. DOI: 10.1080/00223131.2015.1120245.

[92] "16 - Selenium, Tellurium and Polonium". In: *Chemistry of the Elements*. Ed. by N.N. Greenwood and A. Earnshaw. Second Edition. Oxford: Butterworth-Heinemann, 1997, pp. 747 –788. ISBN: 978-0-7506-3365-9. DOI: 10.1016/B978-0-7506-3365-9.50022-5.

[93] M. Laurie, P. March, B. Simondi-Teisseire, and F. Payot. "Containment behaviour in Phébus FP". In: *Annals of Nuclear Energy* 60 (2013), pp. 15 –27. ISSN: 0306-4549. DOI: 10.1016/j.anucene.2013.03.032.

[94] A.E. Pasi, H. Glänneskog, M.R. St.-J. Foreman, and C. Ekberg. "Tellurium Behavior in the Containment Sump: Dissolution, Redox, and Radiolysis Effects". In: *Nuclear Technology* 0.0 (2020), pp. 1–11. DOI: 10.1080/00295450.2020.1762456.

[95] Committee on the Safety of Nuclear Installations. *Updated Knowledge Base for Long Term Core Cooling Reliability*. Project number:JT03350703. Nuclear Energy Agency, 2013.

[96] T. Lavonen. *Chemical effects in the sump water pool during post-LOCA conditions: literature review*. Lappeenranta University of Technology: Department of Information Technology. Research report. Project code: 81524/FISKES2013. Finland: VTT Technical Research Centre of Finland, 2014.

[97] T. Kärkelä, U. Backman, A. Auvinen, R. Zilliacus, M. Lipponen, T. Kekki, U. Tapper, and J. Jokiniemi. "Experiments on the behaviour of ruthenium in air ingress accidents". English. In: *SAFIR: The Finnish Research Programme on Nuclear Power Plant Safety 2003-2006*. VTT Tiedotteita - Research Notes 2363. Finland: VTT Technical Research Centre of Finland, 2006, pp. 253–262. ISBN: 951-38-6886-9.

[98] T. Kärkelä, I Kajan, U Tapper, A. Auvinen, and C. Ekberg. "Ruthenium transport in an RCS with airborne CsI". In: *Progress in Nuclear Energy* 99 (2017), pp. 38 –48. ISSN: 0149-1970. DOI: 10.1016/j.pnucene.2017.04.019.

[99] R.K. Hilliard, A.K. Postma, J.D. McCormack, and L.F. Coleman. "Removal of Iodine and Particles by Sprays in the Containment Systems Experiment". In: *Nuclear Technology* 10.4 (1971), pp. 499–519.

[100] W.N. Bishop and D.A. Nitti. "Stability of Thiosulfate Spray Solutions". In: *Nuclear Technology* 10.4 (1971), pp. 449–453.

[101] B.A. van Brussel and J.Th.M. De Hosson. "Glancing angle x-ray diffraction: A different approach". In: *Applied Physics Letters* 64.12 (1994), pp. 1585–1587. DOI: 10.1063/1.111847.

[102] X. Ning, I.W. Selesnick, and L. Duval. "Chromatogram baseline estimation and denoising using sparsity (BEADS)". In: *Chemometrics and Intelligent Laboratory Systems* 139 (2014), pp. 156 –167. ISSN: 0169-7439. DOI: 10.1016/j.chemolab.2014.09.014.

[103] L. Duval. *BEADS Baseline Estimation And Denoising with Sparsity*. Accessed Jan. 20, 2020. URL: https://www.mathworks.com/matlabcentral/fileexchange/49974-beads-baseline-estimation-and-denoising-with-sparsity.

[104] M.K. Bahl, R.L. Watson, and K.J. Irgolic. "X-ray photoemission studies of tellurium and some of its compounds". In: *The Journal of Chemical Physics* 66.12 (1977), pp. 5526–5535.

[105] N.G. Krishnan, W.N. Delgass, and W.D. Robertson. "Electron binding energies of core levels in caesium adsorbed on a nickel (100) surface". In: *Journal of Physics F: Metal Physics* 7.12 (1977), pp. 2623–2635. DOI: 10.1088/0305-4608/7/12/021.

[106] W.E. Sartz, K.J. Wynne, and D.M. Hercules. "X-ray photoelectron spectroscopic investigation of Group VIA elements". In: *Analytical Chemistry* 43.13 (1971), pp. 1884–1887. DOI: 10.1021/ac60307a044.

[107] G. Ebbinghaus and A. Simon. "Electronics structures of Rb, Cs and some of their metallic oxides studied by photoelectron spectroscopy". In: *Chemical Physics* 43.1 (1979), pp. 117 –133. ISSN: 0301-0104. DOI: 10.1016/0301-0104(79)80111-1.

[108] N.J. Shevchik, M. Cardona, and J. Tejeda. "X-Ray and Far-uv Photoemission from Amorphous and Crystalline Films of Se and Te". In: *Phys. Rev. B* 8 (6 1973), pp. 2833–2841. DOI: 10.1103/PhysRevB.8.2833.

[109] W.E. Morgan, J.R. Van Wazer, and W.J. Stec. "Inner-orbital photoelectron spectroscopy of the alkali metal halides, perchlorates, phosphates, and pyrophosphates". In: *Journal of the American Chemical Society* 95.3 (1973), pp. 751–755. DOI: 10.1021/ja00784a018.

[110] A.J. Ricco, H.S. White, and M.S. Wrighton. "X-ray photoelectron and Auger electron spectroscopic study of the CdTe surface resulting from various surface pretreatments: Correlation of photoelectrochemical and capacitance-potential behavior with surface chemical composition". In: *Journal of Vacuum Science & Technology A* 2.2 (1984), pp. 910–915. DOI: 10.1116/1.572547.

[111] W.F. Moulder J.F. nad Stickle, P.E. Sobol, and K.D. Bomben. *Handbook of X-ray Photoelectron Spectroscopy*. Ed. by J. Chastin. Minnesota, USA: Perkin-Elmer Corporation, 1979. ISBN: 978-0-12-388446-6. DOI: 10.1016/B978-0-12-388446-6.00001-0.

[112] F. Garbassi, J.C.J. Bart, and G. Petrini. "XPS study of tellurium—niobium and tellurium—tantalum oxide systems". In: *Journal of Electron Spectroscopy and Related Phenomena* 22.2 (1981), pp. 95 –107. ISSN: 0368-2048. DOI: 10.1016/0368-2048(81)80019-9.

[113] L. Soriano, L. Galan, and F. Rueda. "An XPS study of Cs_2Te photocathode materials". In: *Surface and Interface Analysis* 16.1-12 (1990), pp. 193–198. DOI: 10.1002/sia.740160138.

[114] P.M.A. Sherwood. "X-ray photoelectron spectroscopic studies of some iodine compounds". In: *Journal of the Chemical Society, Faraday Transactions 2: Molecular and Chemical Physics* 72 (0 1976), pp. 1805–1820. DOI: 10.1039/F29767201805.

[115] J. Kučera, A.E. Pasi, F. Espergen, T. Kärkelä, H.V. Lerum, J.P. Omtvedt, and C. Ekberg. "Tellurium determination by three modes of instrumental neutron activation analysis in aerosol filters and trap solutions for the simulation of a severe nuclear accident". In: *Microchemical Journal* 58 (2020), p. 105139. ISSN: 0026-265X. DOI: 10.1016/j.microc.2020.105139.

[116] NuDat 2.8. *Interactive Chart of Nuclides*. 2020-04. URL: https://www.nndc.bnl.gov/nudat2/ (visited on 06/02/2020).

[117] W.C. Hinds. *Aerosol Technology: Properties, Behavior, and Measurement of Airborne Particles*. 2nd ed. New York: Wiley, 1999. ISBN: 0471194107.

[118] V.P. Itkin and C.B. Alcock. "The O-Te (oxygen-tellurium) system". In: *Journal of Phase Equilibria* 17.6 (1996), pp. 533–538. DOI: 10.1007/BF02666000.

[119] M. Bouroushian. "Electrochemistry of the Chalcogens". In: *Electrochemistry of Metal Chalcogenides*. Berlin, Heidelberg: Springer Berlin Heidelberg, 2010, pp. 57–75. ISBN: 978-3-642-03967-6. DOI: 10.1007/978-3-642-03967-6_2.